

AALBORG UNIVERSITY

---

# Model Predictive Control of a Sewer System

---

Control and Automation:  
Master Thesis

Group:  
CA10-1030

7 June 2018





**AALBORG UNIVERSITY**  
STUDENT REPORT

**Master thesis**

Control and Automation  
Fredrik Bajers Vej 7  
DK-9220 Aalborg Ø, Danmark  
<http://www.es.aau.dk>

**Title:**

Model predictive control  
of a sewer system

**Project period:**

P10, Spring semester 2018

**Projectgroup:**

CA10-1030

**Participants:**

Jacob Naundrup Pedersen  
Thomas Holm Pilgaard

**Supervisors:**

Carsten Skovmose Kallesøe  
Palle Andersen  
Tom Søndergaard Pedersen

**Copies: 6**

**Pages: 91**

**Appendix: 18**

**Completed: 07-06-2018**

**Abstract:**

This project deals with control of wastewater management in sewers, where Fredericia has been used as a case. In Fredericia, there are multiple large industries, which dispose large amounts of wastewater into the sewer. This results in a fluctuating input to the wastewater treatment plant (WWTP). This causes problems for the bacteria which consumes wastewater compound. To optimize the performance of the WWTP a solution to obtain a sewage flow where the variations are minimized is desired. This results in the following problem statement: *How can a simulation environment be constructed, which mimic the behavior of a real sewer system, where MPC is utilized as the control scheme to obtain stable sewage output such that optimal performance can be obtained from a WWTP.* The Nonlinear Saint-Venant equations are used to simulate flow in sewer pipes and together with a linear tank model they are used to construct a simulation environment. Furthermore, the environment can simulate sewer pipes with disturbance side input to increase the complexity of the setup. Due to the nature of the linearization and the sizable amount of components, problems occurred during the design of MPC. A satisfying result was therefore not obtained with MPC.



# Preface

---

This report has been created by Jacob Naundrup Pedersen and Thomas Holm Pilgaard. The project is made on the master thesis of the master in Control and Automation at Aalborg University.

The report is intended for people with knowledge corresponding to a master student at Control and Automation. MATLAB is used as the primary software tool for this project. Figures are constructed by the group, unless a reference is included in the figure text to the source.

Units are indicated by square brackets after the parameter has been elaborated e.g. Q is flow  $\left[\frac{m^3}{s}\right]$ .

Sources are indicated by [name,year], and can be found in the bibliography list at the given [name,year].

Data-sheets, raw flow profiles from Fredericia and the simulation model can be found in the Attachment.

---

Jacob Naundrup Pedersen  
jnpe12@student.aau.dk

---

Thomas Holm Pilgaard  
tpilga12@student.aau.dk



# Contents

---

<b>Nomenclature</b>	<b>ix</b>
<b>1 Introduction</b>	<b>1</b>
1.1 General sewer construction . . . . .	1
1.2 Chemical and biological processes . . . . .	3
1.2.1 Chemical reactions in sewer lines . . . . .	4
1.2.2 Wastewater treatment plant . . . . .	4
1.3 Challenges of wastewater treatment . . . . .	6
1.4 Problem statement . . . . .	8
<b>2 System description</b>	<b>9</b>
<b>3 Simulation solutions &amp; limitations</b>	<b>17</b>
<b>4 Modeling</b>	<b>19</b>
4.1 Hydraulics of sewer line . . . . .	19
4.2 Transport of concentrate . . . . .	26
4.3 Sewer interconnection . . . . .	28
4.4 Tank model . . . . .	29
<b>5 Simulation</b>	<b>33</b>
5.1 Structure . . . . .	33
5.2 Preissmann scheme . . . . .	38
5.2.1 Stability & Precision . . . . .	43
5.3 Concentrate scheme . . . . .	46
5.4 Tank scheme . . . . .	47
5.5 Implementation . . . . .	48
<b>6 Control</b>	<b>67</b>
6.1 Linearization . . . . .	67
6.2 Model predictive control . . . . .	73
6.2.1 Constraints . . . . .	78
6.2.2 Implementation of MPC . . . . .	80
<b>7 Results</b>	<b>85</b>
<b>8 Discussion</b>	<b>89</b>
<b>9 Conclusion</b>	<b>91</b>
<b>Bibliography</b>	<b>93</b>
<b>A Appendix</b>	<b>95</b>
A.1 Summary of company visits . . . . .	95
A.2 Pump information . . . . .	97
A.3 Flow profiles . . . . .	98
A.4 Formulas . . . . .	112



# Nomenclature

---

## Abbreviation

Abbreviation	Definition
GIS	Geographically Information System
WATS	Wastewater of Aerobic/Anaerobic Transformations in Sewers
WWTP	Wastewater Treatment Plant
MPC	Model Predictive Control

## Symbols

Symbol	Description	Units
$A$	Wetted area	$m^2$
$Q$	Water flow	$m^3/s$
$Q_f$	Water flow for a filled pipe	$m^3/s$
$q$	Lateral inflow of water	$m^2/s$
$q_c$	Lateral flux input of concentrate	$g/(s \cdot m)$
$d$	Diameter meter	$m$
$r$	Radius	$m$
$F$	Force	$N$
$v$	Velocity	$m/s$
$M$	Mass	$kg$
$V$	Volume	$m^3$
$\rho$	Density	$kg/m^3$
$l$	Length	$m$
$g$	Gravitational acceleration	$m/s^2$
$T$	Temperature	$^{\circ}C$
$m$	Mass flow	$kg/s$
$\phi$	Flux	$g/s$
$C$	Concentrate	$g/m^3$
$R$	Hydraulic radius = wetted area / wetted perimeter	$m$
$f$	Friction factor	.
$b$	pipe width	$m$
$h$	Height	$m$
$\mathcal{J}$	Cost function	.
$\bar{H}$	Average flow height	$m^3/s$
$S_f$	Friction coefficient	.
$S_b$	Slope of the pipe	$\%_0$
$Q$	weighting parameter	.
$\mathcal{M}$	Momentum	$kg \cdot m/s$
$Re$	Reynolds number	.
$k$	Roughness coefficient	.
$n$	Mannings number	$s/m^{-1/3}$
$f$	Weisbach resistance coefficient	.



Sewers were created to solve the seemingly simple problem of removal of wastewater. The first sewers, registered, dates back to 7000 B.C. in urban settlements and were created to remove wastewater from houses and surface runoff created by precipitation. To avoid clogging and wear of the sewers grit chambers was constructed. They work by slowing the flow of sewage in long narrow channels making the solids, such as sand, end up as sediments in the channels due to gravity. The complexity of sewers increased in ancient Rome where large underground systems were created leading to the main sewer system called "Cloaca Maxima" making it possible to have latrines with running water within households, though mostly made available for the rich [Hvitved-Jacobsen et al., 2013].

During night time the population, without immediate access to a latrine in their household, still disposed waste onto the streets. The reason for this was that they simply did not want to put in the effort to properly dispose of the waste at night. Because of this, the ancient Rome suffered from illnesses related to waste lying in the streets. The hygienic aspect of proper disposal of wastewater in relation to drinking water was not considered until the 19th century, where several European cities saw a large outbreak of cholera causing the deaths of millions [Hvitved-Jacobsen et al., 2013].

The growth in waste furthermore caused the expansion of 26 km sewer network in Paris to 600 km during the 19th century. But it is not until the start of the 20th century that the chemical and microbial processes in sewers are considered. The microbial cause of cholera was identified by the German doctor Robert Koch in 1883, a discovery for which he in 1905 received the Nobel Prize in physiology and medicine. The growing industries and technological progress in the 20th century meant that more chemicals were disposed into the sewers having severe consequences for the organic life downstream of the receiving waters. Wastewater treatment plants were introduced to reduce the pollution, but several countries did not have any wastewater treatment plants before after World War II. Today disposal of sewage and setup of wastewater treatment plants is a given part of a construction of new settlements, even in poor regions of the world [Hvitved-Jacobsen et al., 2013].

## 1.1 General sewer construction

This section will elaborate on the general construction of sewers. Furthermore, a brief explanation, of the flow into the sewer to the output from the wastewater treatment plant (WWTP), is given.

Generally, sewer construction can be put into two categories which are gravity and pressurized sewers. Gravity sewers utilize the topographic advantages of the area in which they are constructed. But in places where the level of the surface area does not accommodate a slope of the sewer pipe, such that wastewater flow in the desired direction,

wells with pumps are used to transport the wastewater to an elevated level. An illustration of gravity and pressurized sewer lines can be seen in figure 1.1.

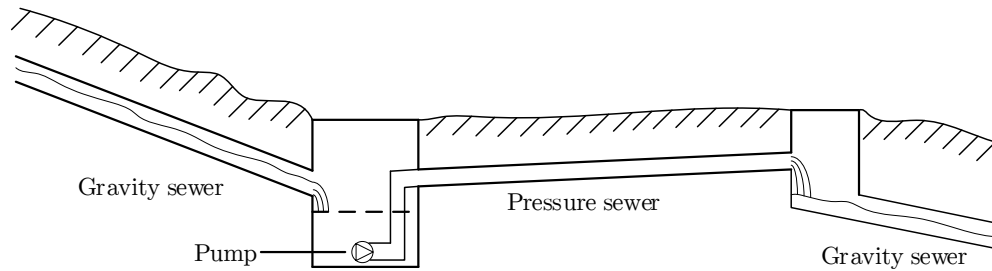


Figure 1.1: Illustration of flow in gravity and pressurized sewer lines.

Design of sewer systems involves careful considerations, such that as much of the network utilize gravity for transport of wastewater, to minimize the energy consumption. Therefore, the WWTP is typically located in a low topographic area near a river, fjord or the sea. Other design parameters involve dimensioning of the pipes to avoid overflow and to compensate for groundwater ingress into the sewer lines. Also, the depth should be sufficient, such that subzero temperatures does not prevent the flow in the sewers at any time. Furthermore, the slope of the pipes must be chosen such that sufficient flow is obtained and clogging is avoided. Different materials used to create the pipes gives different amount of friction e.g. a concrete surface will be rougher than polyethylene and thereby have a higher friction. This means that a larger slope of a concrete pipe is needed to avoid clogging. Typically, gravity sewer pipes are made of concrete and pressurized sewer pipes of polyethylene [Hvitved-Jacobsen et al., 2013].

In figure 1.2 a block diagram of the flow of wastewater is seen.

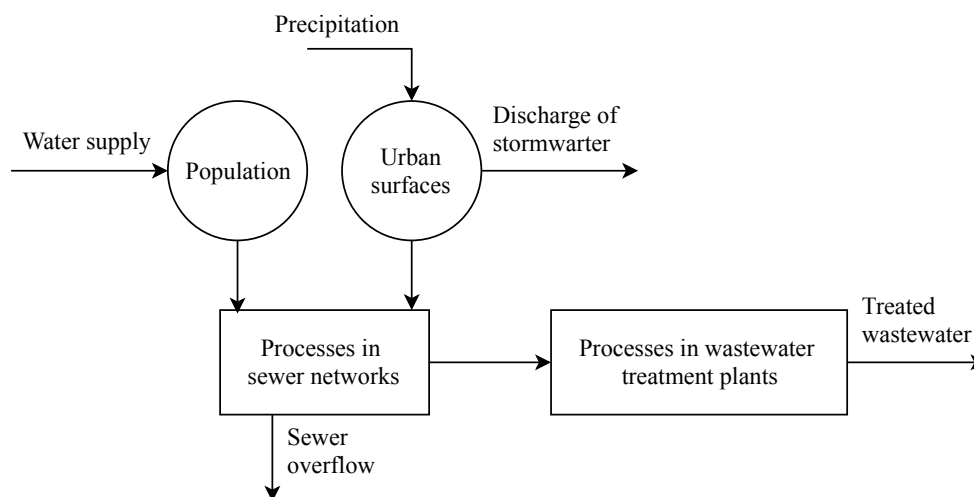


Figure 1.2: General overview of wastewater processes from inputs to treated output [Hvitved-Jacobsen et al., 2013].

Starting at the left side in the figure, precipitation from urban surfaces and roads are let into the sewer by inlets placed at the gutter. In recent times separate sewer systems for

surface runoff are constructed, which are also called storm water sewers. The water in these sewers is typically led into stormwater basins, rivers or the sea. In areas with older sewer constructions, storm water is let into sewers where it is mixed with wastewater. The wastewater comes from households or industry disposing of substances of varying consistency. Heavy precipitation can cause the sewers to be filled, and to avoid overflow, into a household or on roads, the wastewater is let into rivers or the sea during such events. The reason for designing storm water sewers is partly to avoid letting untreated sewage into nature, but also to better be able to control the cleansing process at the WWTP. When wastewater is received at the treatment plant it undergoes several processes to separate the unwanted substances from the received wastewater. The cleansed water is then released into nearby rivers or the sea. Due to the sizes of sewer networks, which can have inlets several kilometers from the WWTP, chemical reactions also occur in the sewer pipes [Hvitved-Jacobsen et al., 2013]. The chemical and microbial reactions happening in the sewer lines is discussed in subsection 1.2.1. The processes which the wastewater undergoes at the treatment plant is discussed in subsection 1.2.2.

## 1.2 Chemical and biological processes

This section will give an overview of the chemical and biological processes that wastewater undergoes from it is led into the sewer till it is cleansed at the WWTP. The various processes occurring at the WWTP is described, to clarify the problems that may arise during operation.

Within wastewater, there is a large number of living organisms. It contains somewhere between 100.000 to 1.000.000 microorganisms per milliliter. These organisms originate from sanitary waste and soil. They are a natural living part of the organic matter and they are an important part of the cleansing at the WWTP. To be able to obtain a high water quality at the output of the WWTP it is necessary to have a thorough understanding of these microorganisms [College, 2018].

Nearly all microorganisms found in wastewater are not harmful and do not cause illness in humans. However, a small group of the microorganisms can cause illness, and these are of great concern in wastewater treatment. The most known diseases to occur are typhoid fever, dysentery, cholera, and hepatitis [College, 2018].

The microorganisms in the WWTP have a specific role in the decomposition of the waste. The three most notable microorganisms in the biological treatment process are bacteria, fungi, and protozoa. The bacteria have the primary role of degrading the wastewater compounds. Bacteria is a single cell organism and is capable of reproducing rapidly when in contact with water. They feed off the waste by absorbing it through the cell wall turning it into sediment solids [College, 2018]. Fungi like bacteria decompose the organic waste, however, they also pose a significant problem for the treatment process as the fungi can proliferate to an extent where it affects the quality of the output from the WWTP [AquaEnviro, 2010]. Lastly, protozoa act as a predator toward the present bacterial population such that it can be controlled [College, 2018]. Reactions in sewer lines is discussed in subsection 1.2.1 and the processes at the treatment plant in subsection 1.2.2.

### 1.2.1 Chemical reactions in sewer lines

Wastewater is subject to a variety of mass changes in sewers. This is caused by free electrons in the wastewater, which causes chemical reactions and thereby leading to new compounds being created. The chemical reactions occurring is called redox reactions. A Redox reaction is the transfer of electrons between two compounds at an atomic scale. Chemical reactions are determined by the electron acceptors that are present in the wastewater. The electron acceptor is the compound that receives electrons in a redox reaction. Examples of dissolved acceptors are oxygen ( $O_2$ ), nitrate ( $NO_3^-$ ) and sulfate ( $SO_4^{2-}$ ). These acceptors are present, respectively, when aerobic, anoxic or anaerobic conditions exist in the sewer. The redox reaction converts these three compounds in the wastewater to new compounds such as water ( $H_2O$ ), molecular nitrogen ( $N_2$ ) and hydrogen sulfide ( $H_2S$ ) [Hvitved-Jacobsen et al., 2013].

Where redox reactions occur in a sewer line is, to a great extent, determined by the design of the sewer. The aerobic, anaerobic and anoxic conditions do not exist in the same part of the sewer, and the last only occurs if nitrate is artificially added to the wastewater. If the sewer is in an aerobic state then the typical characteristics of the sewer are either partly filled gravity sewer or an aerated pressure sewer. This means that there are free oxygen ( $O^+$ ) molecules, and these will bind to hydrogen molecules to create water. If the sewer is in an anoxic state, which occurs in pressure sewers, then the addition of nitrate to the wastewater results in molecular nitrogen. If the sewer is in an anaerobic state the characteristic of the sewer is either a pressure line or a full flowing gravity line. Reactions which occurs will result in hydrogen sulfide as the sulfate will bind with the hydrogen molecules. With the knowledge of these condition, sewers can actively be designed to achieve a specific state [Hvitved-Jacobsen et al., 2013]. The two desired states in sewers are aerobic in gravity lines and anoxic in pressure lines to avoid malodorous dissipation into the urban atmosphere.

To model, the chemical and biological reactions in sewer lines a model concept, Wastewater Aerobic/Anaerobic Transformation in Sewers (WATS), is used. The WATS model is expressed as differential mass balance equations which are suitable for numerical computation. It can, therefore, be included in simulations for a specific objective e.g. model of water and gas phase transformations. The WATS model can be applied to a sewer as long as a fundamental understanding of the sewer is available. Whether it is aerobic, anoxic or anaerobic conditions that dominate the sewer, furthermore the soil composition and the pH concentration of the wastewater must also be known and included in the WATS model [Hvitved-Jacobsen et al., 2013].

### 1.2.2 Wastewater treatment plant

Wastewater from households and industry contains organic and inorganic matter and if it is released into the environment it will result in a polluted environment. This can cause oxygen depletion and thereby affect the wildlife in the water environment negatively. In the following section, the process that wastewater undergoes in a WWTP is elaborated.

In figure 1.3 the various treatments wastewater undergoes is illustrated.

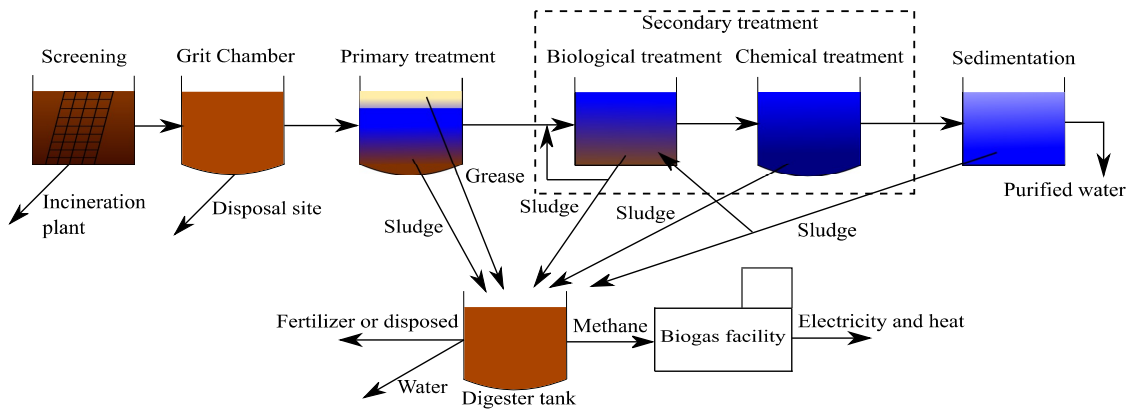


Figure 1.3: General overview of a wastewater treatment plant.

The first stage of cleansing the wastewater is screening, where larger objects are removed from the wastewater which either could cause congestion or damage the equipment. Examples of objects that are filtered from the wastewater are bottles, plastic bags, and diapers [Eschooltoday, 2017]. The wastewater is then lead to the primary treatment, where it first will enter a grit chamber, where objects as sand and stones will settle to the bottom of the tank. These grit chambers are crucial in WWTP that are connected with combined sewer systems. As storm-water may wash sand, stones, and gravel into the sewer these objects will be extracted in this process [EPA, 1994]. The collected objects are disposed at a disposal site. After the screening process the wastewater, still containing organic and inorganic matter, is lead into the primary treatment tank where flow and turbulence are reduced. The organic matter will sediment in the tank, while grease will accumulate at the surface. The grease is scrapped from the surface and lead into the digester tank. The matter that has sedimented is now called sludge or raw primary bio-solids. At the bottom of the tank, large scrappers are moving the sludge to the center of the tank where it is pumped into the digester tank [EPA, 1994].

In the secondary treatment, the wastewater is lead into an aeration tank where the air is pumped in at the bottom. This is called the biological treatment. By aeration of the wastewater, the bacteria gain optimal conditions for respiration. This will speed up the process of decomposing the remaining organic matter from the primary treatment process. In the process of decomposing the organic matter, the bacteria will produce  $CO_2$  that will dissipate into the atmosphere. Furthermore, when the bacteria have consumed the organic matter they will start to produce heavier particles that will sediment in the tank [Rinkesh, 2009]. In figure 1.4 this process is illustrated.

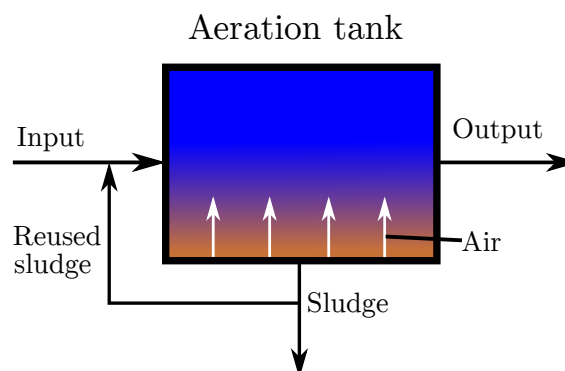


Figure 1.4: Illustration of the aeration tank in the biological treatment process.

This is called the activated sludge process, because some of the sludge is reused in the aeration phase to retain a high bacteria population. The reused sludge contains millions of microorganisms which increase the efficiency of cleansing the wastewater. After some time the aeration is stopped which causes anaerobic conditions. Other bacteria is then activated in a process called denitrification, where it absorbs oxygen molecules from the nitrate converting it to nitrite. The nitrite flows to the surface in the tank and dissipates into the atmosphere. The remaining sludge that has sedimented is pumped to the digester tank [EPA, 1994, Rossi et al., 2014]. Hereafter a chemical treatment is performed to remove the inorganic matter that is left in the wastewater. Chemicals which is non-damaging to the environment is added to the wastewater. This will create chemical reactions and thereby create new compounds, that will sediment in the tank, which is pumped into the digester tank [Sjøholm, 2016].

After these treatment processes, there are still some particles left in the wastewater. It is therefore lead to a sedimentation tank where the remaining bacteria and sludge will settle before the wastewater is released into receiving waters. The sedimented particles or sludge will either be pumped to the digester tank for further processing or reused in the activated sludge process.

The sludge collected in the digester tank also undergoes further treatment, as the remaining water in the sludge is separated. The water is lead back to the wastewater treatment process where it will undergo the same process again. The sludge then undergoes anaerobic digestion for about a month, where the resulting bio-solids can be used as fertilizer. The methane gas created in the process can be used at a bio-gas facility to produce electricity and heat [Rinkesh, 2009].

### 1.3 Challenges of wastewater treatment

In the following section various challenges, such as flow and concentrate variations, which affects the treatment efficiency of the WWTP is discussed. Furthermore, this section will mostly be based on information obtained from a meeting with a WWTP, namely Fredericia Spildevand og Energi A/S. A summary of this meeting can be found in appendix A.1. A general daily intake of wastewater from a small town is illustrated in figure 1.5.

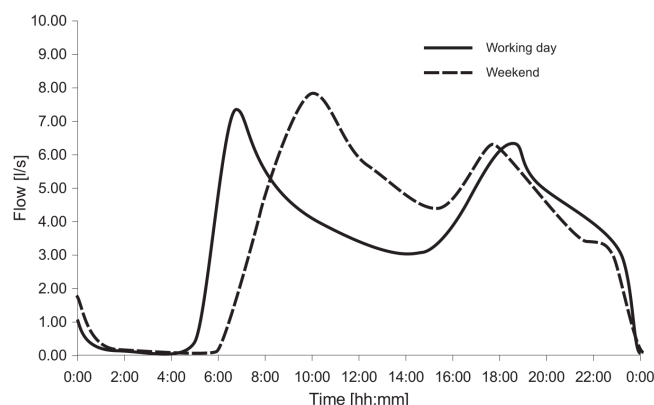


Figure 1.5: Typical daily flow pattern from the town Frejlev, with approximately 2000 residents [Schlütter, 1999].

At approximately 06:00 there is a steep increase in flow, which is due to people preparing

for work. During the day the flow lessens, until 16:00 where people start returning home from work. The flow increases due to typical household activity such as cooking, bathing, toilets flushing. During night time the flow is at a minimum as most people are at sleep. During weekends the flow patterns change slightly, which could be because of a different sleep pattern than during weekdays.

The flow variations created by human routines is challenging for the treatment process. As mentioned in subsection 1.2.2 sludge is reused to accommodate a sufficient amount of microorganisms to be able to cleanse the wastewater. When a sudden peak in flow occurs, there might not be enough microorganisms available to achieve a satisfying result from the cleansing process. Furthermore, it is not possible to store sludge, with the purpose of using the microorganisms at a later time, as they have a short span of life if the right conditions are not in place.

In Fredericia e.g. there are multiple large companies, which disposes large amounts of wastewater into the sewer. At day to day operation the wastewater flow into the WWTP is not a problem. But random occurrences of sudden large outlets of wastewater from the industry is seen. This could, for example, be from the dairy where a failed batch of cream is let into the sewer such that the tanks can be used to produce a new product. In some cases, the companies contact the WWTP to warn on the incoming amount of wastewater or to agree on the discharge flow of the discarded product. This is not something that the companies are required to do, and does not always happen. This means that the WWTP soonest discovers the added load at the inlet, and therefore has limited possibilities to react on the sudden change of flow. These outlets pose a problem for the WWTP. Not only because of the change in flow, but also because the concentrate of the various compounds in the wastewater is usually higher from the larger companies. Typically, the industry is efficient in letting out wastewater within certain pH levels at reasonable flow levels. The only countermeasure, for these incidents of sudden discharge, is to prevent overflow. This is done by letting some of the wastewater, in the later unfinished stages of the cleansing process, through into the fjord. Furthermore, changes in chloride concentration, from either industry outlets or back-flow from the fjord due to heavy precipitation, is problematic for the bacteria. Meaning that changes in concentrate cause a drop in efficiency until the bacteria have acclimated. Contrary, a static level of chloride does not pose a problem for the bacteria.

To sum up, the typical problems which a WWTP encounters. Flow variations are problematic as the cleansing process reuse sludge. The random changes are either caused by larger industry or as a result of heavy precipitation. Outlets by the industry are more of a concern when considering the concentration of the wastewater. Changes in concentration can cause inefficiency at the WWTP as the bacteria need time to acclimate to changes. Precipitation is a problem as a result of the large increase in flow it causes, which can lead to capacity problems at the WWTP.

## 1.4 Problem statement

Based on the information in the previous sections, which states that several problems occur during wastewater treatment, the problems can be summed to the following points:

1. Flow variations due to large industries and natural phenomenons
2. Concentration variations due to large industries and natural phenomenons
  - a) Chloride variations
  - b) Phosphorus variations
  - c) Nitrogen variations
  - d) Organic matter variations

To be able to implement countermeasures towards these problems, information is needed about the flow of wastewater in the sewer lines. As measurements is rarely available for entire sewer networks or even parts of it, an ideal solution would be to construct a simulation environment where different scenarios can easily be setup [Fredericia-Spildevand, 2018b]. Furthermore, a control scheme is needed to be able to implement an efficient countermeasure. It has been decided to utilize model predictive control (MPC) as the control scheme for this project. This control scheme excels in obtaining optimal control action, when operating systems close to limitations, as constraints can be applied. Thus it could be an ideal control solution for this project. From this a problem statement can be formulated:

*How can a simulation environment be constructed, which mimic the behavior of a real sewer system, where MPC is utilized as the control scheme to obtain stable sewage output such that optimal performance can be obtained from a WWTP.*

# System description 2

---

This section will go into details of the structure of the sewer network for which the further work of this project will be based upon.

As mentioned in section 1.3 a steady flow of sewage with a fixed level of contaminants is desired such that an optimal utilization of the wastewater treatment plant can be obtained. An area of interest is Fredericia with a sizable population of approximately 40.000 people and industries where some of the largest consists of a brewery, bottling plant, refinery and a dairy plant [Statistics-Denmark, 2018]. All of these industries are placed at the outskirts of the city, meaning that the wastewater discharged into the sewer goes through populated areas creating an uneven flow of wastewater to the WWTP. Two main sewer lines separate the northern and southern part of the city. To limit the scope of the project only the northern main sewer line is considered. This line covers the largest part of the households and the industry, located in the city. In figure 2.1, a simplified overview is given of the northern main sewer line in Fredericia. The placement of the sewers shown in the figure is obtained from a Geographically Information System (GIS) map, which is made publicly available by the municipal of Fredericia [Fredericia-Spildevand, 2018a]. The red and green lines indicate sewers with flows of wastewater only and combined sewers with flows of wastewater and surface runoff, respectively. The populated areas are indicated by blue and green transparent colors, to easier be able to distinguish between the different parts of the sewer network. The red transparent areas indicate small to medium sized industry. Only the sewer lines out of or between the separate areas are shown. Furthermore, the areas connected by a red line has a separate sewer system for surface runoff, which is lead into various ponds or the sea, minimizing the load on the wastewater treatment plant. The bottling plant, refinery and the brewery are marked by the purple, brown and black rings, respectively. Furthermore, several inlets for surface runoff connected directly to the main sewer line exists.

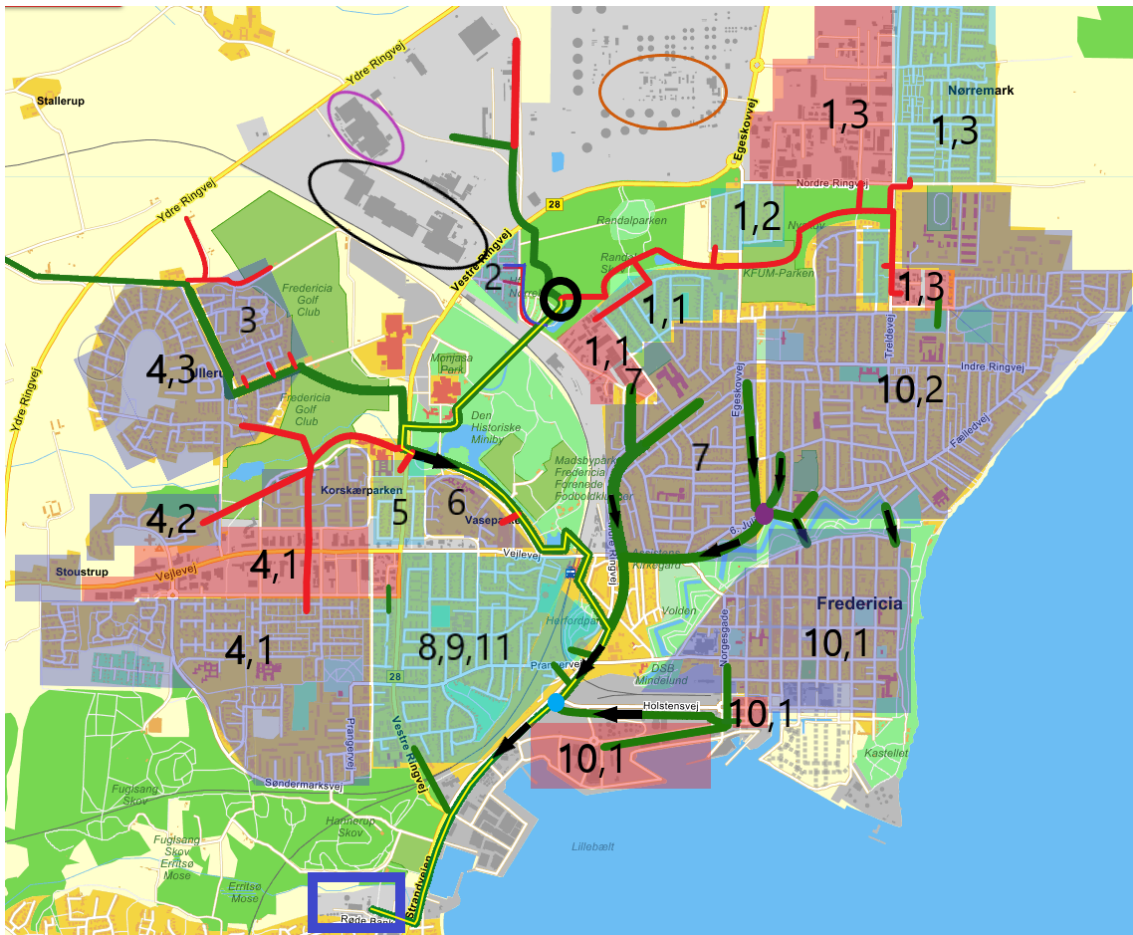


Figure 2.1: Simplified mapping of the northern part of the sewer network in Fredericia. The blue and green transparent colors indicate populated areas and the red transparent area indicate industry. Red and green lines are sewers with flows of wastewater and combined wastewater and surface runoff respectively. The bottling plant, refinery, and brewery are marked by purple, brown and black circles respectively. The black circle denotes the starting point of the main sewer line. The green line with a yellow stripe within represents the main sewer line. The purple dot is a connecting point with two incoming and two outgoing sewer lines. The blue dot is a wastewater pumping station which elevates sewage such that gravity can be utilized for the remaining transport into the treatment plant. Blue rectangle marks the location of the wastewater treatment plant [Eniro, ] [Fredericia-Spildevand, 2018a].

The various enumerated parts in figure 2.1 is shown by order of attachment to the main sewer line, together with distance between each attachment, in figure 2.2.

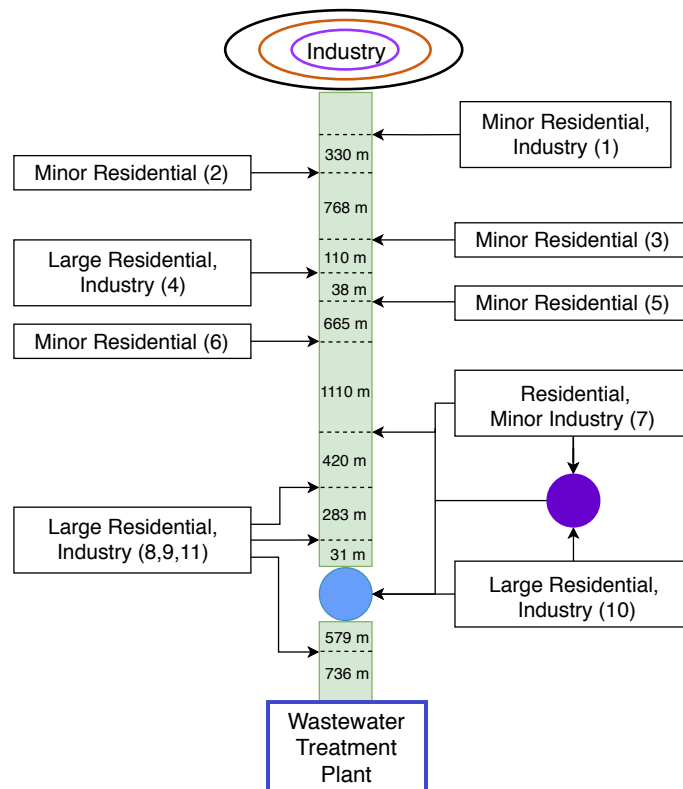


Figure 2.2: Simplification of the attachments to the main sewer line shown in figure 2.1. The numbers correspond to which area is connected to the main sewer line farthest from the wastewater treatment plant, with the distance between them [Fredericia-Spildevand, 2018a].

Furthermore, the different sections consist of pipes with varying diameters which can be seen in table 2.1.

Pipe section	Pipe length (meter)	Inner pipe diameter (mm)	Bed datum in (m)	Bed datum out (m)	Bed slope (‰)
1 → 2	303	900	11,56	10,65	3,00
	27	1000	10,65	10,57	3,00
2 → 3	155	1000	10,57	9,94	4,10
	295	800	9,94	6,33	12,20
	318	900	6,33	4,71	5,30
3 → 4	110	900	4,71	4,31	3,60
4 → 5	38	1000	4,31	4,40	-2,40
5 → 6	665	1000	4,40	2,43	3,00
6 → 7	155	1000	2,43	2,31	0,80
	955	1200	2,31	-0,48	2,90
7 → 8	293	1200	-0,48	unknown	
	11	1300	unknown	-1,38	
	116	1200	-1,38	-1,62	2,10
8 → 9	283	1400	-1,62	-2,09	1,70
9 → 10	31	1400	-2,09	-2,15	1,90
10 → 11	125	1600	0,31	0,05	2,10
	94	1500	0,05	-0,07	1,30
	360	1600	-0,07	-1,72	4,60
11 → WWTP	736	1600	-1,72	-2,60	1,20
Total length 1 → WWTP	5070				

Table 2.1: Table of the various lengths and the approximate inner diameter of a pipe, appearing in order, in the main sewer line. Pipe section indicate the length of a pipe between the attachment of the various areas to the main sewer line [Fredericia-Spildevand, 2018a].

Some assumptions are made to avoid possible complications during simulation. The negative slope of the section between connection point four and five is flipped such that no permanent storage of sewage happens. The reason for this assumption is that it will ease the computation, of the free flow in that section, if storage in the pipe sections could be disregarded during simulation. Furthermore, the new slope is deemed acceptable based on the obtained slopes of the remaining pipe sections. The two pipe sections between point seven and eight, where out- and input datum is unknown, are gathered into a single pipe section. This section will be designated an inner diameter of 1200 mm as the section with the larger diameter, because of its short length, is assumed insignificant when considering the free flow at the end point of the combined section.

Pipe section	Pipe length (meter)	Inner pipe diameter (mm)	Bed slope (‰)
4 → 5	38	1000	2,40
7 → 8	304	1200	3,00
	116	1200	2,10

Table 2.2: New slope values for sections with negative slope and unknown values.

To be able to simulate how the wastewater propagates throughout the main line the flows in each residential and industrial area is needed. However, Fredericia Spildevand og Energi A/S does not have measurements of the flow or concentration from the specific areas.

Only at a limited amount of pumping stations, at various positions in the city are flow measurements available. Therefore flow profiles for the various inputs shown in figure 2.2 needs to be designed. For this purpose the flow profile, seen in figure 1.5, is utilized for the residential and minor industry areas, as an estimate of the flow during a 24 hour period. The flow profiles are scaled to fit the size of each area and delayed approximately with the distances to the main line seen in figure 2.1.

From figure 2.2 it can be seen that 11 different flow profiles are to be constructed, to cover wastewater contribution to the main line from each residential and industrial area. By knowing the area and density of the population a flow profile can be scaled to each of the residential and industrial areas. On average there are 2,6 residents per house in Denmark which will henceforth be the foundation for obtaining population for the various areas [Nykreid, 2018]. Furthermore, it is assumed that the urban areas one to six together with eight, nine and eleven are single-family houses and zone seven and ten are apartments in buildings with several floors, meaning that area seven and ten have a higher density of population per square kilometers. As the northern part of Fredericia consists of the largest part of the city, the assumption is that around 30.000 of the approximately 40.000 people resides there. The residential area 1,1 is used to obtain an approximate density of people per square kilometer within the urban areas. The number of houses located in this area is found to be 199 which gives an approximated average urban population density of 3098,2 per square kilometer. The approximated size of the various areas is found and from that the population by multiplying with the average population density. The remaining of the population is divided between area seven and ten. As area seven is approximately a third of the combined area it is given a third of the remaining population leaving the remaining to area ten. In table 2.3 the approximated size of the residential and industrial areas, together with the population of the residential areas, are shown.

Zone	Residential area [ $km^2$ ]	Industrial area [ $km^2$ ]	Population per area
1,1	0,167	0,0083	517
1,2	0,111	-	344
1,3	0,458	0,543	1418
2	0,056	-	173
3	0,167	-	517
4,1	1,125	0,375	3485
4,2	0,167	-	517
4,3	0,580	-	1797
5	0,104	-	322
6	0,115	-	356
7	0,771	0,014	5874
8 - 9	0,667	0,021	2067
10,1	0,903	0,333	3916
10,2	1,781	-	7832
11	0,278	-	865
total	7,45	1,294	30000

Table 2.3: Table of the sizes of the residential and industrial areas and the population in the residential areas [Nykreid, 2018].

In figure 2.3 a flow profile is shown for residential area 1,1.

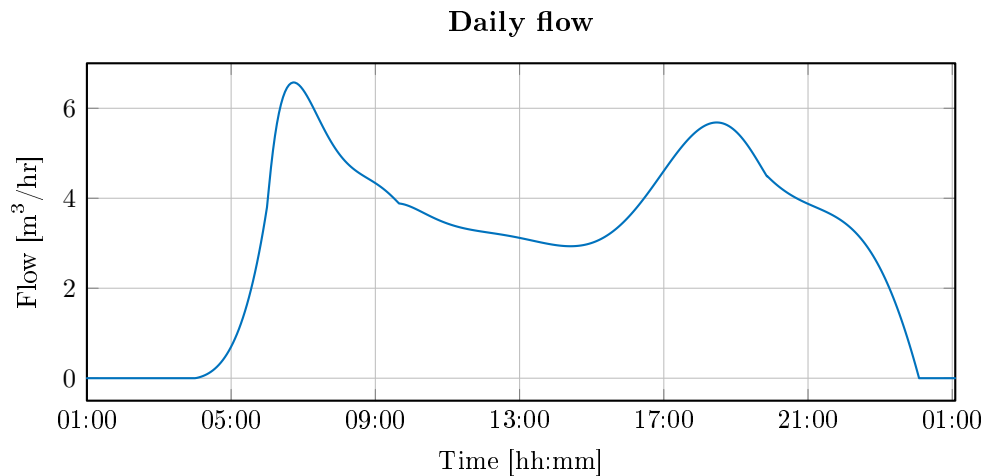


Figure 2.3: Flow profile of residential area 1,1.

Creation of the flow profiles for the various residential and minor industry areas can be found in appendix A.3.

Lastly profiles are needed for the larger industry which counts brewery, bottling plant and the refinery. In figure 2.4 the combined flow from the brewery and bottling plant during 24 hours is seen.

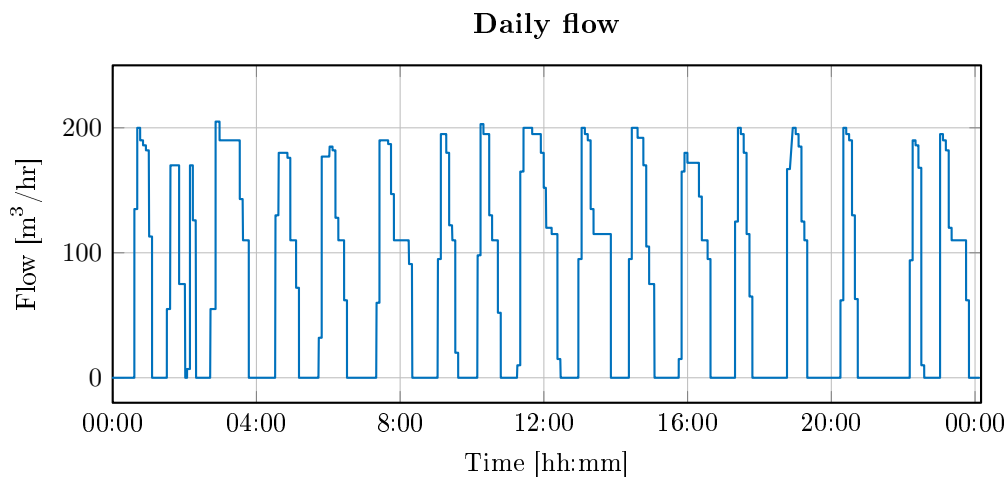


Figure 2.4: Combined outflow from brewery and bottling plant during 24 hours.

From the figure, it can be seen that the combined outflow from the brewery and bottling plant arrives in pulses of up to  $200 \text{ m}^3/\text{hr}$ . The longest pulse last approximately an hour and the shortest approximately 10 minutes. The duration between ranges approximately from three minutes to one and a half hour. This data will be used to create the inflow profile, to the main sewer line, from the industry.

In figure 2.5 the inflow to the WWTP can be seen.

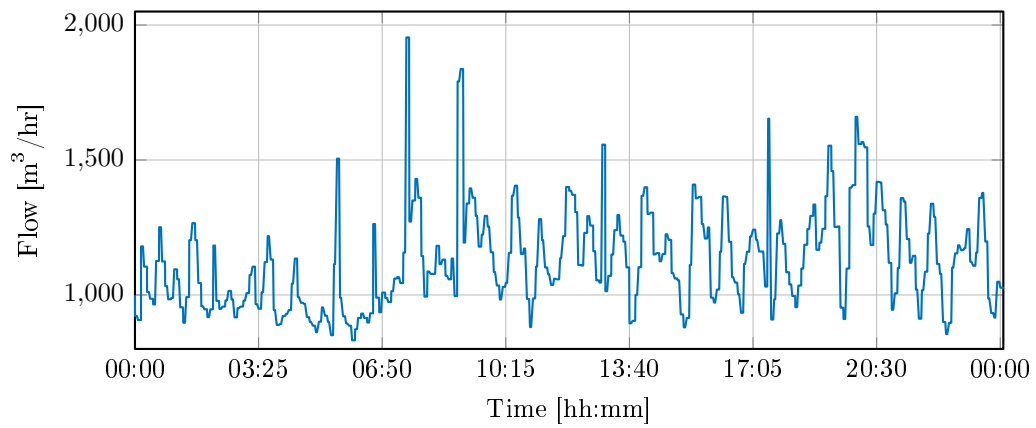


Figure 2.5: Typical dry weather Inflow at Fredericia wastewater treatment plant during 24 hours.

Unfortunately, concentrate measurements were not available from the industry. For that reason, it is decided to lessen the focus on the various chemicals and implement it as a single component. Measurements are available from the inflow to the WWTP, but due to dispersion of the concentrate during transport from the industry to the WWTP, it is not possible to recreate a proper profile for the industry. In appendix A.3 figure A.19, A.20 and A.21 show COD, phosphorus and nitrogen measurements respectively at the inflow of the WWTP.



# Simulation solutions & limitations 3

---

In this chapter, different solutions will be discussed to find a suitable solution, which can be implemented in Fredericia to limit the flow and concentration variations into the WWTP. To limit the variations in flow and concentration into the WWTP, a mechanism is needed to retain wastewater. This could either be done by placing a valve within a pipe that would be able to limit the flow through the pipe or by placing tanks in the sewer network. Using a valve to retain wastewater corresponds to using the pipe as a tank. Depending on the storage capacity of the pipe this could lead to overflow if not controlled properly, and thereby cause wastewater to flow onto streets and into the surrounding environment. This issue was discussed with the wastewater department in Fredericia and they pointed out that storage capacity is limited in sewer pipes due to their dimensions and the constant flow. In this project, it is therefore decided to use one or more tanks as a solution to limit flow and concentration variations into the WWTP. However, the tank must be controlled in a way where overflow in the tank is not permitted.

In addition, from the meeting at Fredericia, it was informed that if tanks are used as a solution it is necessary to keep retention time of the stored wastewater in mind. The reason for this is, that if the wastewater is kept in the tank for a longer period of time, it will start to produce malodorous gas. This is due to oxygen depletion, as the environment in the tank will go from an aerobic to an anaerobic state. The level of dissolved oxygen is something that can be measured, but current sensors require regular maintenance [Emerson, 2009]. Furthermore, complex models of chemical reactions do exist and could be used to predict the level of dissolved oxygen. Due to the delimitation of the concentrate to a single component, further research is not performed on the subject of retention time in tanks. In Denmark sewers are made of concrete and the inner channel is constructed with a circular cross section area [Dansk-betonforening, 2013]. For this reason, the simulation will be limited to work with sewer pipes of this form.



# Modeling 4

---

This chapter will in detail explain the modeling procedure of the various components comprising the sewer system seen in figure 2.1. In the following, methods to model the components such as, flow in gravity sewer lines (section 4.1), transport of concentrate in the wastewater flowing in the main sewer line (section 4.2), interconnections such that disturbances can be added to the main sewer line (section 4.3) and tanks in the sewer network (section 4.4) are described.

## 4.1 Hydraulics of sewer line

A method to model the hydraulics of gravity sewer lines is explained in the following.

Modeling fluids are almost always done by considering it as a control volume. The reason is that it is rarely efficient, computational wise, or possible to consider the individual fluid particles. Henceforth the control volume will be denoted by the letter  $\Omega$  which will correspond to some amount of fluid in a length of a sewer line.

The open channel flow in gravity sewer lines can be described by the Saint-Venant equations which give an expression for conservation of mass and momentum. Some assumptions are made when deriving the Saint-Venant equations [Schütze et al., 2011]:

1. The flow in the channel is one dimensional and prismatic, and as such any curvature or change in the width of the sewer line is considered negligible.
2. Fluid in the sewer line is considered incompressible.
3. The pressure is assumed hydrostatic.
4. The only forces considered is friction, pressure and gravity.
5. The water height and velocity is uniform in the cross section and only changes horizontally i.e. turbulence in the fluid is not considered.
6. The slope of the channel bed is small.

**Continuity** equation for conservation of mass gives an expression for the amount of fluid flowing into and out of the control volume plus the fluid stored in it. In figure 4.1 a flow in a channel is shown.

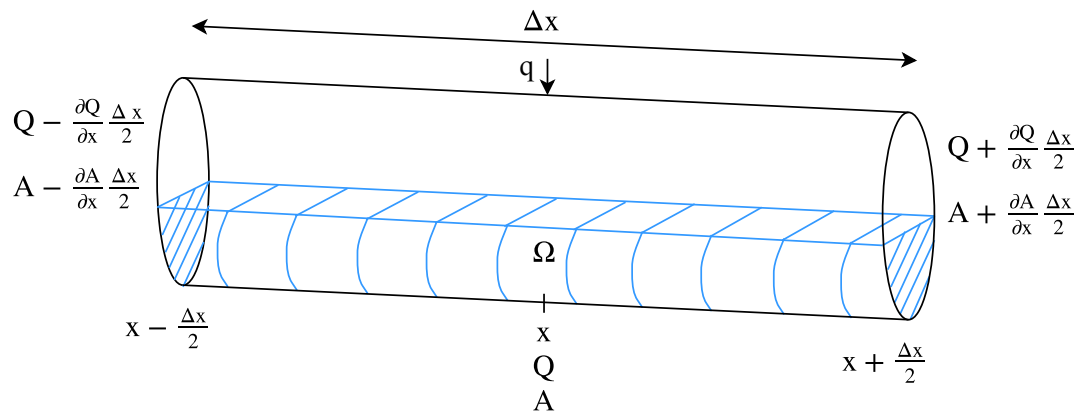


Figure 4.1: Illustration of a control volume,  $\Omega$ , of fluid in a sewer pipe, where  $Q$  is flow into the end of the channel,  $q$  is lateral flow into the channel and  $A$  is the cross section area of the flow.

In figure 4.1, the flow and the cross section area of it, also know as wetted area, is dependent on time and position.

Flow into the control volume, where  $Q$  is the flow considered from the middle of the control volume, is given as:

$$Q_{in} \cdot \Delta t = \left( Q - \frac{\partial Q}{\partial x} \cdot \frac{\Delta x}{2} \right) \cdot \Delta t + q \cdot \Delta x \cdot \Delta t \quad (4.1)$$

Where  $q$  is lateral inflow across the entire channel [ $m^2/s$ ] and  $Q$  is the flow in the channel [ $m^3/s$ ]. Lateral inflow could e.g. come from adjoining sewer pipes or gutter drain. The discharge flow of the channel is given as:

$$Q_{out} \cdot \Delta t = \left( Q + \frac{\partial Q}{\partial x} \frac{\Delta x}{2} \right) \cdot \Delta t \quad (4.2)$$

Average change in the stored fluid in the channel is given as:

$$\begin{aligned} \frac{\partial}{\partial t} \left( \Delta x \cdot \frac{A - \frac{\partial A}{\partial x} \frac{\Delta x}{2} + A + \frac{\partial A}{\partial x} \frac{\Delta x}{2}}{2} \right) \cdot \Delta t &= \frac{\partial}{\partial t} \left( \Delta x \frac{2A}{2} \right) \cdot \Delta t \\ &= \frac{\partial A}{\partial t} \cdot \Delta x \cdot \Delta t \end{aligned} \quad (4.3)$$

As the flow into the channel minus the flow out is equal to the change in the stored fluid in the channel, then due to the assumption of incompressible fluid and uniformity, the following can be written:

$$Q_{in} \cdot \Delta t - Q_{out} \cdot \Delta t = \frac{\partial A}{\partial t} \cdot \Delta x \cdot \Delta t \quad (4.4)$$

Inserting equations 4.1 and 4.2 in 4.4 the following is obtained:

$$\begin{aligned} \left( Q - \frac{\partial Q}{\partial x} \cdot \frac{\Delta x}{2} \right) \cdot \Delta t + q \cdot \Delta x \cdot \Delta t - \left( Q + \frac{\partial Q}{\partial x} \frac{\Delta x}{2} \right) \cdot \Delta t &= \frac{\partial A}{\partial t} \cdot \Delta t \cdot \Delta x \\ \Downarrow & \\ q \cdot \Delta x \cdot \Delta t - \frac{\partial Q}{\partial x} \cdot \Delta x \cdot \Delta t &= \frac{\partial A}{\partial t} \cdot \Delta t \cdot \Delta x \end{aligned} \quad (4.5)$$

Equation 4.5 can be reduced to the following by isolating and dividing with  $\Delta x$  and  $\Delta t$ , on both sides, yielding the mass conservation part of the Saint-Venant equations.

$$\frac{\partial A(x, t)}{\partial t} + \frac{\partial Q(x, t)}{\partial x} = q(x, t) \quad (4.6)$$

For channel flows without lateral input the mass conservation is given as:

$$\boxed{\frac{\partial A(x, t)}{\partial t} + \frac{\partial Q(x, t)}{\partial x} = 0} \quad (4.7)$$

**Momentum** of the control volume  $\Omega$  shown in figure 4.2 can be found by utilizing Newtons second law which states that force is equal to mass times acceleration. Basically this means that the momentum of the control volume can be found by integrating the sum of forces in the following differential equation:

$$\frac{d\mathcal{M}(t)}{dt} = \sum_i F_i(t) \quad (4.8)$$

Where  $\mathcal{M}(t)$  is the momentum, given as mass times a velocity vector, of the control volume at time  $t$  and  $F_i(t)$  is the various external forces affecting the control volume. The forces are given by the various hydrodynamic and hydrostatic effects which affect the control volume.

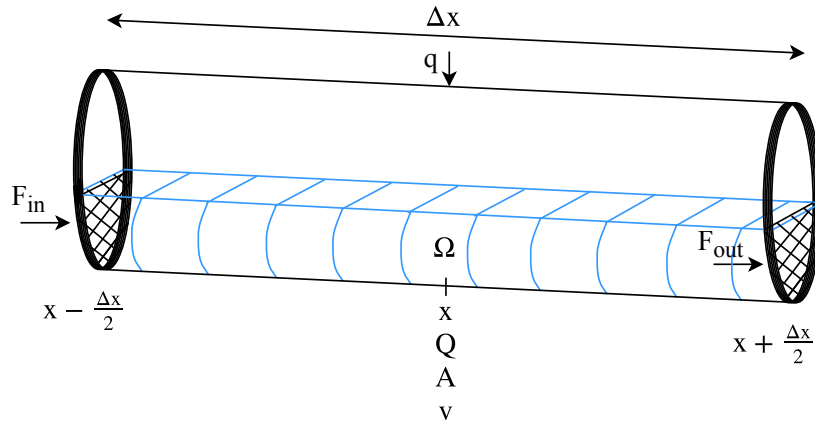


Figure 4.2: Illustration of the control volume  $\Omega$ , where the marked end pieces illustrates infinitely small slices, and  $v$  is the velocity.

If an infinitely small slice of the cross section in the control volume is considered, illustrated at the ends of the pipe in figure 4.2, and utilizing the product rule on the hydrodynamic force acting on the slice, the following is obtained:

$$F = \frac{d\mathcal{M}}{dt} = \frac{d(M \cdot v)}{dt} = M \cdot \frac{dv}{dt} + \frac{dM}{dt} \cdot v \quad (4.9)$$

Where  $M$  is the mass of the control volume. The term  $dM/dt$  is the mass in an infinitely small slice of the control volume, and  $v$  is the velocity of this slice into the control volume. Due to the assumption of incompressible fluid in the control volume the mass derivative term in equation 4.9 can be rewritten to:

$$\frac{dM}{dt} = \rho \frac{dV}{dt} = \rho \cdot Q \quad (4.10)$$

If assuming static speed then the acceleration term can be neglected. By inserting equation 4.10 into equation 4.9 the force, given by the slice of fluid particles, can be written as:

$$F = \rho \cdot Q \cdot v \quad (4.11)$$

The hydrodynamic force given, by the in- and output of fluid particles in the control volume, when considering a slice of fluid particles at the center of the control volume, is given as:

$$F_{in} = \rho \cdot v \cdot Q - \frac{\partial}{\partial x}(\rho \cdot v \cdot Q) \cdot \frac{\Delta x}{2} \quad (4.12)$$

$$F_{out} = \rho \cdot v \cdot Q + \frac{\partial}{\partial x}(\rho \cdot v \cdot Q) \cdot \frac{\Delta x}{2} \quad (4.13)$$

Where subscript "in" denote the force going in through the left side of the channel in figure 4.2 and subscript "out" is the force going out of the right side. The change of particle momentum in the control volume is given as  $F_{in} - F_{out}$  and by replacing velocity with  $Q/A$  the following is obtained:

$$\underbrace{\rho \cdot \frac{Q}{A} \cdot Q - \frac{\partial}{\partial x} \left( \rho \cdot \frac{Q}{A} \cdot Q \right) \cdot \frac{\Delta x}{2}}_{F_{in}} - \underbrace{\left( \rho \cdot \frac{Q}{A} \cdot Q + \frac{\partial}{\partial x} \left( \rho \cdot \frac{Q}{A} \cdot Q \right) \cdot \frac{\Delta x}{2} \right)}_{F_{out}} \quad (4.14)$$

$$= -\rho \frac{\partial}{\partial x} \frac{Q^2}{A} \Delta x$$

The remaining to be found are the forces imposed by gravity, friction and pressure. The force applied by gravity is given as:

$$F_g = \sin(\theta) \cdot g \cdot \rho \cdot \Delta x \cdot A \quad (4.15)$$

Where the slope of the pipe bed  $S_b = \tan(\theta) \approx \sin(\theta)$  for small values of  $\theta$  yields:

$$F_g = S_b \cdot g \cdot \rho \cdot \Delta x \cdot A \quad (4.16)$$

The friction force can be set up as:

$$F_f = S_f \cdot g \cdot \rho \cdot \Delta x \cdot A \quad (4.17)$$

Where  $S_f$  is a friction coefficient. This coefficient can be estimated by different formulas like Manning's or Darcy-Weisbach formula which is seen in equation 4.18 and 4.19 respectively.

$$S_f = \frac{n^2 Q^2}{A^2 R^{4/3}} = \frac{n^2 v^2}{R^{4/3}} \quad (4.18)$$

$$S_f = \frac{fQ^2}{8gRA^2} = \frac{fv^2}{8gR} \quad (4.19)$$

Where  $n$  is Manning's roughness factor [ $\frac{s}{m^{1/3}}$ ],  $f$  is the Weisbach resistance coefficient [ $\cdot$ ] and  $R$  is the hydraulic radius [ $m$ ] given as the wetted area divided by the wetted perimeter [Mays, 2001]. The Weisbach resistance coefficient is found by the Colebrook-White formula seen in equation 4.20.

$$\frac{1}{\sqrt{f}} = -2 \cdot \log \left( \frac{k}{14.84 \cdot R} + \frac{2.52}{4Re\sqrt{f}} \right) \quad (4.20)$$

Where  $k$  is a pipe roughness coefficient and  $Re$  is the Reynolds number.

Last the pressure forces on the x component of the control volume to be found is shown as  $F_{P1}$ - $F_{P3}$  in figure 4.3.

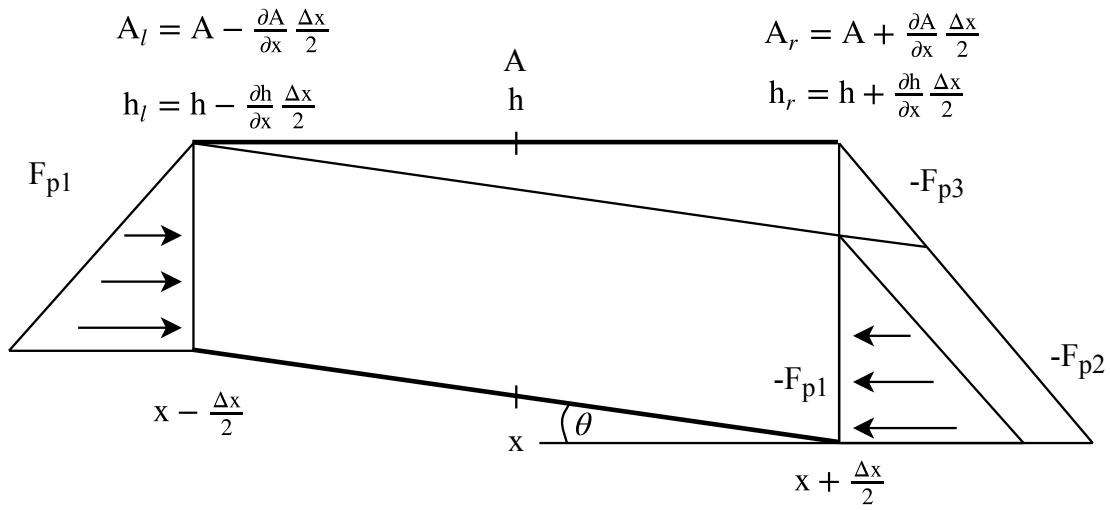


Figure 4.3: Pressure forces acting on a control volume.

By assuming hydrostatic pressure, the pressure in a height,  $z$ , above the bottom of the channel, is given as  $g\rho(h-z)$ , where  $h$  is the height of the fluid. The pressure force acting on the left side of the control volume is given as:

$$F_{P1} = \int_0^{h_l} \rho \cdot g(h_l - z) \cdot b(z) dz \quad (4.21)$$

Where  $h_l$  is the fluid height at the left side of the control volume,  $b(z)$  is the width of the channel given the height  $z$ . The force acting on the right side of the control volume is given as:

$$\begin{aligned} - \int_0^{h_r} \rho \cdot g \cdot (h_r - z) \cdot b(z) dz &= - \int_0^{h_l} \rho \cdot g \cdot (h_l - z) \cdot b(z) dz \\ &\quad - \int_0^{h_l} \rho \cdot g \cdot (h_r - h_l) \cdot b(z) dz \\ &\quad - \int_{h_l}^{h_r} \rho \cdot g \cdot (h_r - z) \cdot b(z) dz \\ &= - F_{P1} - F_{P2} - F_{P3} \end{aligned} \quad (4.22)$$

The pressure force acting on the right side, at a height  $h_l$  from the channel bed, is given by  $F_{P1}$  and  $F_{P2}$ . The remaining force  $F_{P3}$  is given by the height difference from  $h_l$  to  $h_r$ . The force  $F_{P2}$  is given as:

$$\begin{aligned} F_{P2} &= \int_0^{h_l} \rho \cdot g \cdot (h_r - h_l) \cdot b(z) dz \\ &= \int_0^{h_l} \rho \cdot g \cdot \left( h + \frac{1}{2} \frac{\partial h}{\partial x} - \left( h - \frac{1}{2} \frac{\partial h}{\partial x} \right) \right) \cdot b(z) dz \\ &= \rho g \frac{\partial h}{\partial x} \Delta x A_l \end{aligned} \quad (4.23)$$

The remaining pressure force, resulting from the height difference between  $h_l$  and  $h_r$ , is to be found. If, as a result of a small angle, it is assumed that the difference in height at each side is infinitely small. Then the force  $F_{P3}$  is given as:

$$\begin{aligned} F_{P3} &= \int_{h_l}^{h_r} \rho \cdot g \cdot (h_r - z) \cdot b(z) dz \\ &\approx \rho \cdot g \cdot b(h) \cdot \left[ h_r \cdot z - \frac{z^2}{2} \right]_{h_l}^{h_r} \\ &= \rho \cdot g \cdot b(h) \cdot \left( h_r \cdot (h_r - h_l) + \frac{1}{2} \left( \frac{\partial h}{\partial x} \cdot \Delta x \right)^2 \right) \\ &\approx \rho \cdot g \cdot b(h) \cdot \frac{1}{2} \left( \frac{\partial h}{\partial x} \Delta x \right)^2 \end{aligned} \quad (4.24)$$

Taking the sum of forces from equations 4.21 and 4.22:

$$\begin{aligned} F_{P1} - F_{P1} - F_{P2} - F_{P3} &= -\rho g \frac{\partial h}{\partial x} \Delta x A_l - \rho g b(h) \frac{1}{2} \left( \frac{\partial h}{\partial x} \Delta x \right)^2 \\ &= -\rho \cdot g \cdot \frac{\partial h}{\partial x} \cdot \Delta x \left( A_l + \frac{1}{2} b(h) \frac{\partial h}{\partial x} \Delta x \right) \\ &= -\rho \cdot g \cdot \frac{\partial h}{\partial x} \cdot \Delta x \left( A_l + \frac{1}{2} \frac{\partial A}{\partial x} \Delta x \right) \\ &= -\rho \cdot g \cdot \frac{\partial h}{\partial x} \cdot \Delta x \cdot A \end{aligned} \quad (4.25)$$

By summing all the forces from equation 4.14, 4.15, 4.17 and 4.25 and inserting them into equation 4.8 the following is obtained:

$$\begin{aligned} -\sum_i F_i &= -\frac{\partial}{\partial x} \rho \frac{Q^2}{A} \Delta x \\ &\quad - S_b \cdot g \cdot \rho \cdot \Delta x \cdot A \\ &\quad - S_f \cdot g \cdot \rho \cdot \Delta x \cdot A \\ &\quad - \rho \cdot g \cdot \frac{\partial h}{\partial x} \cdot \Delta x \cdot A \end{aligned} \quad (4.26)$$

Lastly the time derivative expression of the momentum, which is given by mass times velocity, are:

$$\frac{dM(t)}{dt} = \frac{\partial}{\partial t} \left( \rho \cdot A \cdot \Delta x \cdot \frac{Q}{A} \right) \quad (4.27)$$

Where mass is given by  $\rho \cdot A \cdot \Delta x$  and velocity by  $Q/A$ .

Having obtained expressions for equation 4.27 and equation 4.26 they can be inserted into equation 4.8 yielding the following expression:

$$\begin{aligned} \frac{\partial}{\partial t}(\rho \frac{Q}{A} A \cdot \Delta x) = & - \frac{\partial}{\partial x} \rho \frac{Q^2}{A} \Delta x \\ & - S_b \cdot g \cdot \rho \cdot \Delta x \cdot A \\ & - S_f \cdot g \cdot \rho \cdot \Delta x \cdot A \\ & - \rho \cdot g \cdot \frac{\partial h}{\partial x} \cdot \Delta x \cdot A \end{aligned} \quad (4.28)$$

Dividing with  $g \cdot \rho \cdot \Delta x \cdot A$  and isolating, then the following definition of the equation is obtained:

$$\boxed{\frac{1}{gA} \frac{\partial Q}{\partial t} + \frac{1}{gA} \frac{\partial}{\partial x} \left( \frac{Q^2}{A} \right) + \frac{\partial h}{\partial x} + S_f - S_b = 0} \quad (4.29)$$

Some or all of the terms in equation 4.29 can be utilized when simulating free channel flow. An overview of the limitations when excluding parts of the momentum equation is given in table 4.1.

Approximation	Kinematic wave (1)	Noninertia wave (2)	Quasi-steady dynamic wave (3)	Dynamic wave (4)
Momentum equation	$S_b = S_f$	$\frac{\partial h}{\partial x} = S_b - S_f$	$\frac{1}{gA} \frac{\partial}{\partial x} \left( \frac{Q^2}{A} \right) + \frac{\partial h}{\partial x} = S_b - S_f$	Equation 4.29
Boundary conditions required	1	2	2	2
Account for downstream backwater effect and flow reversal	No	Yes	Yes	Yes
Damping of flood peak	No	Yes	Yes	Yes
Account for flow acceleration	No	No	Only convective acceleration	Yes

Table 4.1: Limitations when excluding, 1.(inertia and pressure terms), 2.(inertia terms), 3.(pressure term relating to local acceleration) and 4.(none), from the momentum equation [Mays, 2001].

The kinematic wave is the simplest approximation and ignores the terms representing changes in inertia and pressure by assuming that the slope of the water surface is identical to that of the channel bed. Furthermore, only one boundary condition is needed, meaning that only the upper boundary of the channel is needed to solve the Saint-Venant equations. Some considerations are needed when utilizing this approximation. Due to the simplicity of the kinematic wave approximation, attenuation, which occurs in a real free flowing channel,

should not be present. But due to numerical damping, which is induced because of the nature of discretization, it occurs. Some wrongfully attempts to mitigate it by choosing smaller steps of  $\Delta x$  and  $\Delta t$ . Instead, they should be chosen such that the simulated channel flow mimics that of the real channel. Due to its simplicity, the kinematic wave approximation has been used and researched extensively. If the back water effect is not an issue the kinematic wave approximation is often used when dealing with simulation of flows in sewer lines. Furthermore, it is decided to disregard lateral input, i.e. gutter drains or other inputs between ends of the pipe are not taken into consideration. Instead, side input into the main sewer line is assumed attached at the start of the pipe section as shown in figure 2.2 and table 2.1. Further details of modeling sewer interconnection can be found in section 4.3.

## 4.2 Transport of concentrate

A model for transport of concentrate in sewer pipes is obtained in the following. The following assumptions are made obtaining the transport equation.

1. The flow of concentrate is assumed to be steady and uniform in the cross section.
2. The anoxic, anaerobic or aerobic processes occurring in the sewer line is neglected

In figure 4.4 a control volume is seen.

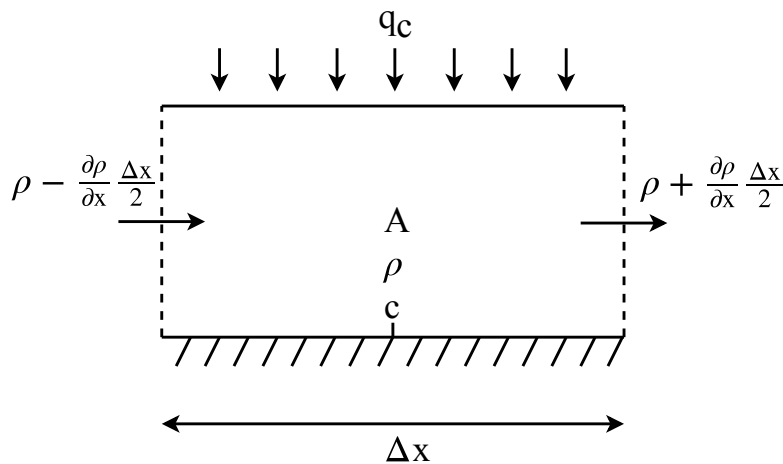


Figure 4.4: Illustration of a control volume containing concentrate.

The conservation of concentrate in the control volume is as in section 4.1 dependent on the change in stored mass and change in flow. This means that the equation for conservation of mass given by equation 4.6, which is shown below, can be utilized.

$$\frac{\partial A}{\partial t} + \frac{\partial Q}{\partial x} = q \quad (4.30)$$

Assuming average concentrate,  $C$ , across the control volume, and multiplying it with the terms of the continuity equation, the following is obtained:

$$\frac{\partial A \cdot C}{\partial t} + \frac{\partial \phi}{\partial x} = q \cdot C_{lat} \quad (4.31)$$

Where  $\phi$  is a flux [ $\frac{g}{s}$ ] term replacing the flow term,  $Q$  and  $C_{lat}$  is lateral concentrate input into the control volume [ $\frac{g}{m^3}$ ] [Vestergaard, 1989].

Depending on the desired approximation the flux and lateral inflow terms can be expanded. The expanded lateral term describes a dead zone at the bottom of the channel, which can be useful to model if dealing with rugged channel bed. Due to the prismatic assumption, in section 4.1 of the sewer channel, the dead zone in the channel is not investigated further. Flux terms describing convective flow and dispersion can be seen in table 4.2.

Approximation	Convective flow	Convective + (dispersion)
Flux term	$\phi = Q \cdot C$	$\phi = Q \cdot C + (-\epsilon \cdot A \frac{\partial C}{\partial x})$
boundary conditions required	1	2

Table 4.2: Table of convective flux term without and with dispersion where  $Q$  is flow,  $C$  is concentrate,  $A$  is area and  $\epsilon$  is a dispersion coefficient [ $\frac{m^2}{s}$ ] [Vestergaard, 1989] .

The dispersion term shown in the above table, also known as Fickian diffusion, gives an expression for how the molecules of the concentrate are spreading. On a molecular level, the concentrate will to some degree disperse upstream and downstream as shown in figure 4.5.

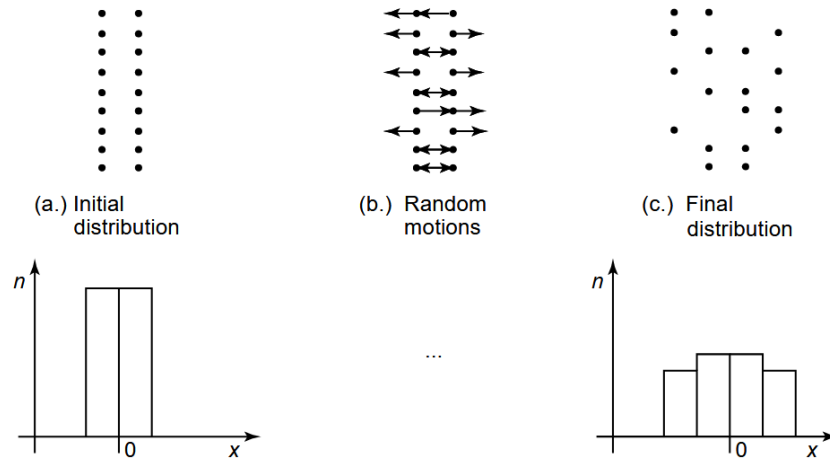


Figure 4.5: Illustration of distribution of convective flow without dispersion (a) and with (c), where dots illustrate molecules of the concentrate within a control volume [Institute of hydromechanics, ].

For various concentrates the dispersion coefficient  $\epsilon$  which varies with temperature can be found in lookup tables [Institute of hydromechanics, ].

Inserting the terms in table 4.2 into equation 4.31 then the following expressions of the continuity equation is obtained:

$$\frac{\partial(A \cdot C)}{\partial t} + \frac{\partial(Q \cdot C)}{\partial x} - \epsilon \cdot \frac{\partial^2(A \cdot C)}{\partial x^2} = q \cdot C_{lat} \quad (4.32)$$

$$\frac{\partial(A \cdot C)}{\partial t} + \frac{\partial(Q \cdot C)}{\partial x} = q \cdot C_{lat} \quad (4.33)$$

In closed environments such as sewers longitudinal dispersion can often be neglected [Vestergaard, 1989]. For this reason and to reduce complexity of the simulation, equation 4.33 is utilized further on. As the change in flow and area in the channel is solved by the Saint-Venant equations, an expression which only considers a change in concentrate suffices. The terms in equation 4.33 can be rewritten to the following:

$$C \cdot \frac{\partial A}{\partial t} + A \cdot \frac{\partial C}{\partial t} + C \cdot \frac{\partial Q}{\partial x} + Q \cdot \frac{\partial C}{\partial x} = q \cdot C_{lat} \quad (4.34)$$

Multiplying equation 4.30 with C yields:

$$C \cdot \frac{\partial A}{\partial t} + C \cdot \frac{\partial Q}{\partial x} = q \cdot C \quad (4.35)$$

Subtracting equation 4.35 from 4.34 then results in the following:

$$A \cdot \frac{\partial C}{\partial t} + Q \cdot \frac{\partial C}{\partial x} = q \cdot (C_{lat} - C) \quad (4.36)$$

Neglecting lateral flow and concentration inputs the following expression is obtained:

$$\boxed{A \cdot \frac{\partial C}{\partial t} + Q \cdot \frac{\partial C}{\partial x} = 0} \quad (4.37)$$

Equation 4.37 can thereby be solved with the solutions of Q and A obtained from the Saint-Venant equations.

### 4.3 Sewer interconnection

This section will explain the scheme on how pipes are interconnected and the concentration is mixed. To limit complexity the following assumptions are made during the modeling of interconnections.

1. Turbulence caused by vertical inflow is neglected.

In figure 4.6 an illustration of two interconnected pipes is seen.

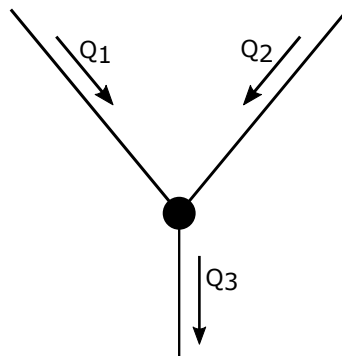


Figure 4.6: Illustration of an interconnection between two flow inputs and one output.

As any turbulence is neglected, when the two flows join, the flow into pipe three is given as:

$$\boxed{Q_3 = Q_1 + Q_2} \quad (4.38)$$

As the concentrate level depends on flow, i.e.  $Q \cdot C$ , it can be derived by the following equation:

$$\begin{aligned} Q_3 \cdot C_3 &= Q_1 \cdot C_1 + Q_2 \cdot C_2 \\ \Downarrow \\ C_3 &= \frac{C_1 Q_1 + C_2 Q_2}{Q_3} \end{aligned} \quad (4.39)$$

Inserting equation 4.38 into 4.39 the following is obtained for the combined concentrate level of the interconnected pipes.

$$\boxed{C_3 = \frac{C_1 \cdot Q_1 + C_2 \cdot Q_2}{Q_1 + Q_2}} \quad (4.40)$$

The two equations for flow and concentrate does not reflect a real interconnection of two flows, but it is assumed to be acceptable on the ground of the assumptions made in section 4.1 and 4.2.

## 4.4 Tank model

In this section, a model for flow and concentrate is derived for a tank. The assumptions made deriving the tank model is:

1. Turbulence, caused by in- or output in the tank, is neglected.
2. Level of concentrate of the fluid in the tank is considered uniform, meaning mixing with the new inflow occurs instantly.

In figure 4.7 an illustration of a tank is shown.

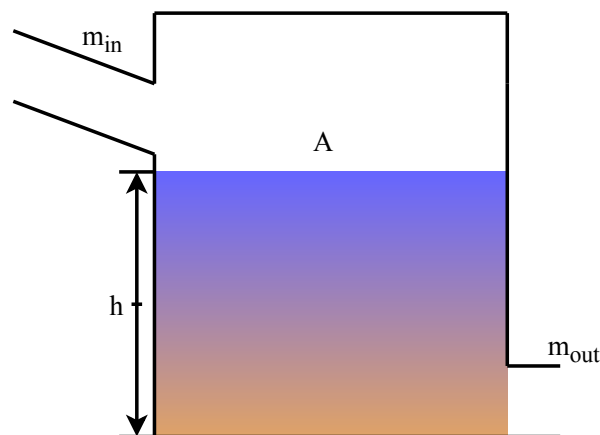


Figure 4.7: Illustration of a tank.

The illustration will be used to derive the model for the tank. From the left, a pipe that discharges fluid into the tank is shown. The fluid going into the tank has a mass flow rate  $m_{in}$  [kg/s]. At the bottom right, the fluid is discharged from the tank with a mass flow rate,  $m_{out}$ . Within the tank the height of the stored fluid is dependent on horizontal cross-section area and the mass in- and outflow. The mass balance equation is derived in [Vojtesek et al., ] and is given as:

$$\frac{dM_{cv}(t)}{dt} = m_{in}(t) - m_{out}(t) \quad (4.41)$$

Where  $M_{cv}$  is the total mass within the control volume [kg], and  $m_{in}$  and  $m_{out}$  is the mass in and outflow rate of the tank [kg/s]. The mass balance can be written as  $M_{cv} = \rho Ah$  where  $\rho$  is the density [kg/m<sup>3</sup>], A is the area [m<sup>2</sup>] and h is the height [m]. The mass flow rate can be written as  $m = \rho Q$ , where Q is the flow [m<sup>3</sup>/s]. Inserting this into equation 4.41 the following is obtained:

$$\frac{d(\rho Ah(t))}{dt} = \rho Q_{in}(t) - \rho Q_{out}(t) \quad (4.42)$$

By assuming incompressible fluid such that density is constant then the in- and outflow can be isolated.

$$\rho A \frac{dh(t)}{dt} = \rho (Q_{in}(t) - Q_{out}(t)) \quad (4.43)$$

Simplifying equation 4.43 by dividing with  $\rho A$ :

$$\frac{dh(t)}{dt} = \frac{1}{A} (Q_{in}(t) - Q_{out}(t)) \quad (4.44)$$

This equation describes the change in height according to in- and outflow. Due to the nature of a sewer system, it is typically not possible to implement a tank where the outflow is controlled by gravity and a valve. For this reason, it is decided to implement an actuator in the form of a pump within the tank, which control the output flow into the adjoining pipe. In figure 4.8 the chosen tank setup is seen.

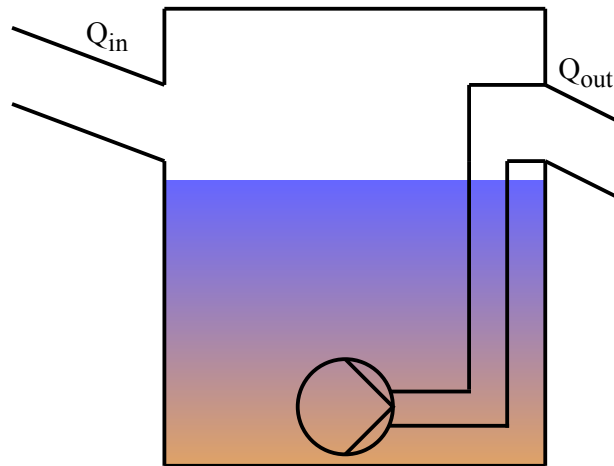


Figure 4.8: Illustration of a tank with a pump inserted to regulate the output flow.

Due to the nature of free flow in pipes, the dynamics of the pump will be mitigated for longer pipes. For this reason, it is decided to disregard pump dynamics and implement a simple linear term where an actuator input controls the output flow.

$$Q_{out}(t) = u(t) \cdot \bar{Q} \quad (4.45)$$

Where  $u$  is pump control input and  $\bar{Q}$  is a fixed operating point which for example could be the maximum flow of the adjoining pipe. By inserting equation 4.45 into equation 4.44 the following is obtained:

$$\boxed{\frac{dh(t)}{dt} = \frac{1}{A} (Q_{in}(t) - u(t) \cdot \bar{Q})} \quad (4.46)$$

Equation 4.46 then gives an expression where a change in height is given as a function of inflow and outflow.

For the concentration part of the tank, there is the ratio of concentrate to consider. At some point, the level of concentrate flowing into the tank might differ from the concentrate level already in the tank. Then as the stored fluid is pumped out of the tank the concentrate level should go towards the inflow concentration. When empty the concentration of the outflow should be equal to the inflow concentration. By the initial assumptions the change in concentration in the tank is given by equation 4.47.

$$\frac{dC_{tank}(t)}{dt} = C_{in}(t) \cdot \frac{Q_{in}(t)}{h(t)} - C_{out}(t) \cdot \frac{Q_{out}(t)}{h(t)} \quad (4.47)$$

As the output concentration is equal to what is in the tank at the current time the following is obtained.

$$\boxed{\frac{dC_{tank}(t)}{dt} = \frac{1}{A} \left( C_{in}(t) \cdot \frac{Q_{in}(t)}{h(t)} - C_{tank}(t) \cdot \frac{Q_{out}(t)}{h(t)} \right)} \quad (4.48)$$

The advantage of this scheme is that flow and height are already known. This keeps the computational power required at a minimum while some realism, in the level of concentrate flowing through the tank, is obtained.

In this chapter, models of gravity sewer, interconnection of sewers, concentration in sewers and a tank are constructed to describe the sewer network seen in figure 2.1. These models will be used in the simulation model that will be explained in the next chapter.



# Simulation 5

---

In this chapter, an overview is given of the design process of the simulation environment. Furthermore, the schemes utilized to be able to simulate the nonlinear parts of the sewage flow, with its various concentrations, is explained. Lastly, the designed environment is implemented and verified. It is decided to utilize MATLAB as the platform to be used for this project. Furthermore, it is assumed that readers are familiar with basic terminology related to MATLAB, and therefore specifics will not be given hereof.

In the following, the basic structure of the simulation and the design of it is explained.

## 5.1 Structure

For the simulation environment to be useful, some basic functionality is needed. The simulation should be easy to setup and adjust if needed. Furthermore, an easy way to view the result of the simulation is needed such that necessary adjustments can easily be made based on the result.

The first overall thing to consider is the composition of components desired to simulate. To make the simulation environment useful it should be able to handle different compositions of pipes and tanks. Meaning that the simulation environment can simulate different setups than the one shown in figure 2.1. For this, a simple setup procedure, where different sizes of pipes with different parameters can be chosen, is needed. The second thing to consider is that the environment should be brought to a steady state before the simulation starts. The reason for this is that unintended results can arise when working with nonlinear systems. Transients caused by the system not to be in a steady state, when starting simulating, can skew the initial data obtained, which is not ideal. Also if a linearized approach to the MPC scheme is chosen a linearized model is necessary, which requires a system in steady state to obtain. The simulation should be able to run for a predefined amount of iterations. Based on this the basic structure of the simulation environment can be split into three parts as shown in figure 5.1.

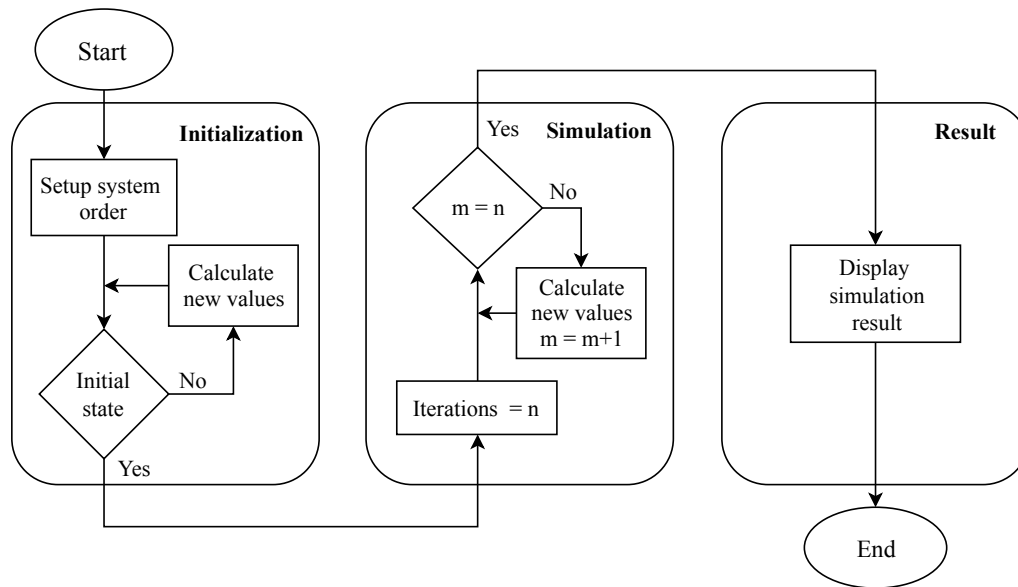


Figure 5.1: Basic overview of simulation environment

The following will go into details, on the thoughts and the considerations made during the design phase, of the three parts shown in the figure.

### Initialization

The initialization process is, as shown in figure 5.1, comprised of several parts. The first part is to set up the desired system of pipes and tanks such that the system is simulated with the chosen components in the right order. Secondly, the system should be brought in to a steady state from which the simulation can start. The reason for this is that the Saint-Venant equations utilized to simulate the flow in the sewer pipes is nonlinear. Because of this, it can be difficult to find a steady state by hand, which do not produce an unintended result when starting simulating. Though it might be possible to find fitting initial values for small setups it is assumed that a larger setup will increase the chance of unintended results when starting simulating.

For the first part, a simple system setup is decided upon, where the desired components are added to a list. The order of the list then decides how the components is connected when simulating. An example of this setup procedure is shown in figure 5.2.

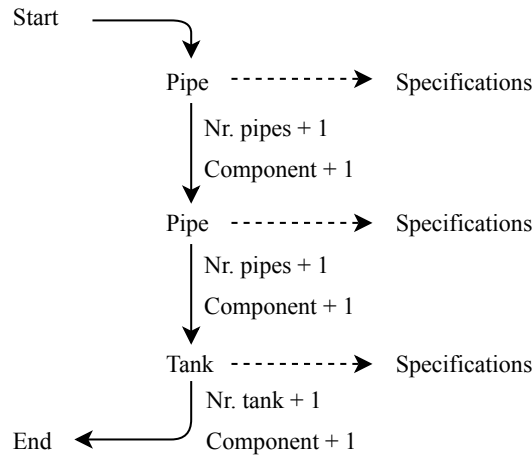


Figure 5.2: Setup scheme of system order initiation.

The specifications for each part in figure 5.2 refers to the parameters needed to run the simulation. The necessary specifications entered for pipe and tank should as a minimum be the required parameters needed to utilize the Preissmann scheme explained in section 5.2 and to simulate in- and outflow of one or more tanks, respectively. Furthermore, constants which are utilized during simulation should be calculated during initialization such that the computational load is kept as low as possible during simulation.

A simple solution to bring the desired system setup to an initial steady state is to give a fixed input flow and iterate. The iteration continues until a satisfactory error between the fixed input and the flow within the designated setup is deemed sufficiently low. For this to work, it is important to have side input or disturbance input in mind. In figure 5.3 a simple setup is shown of a possible setup to be simulated.

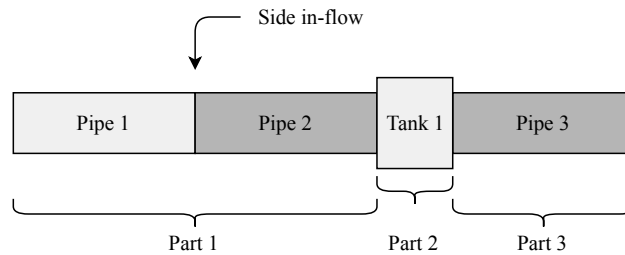


Figure 5.3: Simple setup with three pipes, a tank and a single side input.

To make the steady state iteration scheme work on a dynamic level, the components can be separated into parts where adjoining pipes are seen as a single part. The system can then be brought in to steady state one part at a time. As the pipes are the only nonlinear part of the system, they are the only parts needed to be iterated upon. Taking the first part in figure 5.3 as an example, there are two pipes and the second one has a side input. A general expression of the average flow in the parts containing pipes is given by the following equation:

$$\text{Part-m}_{\text{avg}} = \frac{\sum_{i=1}^n \text{Pipe-input}_i + \text{side inflow}_i}{n_{\text{pipes}}} \quad (5.1)$$

Equation 5.1 can then be used to obtain the desired steady state flow and a current one by utilizing values obtained by solving the Saint-Venant equations. The iteration can then be set to stop when the error between the desired and the measured average is sufficiently low. The next part in figure 5.3 is, in this case, a tank, set to have an in- and outflow equal to the output of the second pipe, which is the combined flow of the first pipe plus the side input. For the third part, the iteration process then starts over with the outflow of the tank as input. As the concentrate flow is depending on the solution of the Saint-Venant equations it is assumed that when the flow is in a steady state the concentrate will have reached steady state as well.

## Simulation

Having obtained a setup in steady state, the next part is to simulate it for the predefined amount of iterations. An important part of the simulation is to store data in a way such that it is easily and intuitively obtainable for purposes such as debugging or customized plots. For this reason, it is decided to store the data, from simulating, into separate blocks. This means that data from individual pipes and tanks should be stored separately in the order given by the initial component setup shown in figure 5.2. In figure 5.4 a simple overview of the simulation procedure is given.

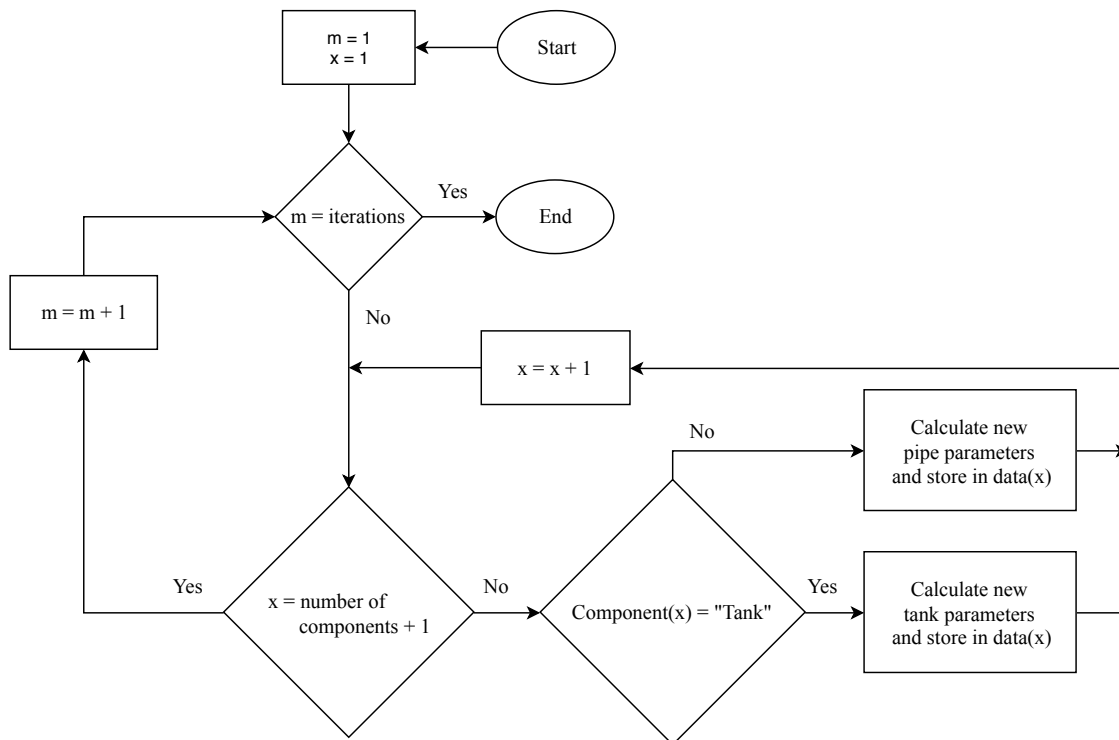


Figure 5.4: Basic overview of the simulation scheme where  $x$  indicates an index going from one to the amount of component in the setup and  $m$  indicates current iteration.

The main idea behind the simulation scheme is to calculate one component at a time and split the calculation of various components into separate functions. This structure

makes it more simple to incorporate new components or insert replacement components if needed further on. A replacement component could e.g. be another scheme to solve the Saint-Venant equations.

## Display result

Having obtained data from simulating the user-defined system an overview of the results is needed. Considerable time can be spent in designing a function which can display the data in various forms. As the data can consist of a large number of components as well as a considerable time span, it can get quite time-consuming to pinpoint parts of interest in time and place. For this reason, it is decided that a solution which can give an overview of the obtained data is needed. The chosen solution is a function which can playback the simulated data at a user defined speed and interval. Furthermore, it should be possible to pause and start the playback at a user-defined iteration. Furthermore, the chosen areas of interest to be displayed is chosen to be flow, height, concentrate and concentrate flow for pipes. Tanks should when present be shown with a split axis on the right side of the flow, height and concentrate pipe plots.

In figure 5.5 an illustration of the solution is seen.

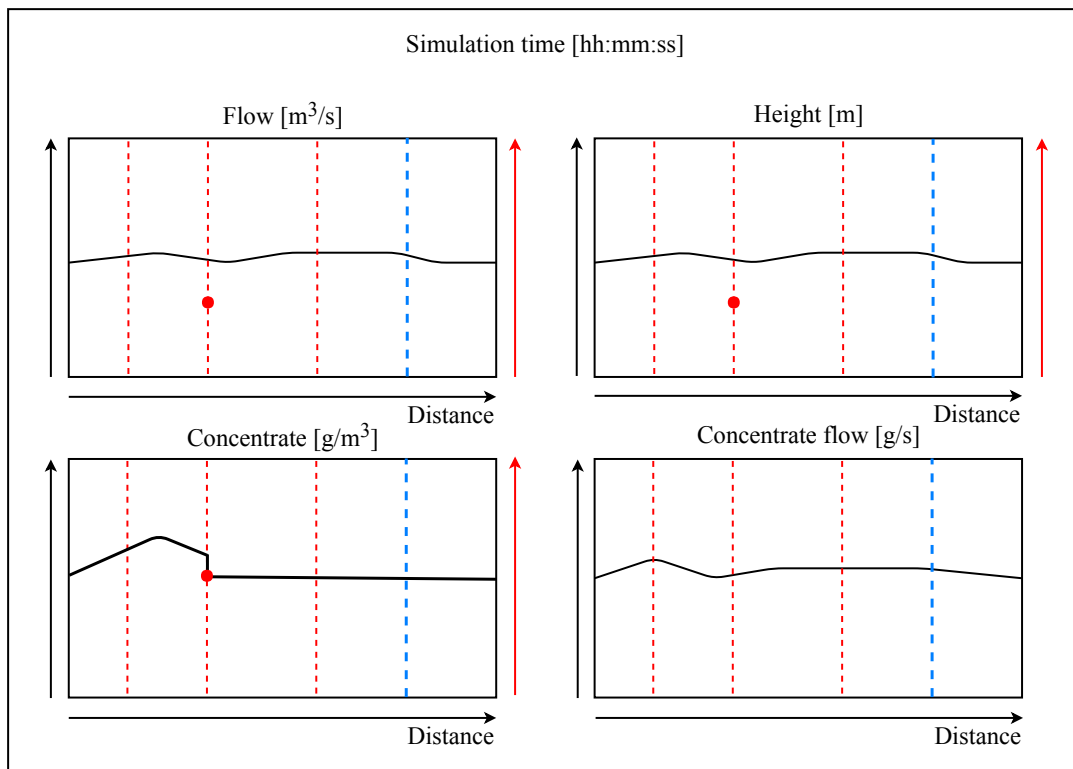


Figure 5.5: Illustration of the desired visual interface for the playback function where flow, height, concentrate and concentrate flow in the sewer network is seen. The red dashed lines indicate interconnection of pipes, the red dot denotes that a tank is placed at that position and the right y-axis indicates height in that tank. The blue dashed line indicates a pipe with side inflow.

The visual interface should make it possible with limited effort to examine the simulation data acquired such that verification or adjustments can be made to the constructed setup. Having outlined the basic details of the construction of the simulation environment the

scheme needed to solve the nonlinear Saint-Venant equations is explained in detail in the next section.

## 5.2 Preissmann scheme

In this section, a numerical method for solving the Saint-Venant equations are chosen and elaborated on. According to table 4.1 various approximations of the momentum equation can be used. Common for the most part of them is that boundary conditions are needed up- and downstream. The problem is that downstream boundary conditions are not always known or require extensive information of the WWTP. It is therefore decided to utilize the kinematic wave approximation, as the hydraulic conditions of the WWTP are considered out of scope for this project.

The numerical method chosen, for solving the Saint-Venant equations, is the Preissmann scheme which is based on the box scheme. Other methods exist such as Lax scheme, Abbot-Ionescu scheme, leap-frog scheme, Vasiliev scheme, however, the Preissmann scheme is known for its robustness. Basically, by using the Preissmann scheme the Saint-Venant equations can be discretized, and thereby utilized to simulate the flow and height throughout a pipe [Cunge et al., 1980].

In section 4.1 the Saint Venant equations for conservation of mass and momentum are derived, they are also shown below.

$$\frac{\partial A(x, t)}{\partial t} + \frac{\partial Q(x, t)}{\partial x} = 0 \quad (5.2)$$

$$\frac{1}{gA} \frac{\partial Q}{\partial t} + \frac{1}{gA} \frac{\partial}{\partial x} \left( \frac{Q^2}{A} \right) + \frac{\partial h}{\partial x} + S_f - S_b = 0 \quad (5.3)$$

In figure 5.6 a single mesh for the Preissmann scheme is illustrated.

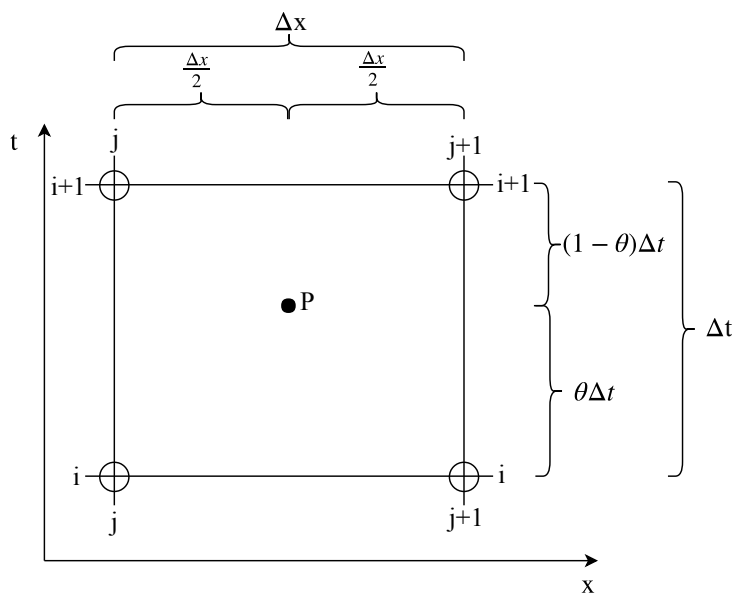


Figure 5.6: Preissmann non-staggered grid scheme.

Where  $\theta$  is a weighting parameter ranging between zero and one,  $j$  is an index of cross section and  $i$  is an index of time. The mesh contains four nodes,  $(j,i)$ ,  $(j+1,i)$ ,  $(j,i+1)$  and  $(j+1,i+1)$ , however in the implementation the dimension of the grid is  $\Delta t \times \Delta x$  for  $0 \leq x \leq L$  and  $0 \leq t$ . Where  $L$  defines the length of the pipe section. The derivatives in equations 5.2 and 5.3 are calculated as an approximation at the point P, which is in the middle of the interval of  $\Delta x$ . The difference between the box scheme and the Preissmann scheme is that the point P should always be located at  $\Delta x/2$ , meaning that the point can only move along the time axis within this mesh by adjusting the weighting parameter  $\theta$ . The effect of this weighting parameter will be elaborated in subsection 5.2.1. An arbitrary function  $f_p(x, t)$  calculated at point P is approximated by [Szymkiewicz, 2010].

$$f_P \approx \frac{1}{2}(\theta \cdot f_j^{i+1} + (1 - \theta)f_j^i) + \frac{1}{2}(\theta \cdot f_{j+1}^{i+1} + (1 - \theta)f_{j+1}^i) \quad (5.4)$$

The numerical approximation for the derivatives in equations 5.2 and 5.3 for time and length are shown below [Szymkiewicz, 2010].

$$\left. \frac{\partial f}{\partial t} \right|_P \approx \frac{1}{2} \left( \frac{f_j^{i+1} - f_j^i}{\Delta t} + \frac{f_{j+1}^{i+1} - f_{j+1}^i}{\Delta t} \right) \quad (5.5)$$

$$\left. \frac{\partial f}{\partial x} \right|_P \approx (1 - \theta) \frac{f_{j+1}^i - f_j^i}{\Delta x} + \theta \frac{f_{j+1}^{i+1} - f_j^{i+1}}{\Delta x} \quad (5.6)$$

The approximations of equation 5.5 and 5.6 can be utilized on the derivative terms in the Saint-Venant equations to achieve the following expressions for equation 5.2 and 5.3 respectively:

$$\theta \frac{Q_{j+1}^{i+1} - Q_j^{i+1}}{\Delta x} + (1 - \theta) \frac{Q_{j+1}^i - Q_j^i}{\Delta x} + \frac{1}{2} \frac{A_{j+1}^{i+1} - A_j^{i+1}}{\Delta t} + \frac{1}{2} \frac{A_j^{i+1} - A_j^i}{\Delta t} = 0 \quad (5.7)$$

$$\begin{aligned} & \frac{1}{gA_p} \left( \frac{1}{2} \left( \frac{Q_{j+1}^{i+1} - Q_j^{i+1}}{\Delta t} + \frac{Q_j^{i+1} - Q_j^i}{\Delta t} \right) \right) + \\ & \frac{1}{gA_p} \left( \frac{\theta}{\Delta x} \left( \left( \frac{Q^2}{A} \right)_{j+1}^{i+1} - \left( \frac{Q^2}{A} \right)_j^{i+1} \right) + \frac{1 - \theta}{\Delta x} \left( \left( \frac{Q^2}{A} \right)_{j+1}^i - \left( \frac{Q^2}{A} \right)_j^i \right) \right) + \end{aligned} \quad (5.8)$$

$$\theta \left( \frac{h_{j+1}^{i+1} - h_j^{i+1}}{\Delta x} \right) + (1 - \theta) \left( \frac{h_{j+1}^i - h_j^i}{\Delta x} \right) +$$

$$S_f - S_b = 0$$

By discretizing the Saint-Venant equations they can be used in a simulation to calculate parameters for the pipe model. The mesh shown in figure 5.6 is used to calculate the value of the node  $(j+1,i+1)$  by knowing the previous values in time and length  $(j,i)$ ,  $(j+1,i)$

and  $(j,i+1)$ . Therefore some initial conditions must be known to be able to calculate the parameters for the pipe at the first iteration. The boundary conditions for the flow, at  $t=0$ , must be known throughout the pipe. Furthermore, the inflow to the pipe for each iteration must be known. This is illustrated with circles in figure 5.7.

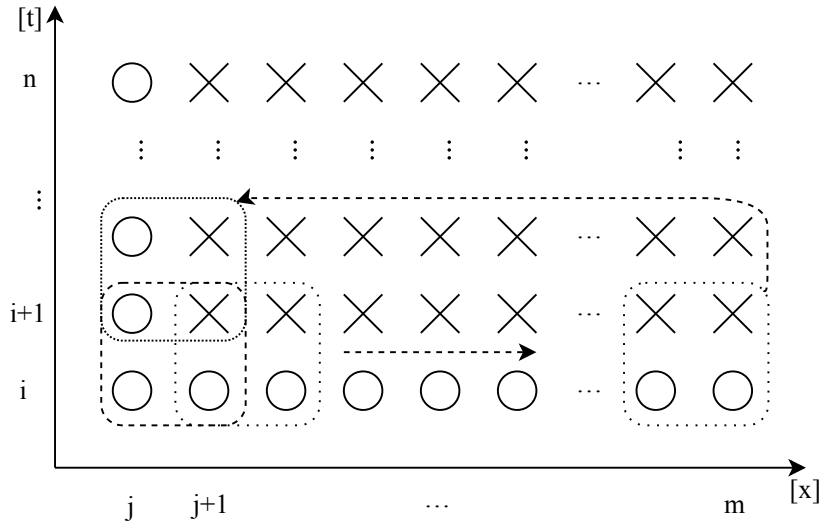


Figure 5.7: Preissmann non-staggered grid scheme example of iteration pattern.

By knowing inflow and specifications of the pipe, area can be calculated at the initialization nodes. With equation 5.7, the flow at  $(j+1,i+1)$  can be calculated by knowing the flow and area at the previous nodes  $(j,i)$ ,  $(j+1,i)$  and  $(j,i+1)$  as illustrated with the box in the left bottom corner in figure 5.7.

The discretized continuity equation, seen below, is solved for the desired flow in equation 5.10,

$$\theta \frac{Q_{j+1}^{i+1} - Q_j^{i+1}}{\Delta x} + (1 - \theta) \frac{Q_{j+1}^i - Q_j^i}{\Delta x} + \frac{1}{2} \frac{A_{j+1}^{i+1} - A_{j+1}^i}{\Delta t} + \frac{1}{2} \frac{A_j^{i+1} - A_j^i}{\Delta t} = 0 \quad (5.9)$$

$$Q_{j+1}^{i+1} = -\frac{1}{2\theta} \cdot (A_{j+1}^{i+1} - H) \cdot \frac{\Delta x}{\Delta t} \quad (5.10)$$

Where H is a parameter containing the previous flows and areas in time and distance, which are known. These have either been calculated or set as boundary conditions as shown in figure 5.7.

$$H = \left( 2 \cdot (1 - \theta) \cdot Q_j^i - 2 \cdot (1 - \theta) \cdot Q_{j+1}^i + 2\theta Q_j^{i+1} \right) \cdot \frac{\Delta t}{\Delta x} - A_j^{i+1} + A_j^i + A_{j+1}^i \quad (5.11)$$

Due to the delimitation to sewer channels with an inner circular cross section and to use the approximated momentum equation for a kinematic wave, the following expression is utilized [Michelsen, 1976].

$$Q = \left( 0.46 - 0.5 \cdot \cos \left( \pi \frac{h}{d} \right) + 0.04 \cdot \cos \left( 2\pi \frac{h}{d} \right) \right) \cdot Q_f \quad (5.12)$$

This equation describes flow in a circular pipe by knowing the diameter ( $d$ ), height ( $h$ ), and flow for a fully filled pipe ( $Q_f$ ) as seen in equation 5.13.

$$Q_f = 72 \cdot \left(\frac{d}{4}\right)^{0,635} \pi \cdot \left(\frac{d}{2}\right)^2 \cdot S_f^{0,5} \quad (5.13)$$

$Q_f$  can be obtained from Manning's equation shown in equation 4.18. The derivation from Manning's equation to equation 5.13 can be seen in appendix A.4.

In equation 5.10 the flow  $Q_{j+1}^{i+1}$  is a function of the unknown area  $A_{j+1}^{i+1}$ , and by subtracting the flow on each side the following is achieved:

$$0 = -Q_{j+1}^{i+1} - \frac{1}{2\theta} \cdot (A_{j+1}^{i+1} - H) \cdot \frac{\Delta x}{\Delta t} \quad (5.14)$$

By naming the right hand side of equation 5.14 for  $V$  yields the following:

$$V = -Q_{j+1}^{i+1} - \frac{1}{2\theta} \cdot (A_{j+1}^{i+1} - H) \cdot \frac{\Delta x}{\Delta t} \quad (5.15)$$

The two unknowns remaining in equation 5.15 is  $Q_{j+1}^{i+1}$  and  $A_{j+1}^{i+1}$ . The flow  $Q_{j+1}^{i+1}$  can be replaced with equation 5.12, which inserted into equation 5.15 gives the following equation:

$$V = -Q_f \cdot \left(0,46 - 0,5 \cdot \cos\left(\pi \frac{h_{j+1}^{i+1}}{d}\right) + 0,04 \cdot \cos\left(2\pi \frac{h_{j+1}^{i+1}}{d}\right)\right) \frac{\Delta t}{\Delta x} - \frac{1}{2\theta} (A_{j+1}^{i+1} - H) \quad (5.16)$$

Inserting  $Q_f$  from equation 5.13 into equation 5.16 yields the following:

$$V = -72 \left(\frac{d}{4}\right)^{0,635} \pi \cdot \left(\frac{d}{2}\right)^2 S_f^{0,5} \cdot \left(0,46 - 0,5 \cdot \cos\left(\pi \frac{h_{j+1}^{i+1}}{d}\right) + 0,04 \cdot \cos\left(2\pi \frac{h_{j+1}^{i+1}}{d}\right)\right) \frac{\Delta t}{\Delta x} - \frac{1}{2\theta} (A_{j+1}^{i+1} - H) \quad (5.17)$$

$V$  is now a function of height  $h_{j+1}^{i+1}$  and  $A_{j+1}^{i+1}$ . Height, being the only unknown parameter for finding the wetted area  $A_{j+1}^{i+1}$ , can be found for a circular pipe by equation 5.18 [Michelsen, 1976].

$$A = \frac{d^2}{4} \cdot \text{acos}\left(\frac{\frac{d}{2} - h}{\frac{d}{2}}\right) - \sqrt{h \cdot (d - h)} \cdot \left(\frac{d}{2} - h\right) \quad (5.18)$$

A numerical solution to obtain height in equation 5.17 is Newton's method. The method is used to find the roots of a real-valued function. The method requires a real-valued function

$f$ , the derivate  $f'$ , and an initial guess  $x_0$  and the approximation is found by the following equation [Szymkiewicz, 2010]:

$$x_1 = x_0 - \frac{f(x_0)}{f'(x_0)} \quad (5.19)$$

Where  $x_1$  is an approximation of a root from the initial guess. Newtons method can be iterated until a sufficiently accurate root is obtained.

$$x_{i+1} = x_i - \frac{f(x_i)}{f'(x_i)} \quad (5.20)$$

To stop the iteration, a tolerance value which stops the iteration can be inserted. When the error between the current approximation and the past is sufficiently low, as shown in equation 5.21.

$$(x_{i+1} - x_i) < \epsilon \quad (5.21)$$

This calculation is performed for each node in the Preissmann scheme, making it an iterative method of obtaining flow in a pipe. In figure 5.8 a flowchart of the Preissmann iterative scheme is seen.

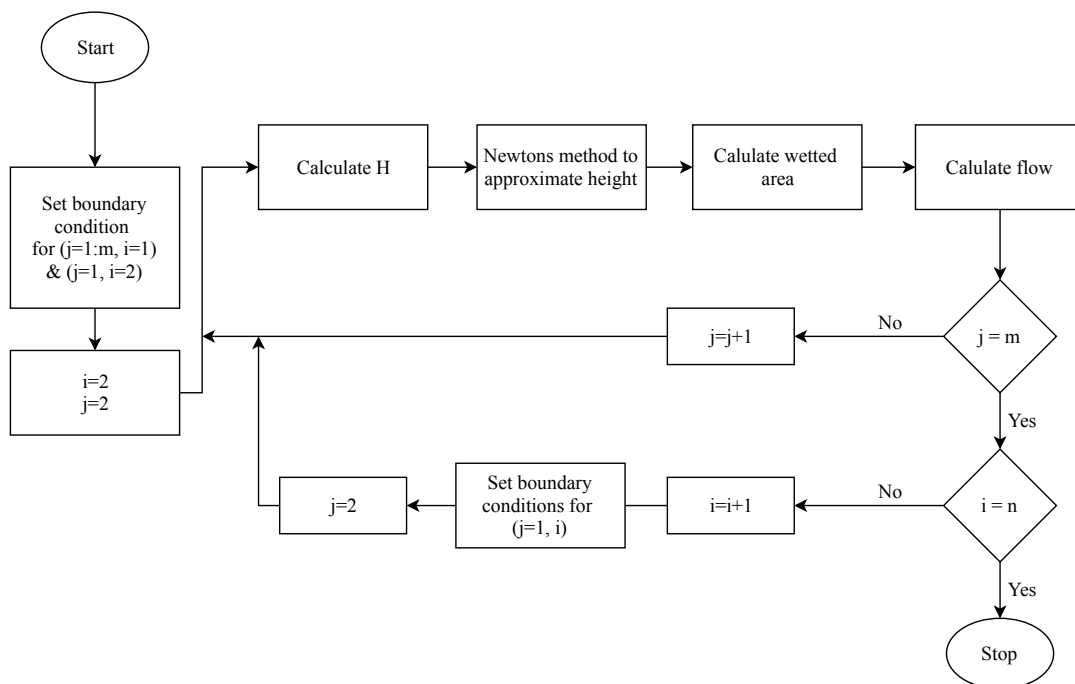


Figure 5.8: Flowchart of the iteration process to calculate the flow in each point.

The iteration scheme starts with setting boundary conditions for flow and height in all sections of the pipe. Thereafter  $i$  and  $j$  are incremented by one before the iteration process starts. The calculation of  $H$ , height, wetted area, and flow are conducted iteratively

throughout the pipe for “m” sections. When the iteration scheme has been through the whole pipe it increments by one in time. This iteration process will go on until “n” time iterations has been performed.

In the following stability and precision for the Preissmann scheme will be elaborated.

### 5.2.1 Stability & Precision

Stability is an important parameter to consider when trying to obtain a solution for nonlinear equations. An advantage of the Preissmann scheme is that if the parameter  $\theta$  is chosen  $0.5 \leq \theta \leq 1$ , then stability is unconditionally guaranteed [Cunge et al., 1980]. But guaranteed stability does not necessarily mean precision in the obtained solution. An accurate solution can be found when  $\theta$  is set to 0,5 and appropriate values of  $\Delta t$  and  $\Delta x$  are chosen. For some explicit schemes, utilized for solving the Saint-Venant equations, the Courant number is often used as a stability criterion. It can also be utilized as an indication of precision of the Preissmann scheme. The Courant number can be obtained by the following equation [Cunge et al., 1980, Szymkiewicz, 2010].

$$C_r = \frac{\sqrt{g \cdot \bar{H}} \cdot \Delta t}{\Delta x} \quad (5.22)$$

Where  $g$  is the gravitational constant,  $\bar{H}$  is average flow height in the pipe,  $\Delta t$  is time step and  $\Delta x$  is distance step. A test clarifying the effect of various Courant numbers is performed on a pipe with the specifications shown in table 5.1.

Length	500 m
Sections	25
$\Delta x$	20 m
Diameter	1.2 m
Ib	3 ‰

Table 5.1: Pipe specifications.

In the above pipe a step in inflow is given from 0,35 m<sup>3</sup>/s to 0,7 m<sup>3</sup>/s and for various Courant numbers,  $\Delta t$  is found by equation 5.22. The results can be seen in figure 5.9.

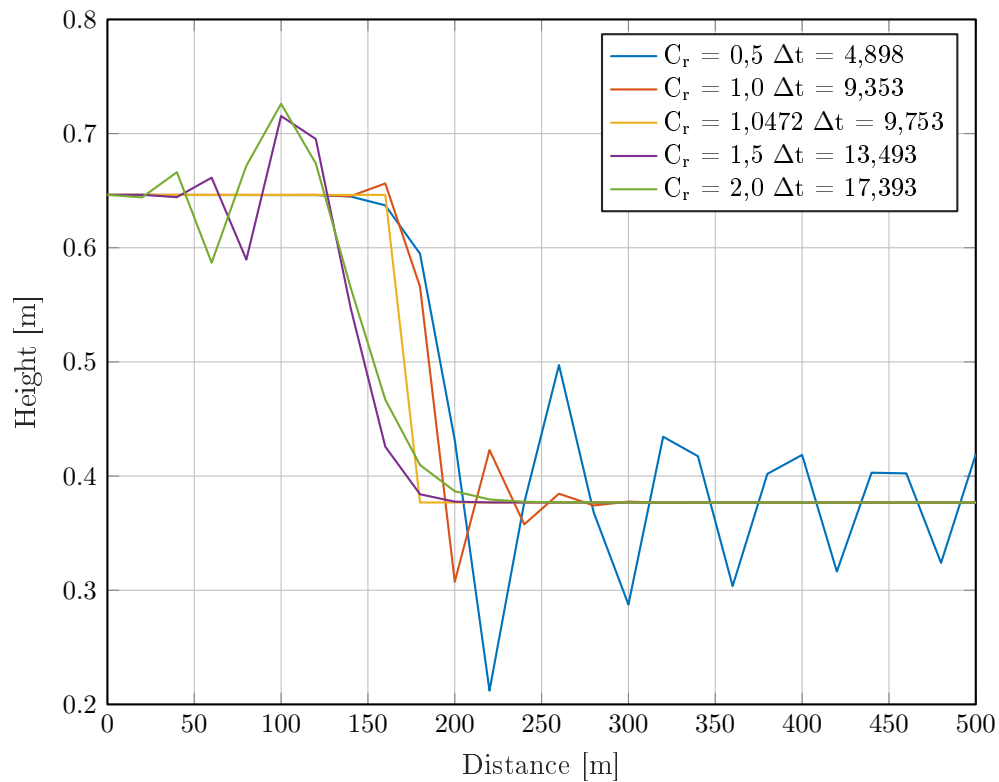


Figure 5.9: Step in inflow given from  $0,35 \text{ m}^3/\text{s}$  to  $0.7 \text{ m}^3/\text{s}$  at first iteration in pipe listed in table 5.1. Plot for all tests is made at approximately  $t = 100$  seconds.

It is clear from the results shown in figure 5.9 that considerations when choosing  $\Delta t$  and  $\Delta x$  should be made, as it can have an undesirable effect on the results. Another anomaly discovered is that the Courant number has to be slightly more than one to obtain a perfect calculation, i.e. no oscillation occurring before or after the wave. An attempt to mitigate the error by minimizing the threshold of the approximation by Newton's method from  $10^{-6}$  to  $10^{-9}$  yielded no change in the obtained result. Further investigations were not made on the subject. The parameter  $\theta$  should not be left out of the equation, as higher values have a dampening effect on the wave. In figure 5.10 various values of  $\theta$  is tested with  $\Delta t$  set to 9,754.

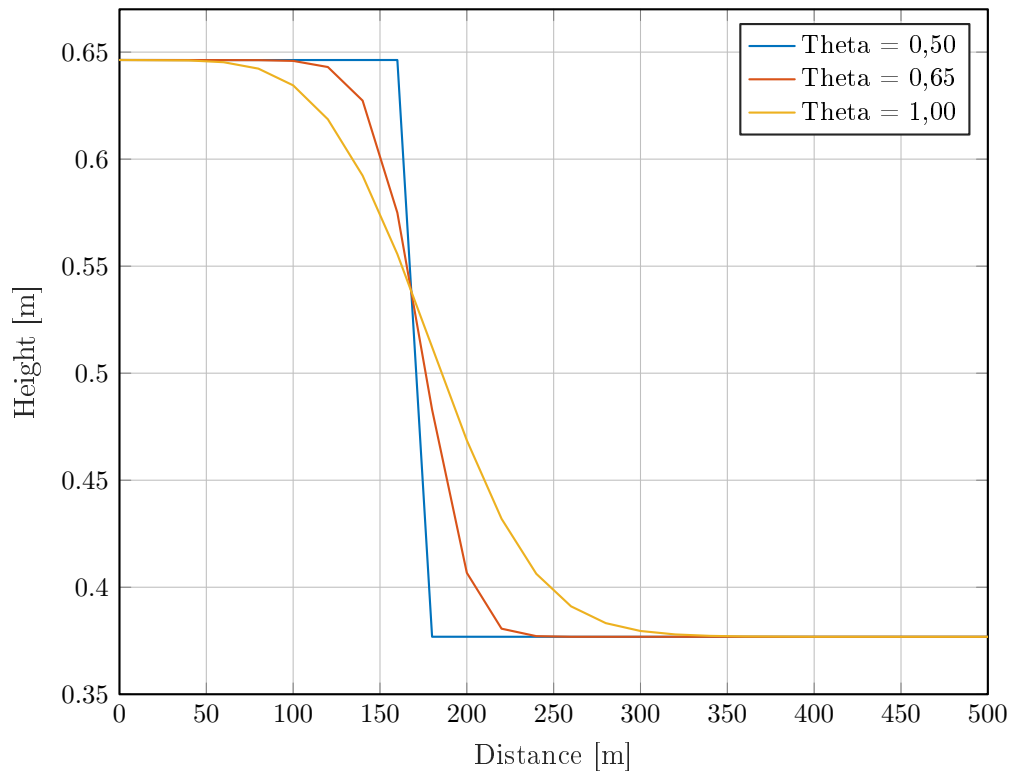


Figure 5.10: Step in inflow given from  $0,35 \text{ m}^3/\text{s}$  to  $0,7 \text{ m}^3/\text{s}$  at first iteration in pipe listed in table 5.1 and  $9,753$  chosen for  $\Delta t$ . Plot for all tests is made at approximately  $t = 97,5$  seconds.

Due to the choice of simplifying, any natural dampening effect has thereby been disregarded, but as seen in figure 5.10 artificial dampening due to numerical errors can be reintroduced. By choosing a proper value of  $\theta$  the simplification can be somewhat rectified, but at the same time, it can mitigate oscillations, which would be bound to happen when pipes of different diameters, slopes and  $\Delta x$  are adjoined. As a consequence of introducing numerical dampening, waves of low amplitude will be dampened out. But due to the lengths sewer pipes typically are it is assumed to be an insignificant consequence compared to the reduction in oscillation which can be obtained. According to [Cunge et al., 1980] a value of approximately  $0,65$  is a reasonable choice for  $\theta$ , and for that reason, it will be used for the remaining part of the project. For comparison the test in figure 5.9 is replicated with the chosen value of  $\theta$  and can be seen in figure 5.11.

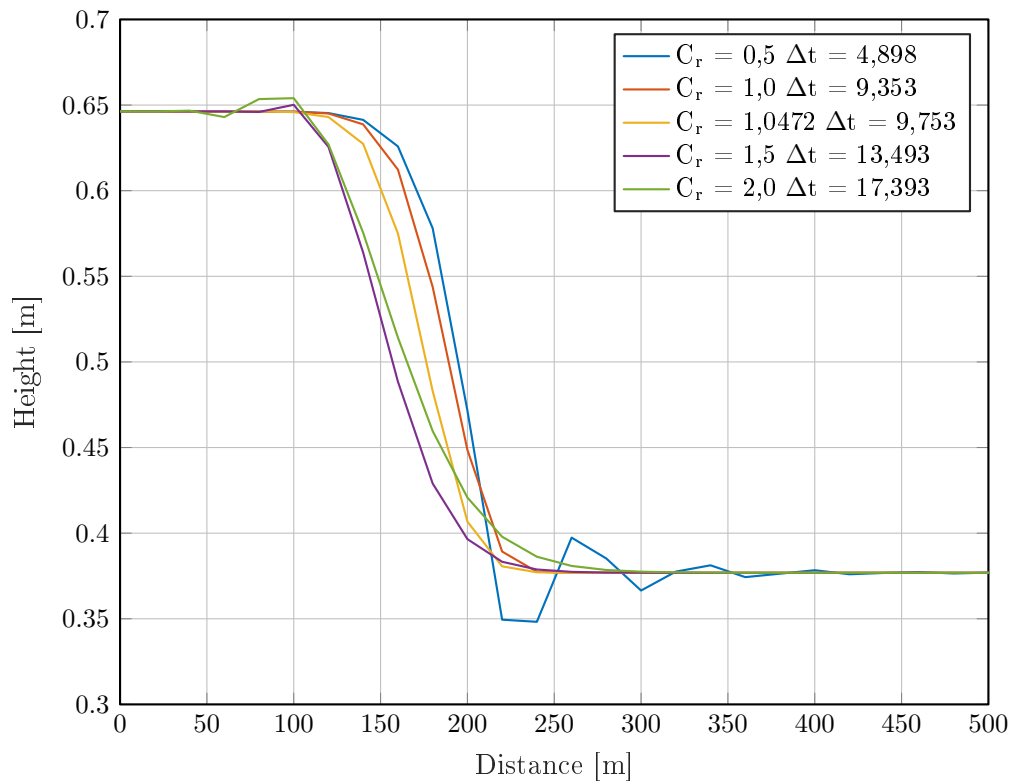


Figure 5.11: Step in inflow given from  $0,35 \text{ m}^3/\text{s}$  to  $0.7 \text{ m}^3/\text{s}$  at first iteration in pipe listed in table 5.1. Plot for all tests is made at approximately  $t = 100$  seconds.

The chosen value of  $\theta$  together with Courant's number as a tuning parameter could be a simple way to obtain values of  $\Delta t$  and  $\Delta x$  for which the simulated results are less affected by distortion caused by numerical errors. To be able to conclude on this as a feasible tuning parameter, further testing would be needed with different pipes with different specifications. Furthermore different steps in both directions of inflow at different initial heights would also be needed to conclude on the uniformity of the Courant number.

### 5.3 Concentrate scheme

Various explicit and implicit schemes exist to solve the transport equation obtained in section 4.2 and shown below.

$$A \cdot \frac{\partial C}{\partial t} + Q \cdot \frac{\partial C}{\partial x} = 0 \quad (5.23)$$

As area and flow are already found by solving the Saint-Venant equations by the Preissmann scheme in section 5.2 a simple discretization of the transport equation suffices. The discretized transport equation is shown below:

$$A(x, t) \cdot \frac{C(x, t) - C(x, t - \Delta t)}{\Delta t} + Q(x, t) \cdot \frac{C(x, t) - C(x - \Delta x, t)}{\Delta x} = 0 \quad (5.24)$$

Isolating for  $C(x,t)$  in steps is shown in the following:

$$\begin{aligned}
A(x,t) \cdot \frac{C(x,t)}{\Delta t} + Q(x,t) \cdot \frac{C(x,t)}{\Delta x} &= A(x,t) \cdot \frac{C(x,t-\Delta t)}{\Delta t} + Q(x,t) \cdot \frac{C(x-\Delta x,t)}{\Delta x} \\
\Downarrow \\
C(x,t) \cdot \left( \frac{A(x,t)}{\Delta t} + \frac{Q(x,t)}{\Delta x} \right) &= A(x,t) \cdot \frac{C(x,t-\Delta t)}{\Delta t} + Q(x,t) \cdot \frac{C(x-\Delta x,t)}{\Delta x} \\
\Downarrow \\
C(x,t) &= \frac{A(x,t) \cdot \frac{C(x,t-\Delta t)}{\Delta t}}{\frac{A(x,t)}{\Delta t} + \frac{Q(x,t)}{\Delta x}} + \frac{Q(x,t) \cdot \frac{C(x-\Delta x,t)}{\Delta x}}{\frac{A(x,t)}{\Delta t} + \frac{Q(x,t)}{\Delta x}} \\
\Downarrow \\
C(x,t) &= \frac{A(x,t) \cdot C(x,t-\Delta t)}{A(x,t) + Q(x,t) \cdot \frac{\Delta t}{\Delta x}} + \frac{Q(x,t) \cdot C(x-\Delta x,t)}{Q(x,t) + A(x,t) \cdot \frac{\Delta x}{\Delta t}}
\end{aligned} \tag{5.25}$$

It can be seen that the concentration can be obtained at current time and place by known values and the solutions of the Saint-Venant equations.

## 5.4 Tank scheme

This section will go through the discretization of equation 4.46 and 4.48. Discretizing equation 4.46, and express it as change in terms of height, the following is obtained:

$$\begin{aligned}
\frac{h(t) - h(t-\Delta t)}{\Delta t} &= \frac{1}{A} (Q_{in}(t) - u(t) \cdot \bar{Q}) \\
\Downarrow \\
h(t) &= \frac{1}{A} (Q_{in}(t) - u(t) \cdot \bar{Q}) \cdot \Delta t + h(t - \Delta t)
\end{aligned} \tag{5.26}$$

Some limitations are needed to be considered during implementation such that outflow can never exceed what is currently in the tank. Solving the equation for a change in level of concentrate in the tank explicit, and discretizing it the following is obtained:

$$\begin{aligned}
\frac{C_{tank}(t) - C_{tank}(t-\Delta t)}{\Delta t} &= \frac{1}{A} \left( C_{in}(t) \cdot \frac{Q_{in}(t)}{h(t)} - C_{tank}(t - \Delta t) \cdot \frac{Q_{out}(t)}{h(t)} \right) \\
\Downarrow \\
C_{tank}(t) &= \frac{1}{A} \left( C_{in}(t) \cdot \frac{Q_{in}(t)}{h(t)} - C_{tank}(t - \Delta t) \cdot \frac{Q_{out}(t)}{h(t)} \right) \cdot \Delta t + C_{tank}(t - \Delta t) \\
\Downarrow \\
C_{tank}(t) &= C_{in}(t) \cdot \frac{1}{A} \frac{Q_{in}(t)}{h(t)} \cdot \Delta t - C_{tank}(t - \Delta t) \cdot \frac{1}{A} \frac{Q_{out}(t)}{h(t)} \cdot \Delta t + C_{tank}(t - \Delta t) \\
\Downarrow \\
C_{tank}(t) &= C_{in}(t) \cdot \frac{1}{A} \frac{Q_{in}(t)}{h(t)} \cdot \Delta t + C_{tank}(t - \Delta t) \cdot \left( 1 - \frac{1}{A} \frac{Q_{out}(t)}{h(t)} \cdot \Delta t \right)
\end{aligned} \tag{5.27}$$

To avoid instability or oscillation when the condition  $h(t) < Q_{out} \cdot \Delta t / A$  occurs, the concentrate level in the tank should be set equal to the inflow level. This condition corresponds to the fluid being in the tank at one-time step has been emptied out of the tank at the next, meaning that the fluid in the tank at the next time step is new inflow.

## 5.5 Implementation

In this section, the implementation of the various parts, which the simulation environment consist of, is explained. The chosen structure, which is described in section 5.1, is seen in figure 5.12.

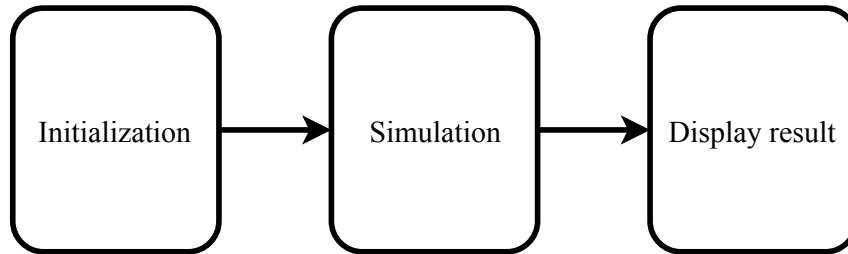


Figure 5.12: Chosen structure of simulation environment.

The first part to be elaborated upon is the initialization.

### Initialization

For the setup procedure of the simulation in list form, the specifications part, shown in figure 5.2, needs to be defined. The necessary parameters in the list for both pipe and tank can be seen in table 5.2.

#### 1. Pipe

- Length [m]
- Sections (Number of sections the pipe should be split in to)
- $S_b$  (Slope) [%]
- $\Delta x = \text{Length} / \text{Sections}$  [m]
- Diameter [meter]
- Theta (parameter used in Preissmann scheme)
- $Q_f$  (maximum flow found by Manning formula, see equation 5.13) [ $\text{m}^3/\text{s}$ ]
- Side/lateral inflow present
- Section location in data

#### 2. Tank

- Size [ $\text{m}^3$ ]
- Height [m]
- Area = Size / Height [ $\text{m}^2$ ]
- Maximum outflow [ $\text{m}^3/\text{s}$ ]
- Section location in data

Table 5.2: List of parameters for pipe and tank.

Some parameters can be found from others and are set to be calculated automatically. Furthermore, an item is added to the list which indicates, where the initial and simulated data, for the specific item can be found. To give an overview of the system to be simulated, and to easily be able to locate specific parameters needed during simulation, three structures are returned to the workspace. These are named “pipe\_spec”, “tank\_spec” and “sys\_setup”. The first two structures holds the information shown in table 5.2 respectively. The last one, “sys\_setup”, holds information about the various parts indexed in the order the system is set up and simulated. In figure 5.13 the content of “sys\_setup” is shown for a setup with two pipes and a tank.

Fields	type	component	sections
1	'Pipe'	1	10
2	'Tank'	1	1
3	'Pipe'	1	10
4	'Total'	3	21

Figure 5.13: Display of structure showing system setup information in MATLAB.

An initialization scheme is constructed as per figure 5.3 where adjoining pipes are considered as one part of the system and each tank is an individual part, which means that tanks are used as a separator between parts consisting of pipes. The iterative scheme is shown in figure 5.7 requires that boundary conditions are found before the iterative Preissmann scheme can be started. It has been decided by the project group that input should be given in flow, as input in height would be needed to be specific for the pipe inserted, to make the simulation universal. This means that from an initial input flow the corresponding height in the pipes needs to be found. By equation 5.12 flow can be obtained from height, but that equation is transcendental, as it can not be solved analytically for height. This means that other means are necessary to obtain height from a flow. Various iterative schemes exist to solve such equations, but due to the desire to keep computation time at a minimum, use of such schemes is refrained from. A solution to the problem is that for each pipe, during initialization, a data set from zero to the diameter of the pipe in sufficient steps is created, and from which the corresponding flow is obtained by equation 5.12. From this data, a curve fitted polynomial can be obtained by the MATLAB curve fitting toolbox or a lookup table can be constructed. Flow data is generated for 10.000 height steps for a pipe with the parameters shown in table 5.3.

Diameter	0,9 meter
Slope ( $I_b$ )	3 ‰
Length	200 meter
Sections	10

Table 5.3: List of parameters used to obtain data shown in figure 5.14.

In figure 5.14 a comparison is shown of the generated data and a ninth order polynomial fitted to the data.

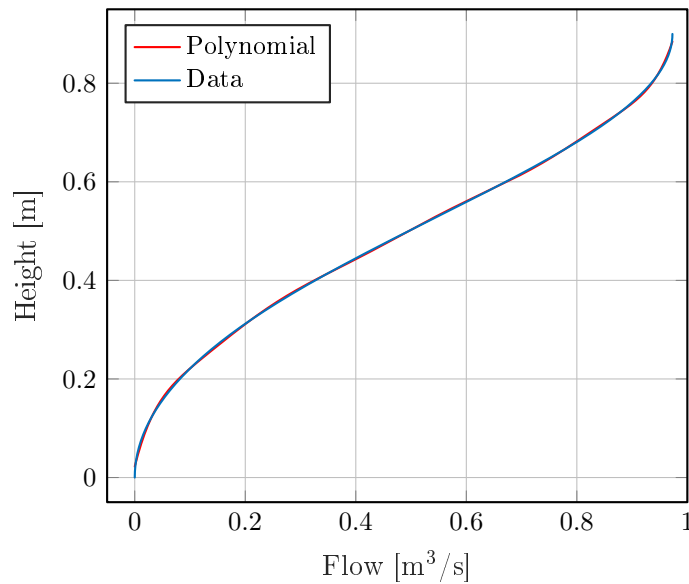


Figure 5.14: Comparison between data obtained by equation 5.12 and the same data curve fitted to a ninth order polynomial.

The two plots in the figure are seemingly identical, but if observed closer the curve fit has what could be described as a low frequency oscillation compared to the plotted data. Furthermore, the curve fit does not reach the same endpoints. This will result in the height at the endpoints never to be zero or the diameter of the pipe when no inflow or maximum inflow is present. In figure 5.15 the plot is separated into three for an easier overview.

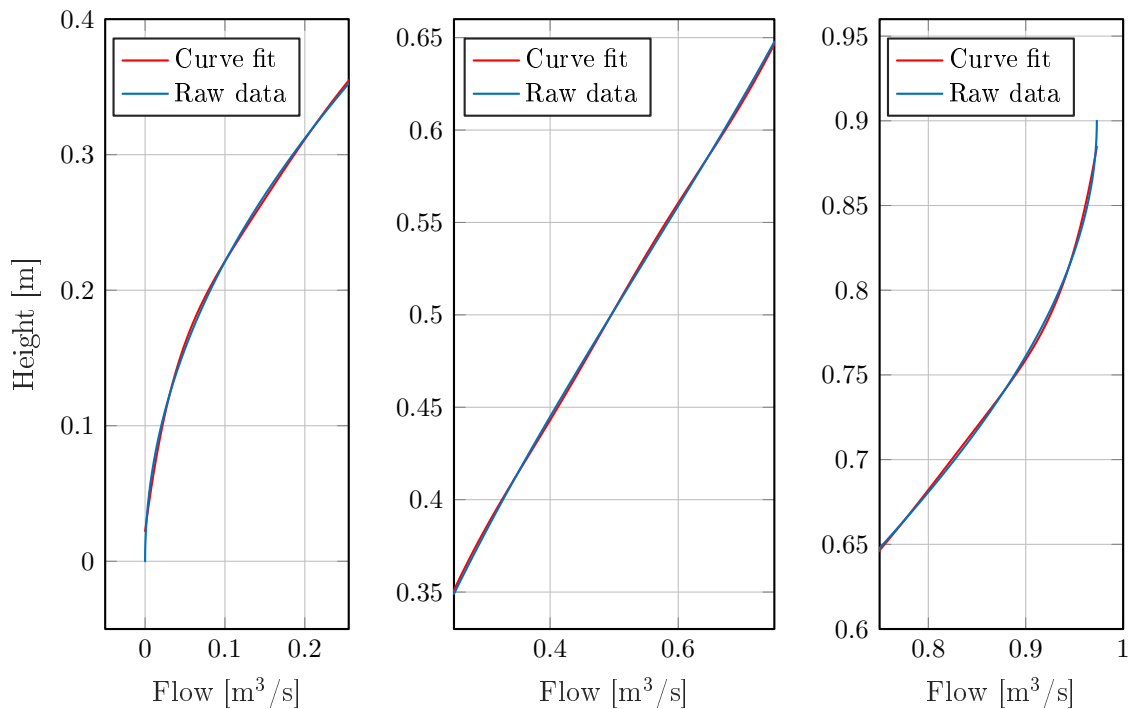


Figure 5.15: Comparison between data obtained by equation 5.12 and the same data curve fitted to a ninth order polynomial.

As discussed in section 5.1, a scheme which brings the system to an initial steady state could

be necessary due to the nonlinear nature of the Saint-Venant equations. A test is performed where two adjoining pipes, with the specifications given in table 5.3, is calculated for a different amount of iterations. The boundary condition is found by the fitted polynomial for each pipe respectively. The result of this test is seen in figure 5.16.

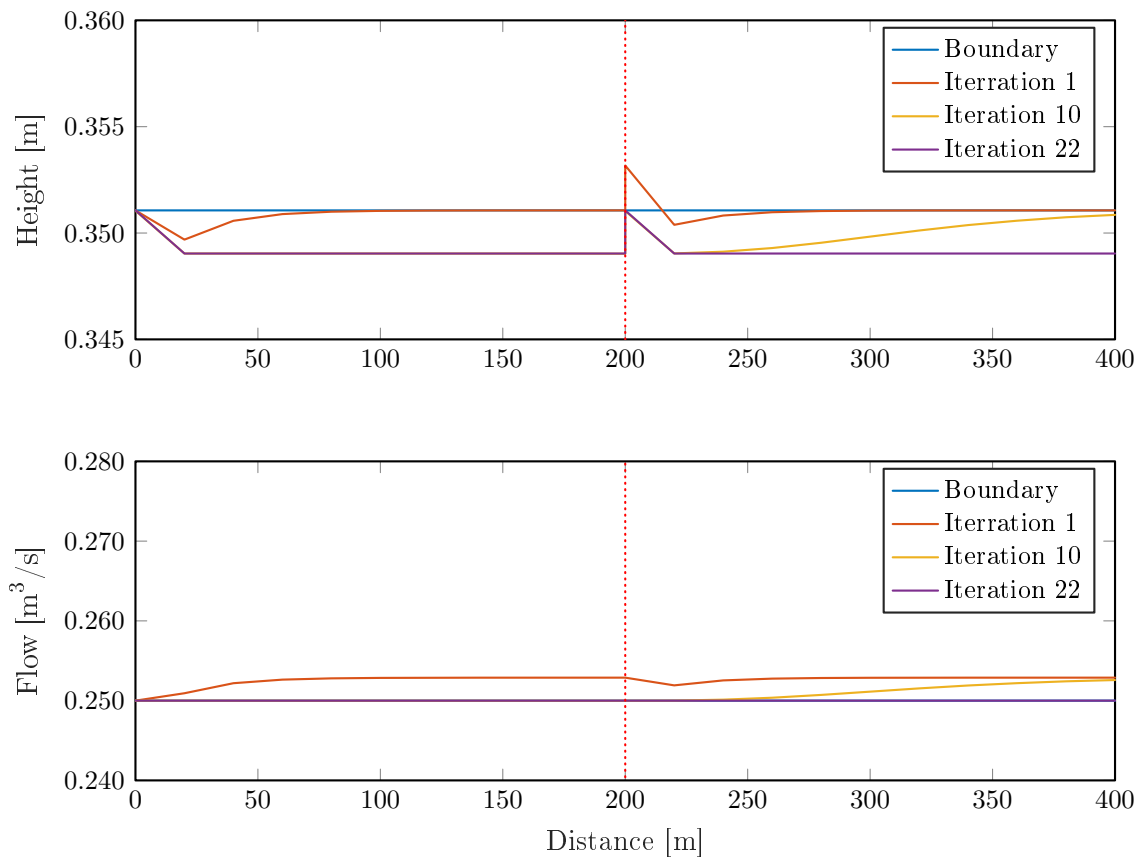


Figure 5.16: Height and flow in two adjoining pipes, with identical specifications given in table 5.3, given boundary conditions found by fitted polynomial, and calculated at various amount of iterations with constant flow input of  $0,25 \text{ m}^3/\text{s}$ . The dotted line indicates an intersection between pipes.

In figure 5.16 a maximum of 22 iterations are performed. The iterations are stopped as the error between the input flow of  $0,25 \text{ m}^3/\text{s}$  desired to be in all sections, and the calculated flow in all the sections of the two pipes is less than  $1 \cdot 10^{-7}$ , which is a preset condition. Some discrepancy in heights can be seen at the start of both pipes. These two points are the boundary conditions that are found by the fitted polynomial. Even though the anomalies are small they could pose a problem when expanding the simulation with more pipes and different slopes.

In figure 5.17 the specifications of the main line of Fredericia mentioned in section 2, and given by table 2.1 with corrections from table 2.2, is seen.

Fields	length	sections	Dx	Sb	d	Theta	Qf	side_inflow	data_location
1	303	15	20.2000	0.0030	0.9000	0.6500	0.9730	0	1
2	27	1	27	0.0030	1	0.6500	1.2843	1	2
3	155	8	19.3750	0.0041	1	0.6500	1.5014	0	3
4	295	14	21.0714	0.0122	0.8000	0.6500	1.4386	0	4
5	318	15	21.2000	0.0053	0.9000	0.6500	1.2932	1	5
6	110	5	22	0.0036	0.9000	0.6500	1.0658	1	6
7	38	2	19	0.0024	1	0.6500	1.1487	1	7
8	665	30	22.1667	0.0030	1	0.6500	1.2843	1	8
9	155	7	22.1429	8.0000e-04	1	0.6500	0.6632	0	9
10	955	40	23.8750	0.0029	1.2000	0.6500	2.0415	1	10
11	304	15	20.2667	0.0030	1.2000	0.6500	2.0764	0	11
12	116	5	23.2000	0.0021	1.2000	0.6500	1.7373	1	12
13	283	12	23.5833	0.0017	1.4000	0.6500	2.3463	1	13
14	31	1	31	0.0019	1.4000	0.6500	2.4805	1	14
15	125	6	20.8333	0.0021	1.6000	0.6500	3.7075	0	15
16	94	4	23.5000	0.0013	1.5000	0.6500	2.4609	0	16
17	360	15	24	0.0046	1.6000	0.6500	5.4872	1	17
18	736	32	23	0.0012	1.6000	0.6500	2.8026	0	18

Figure 5.17: Setup in MATLAB of pipe system from section 2 of the main line in Fredericia.

The amount of sections for each pipe is chosen such that each section is close to being 20 meters, with some sections deviating due to pipe length and others deviate on purpose to see if it affects the outcome. To lessen the design complexity of the simulation environment a limitation is made on side input. It is decided that side input should not consist of pipes in which flow should be simulated. Instead it is chosen that side input is given from premade flow profiles. There is not given any side inflow in the results show in the following figures, as the indication of side inflow listed in figure 5.17 just indicates the possibility of inflow to be given at the inlet of the pipe. In figure 5.18 iterations of the pipe setup shown in figure 5.17 is seen.

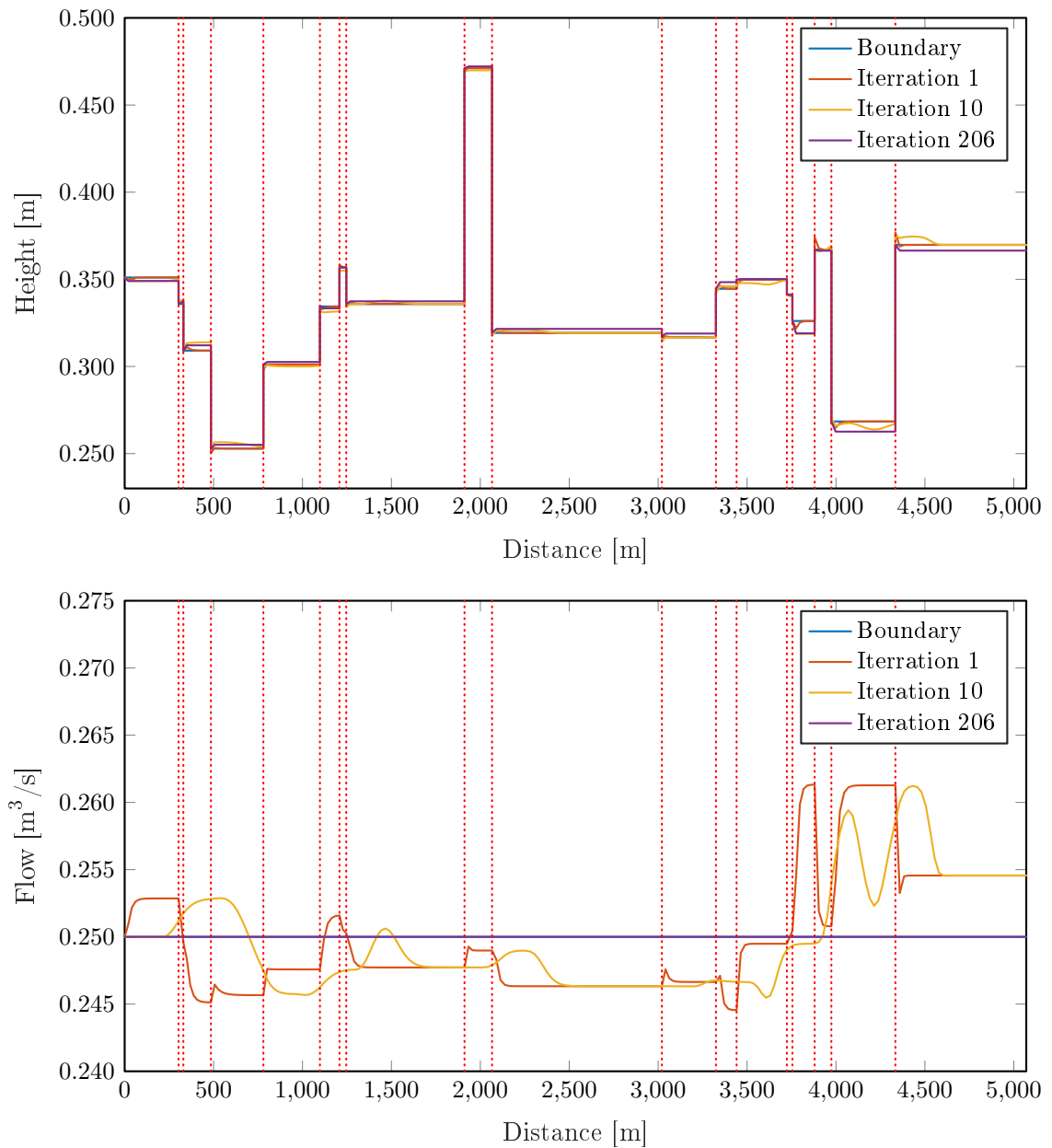


Figure 5.18: Height and flow of pipe setup from part of Fredericia, given by table 2.1 with corrections from table 2.2, where boundary conditions is found by fitted polynomial. Various amount of iterations, with constant flow input of  $0,25 \text{ m}^3/\text{s}$ , is performed. The dotted line indicates pipe intersections.

It is clear that the larger setup increases the undesired behavior seen in figure 5.16. But it can also be seen that the flow can be brought to an acceptable initial state from which the system can start simulating. In figure 5.19 a section of the height plot from figure 5.18 is seen.

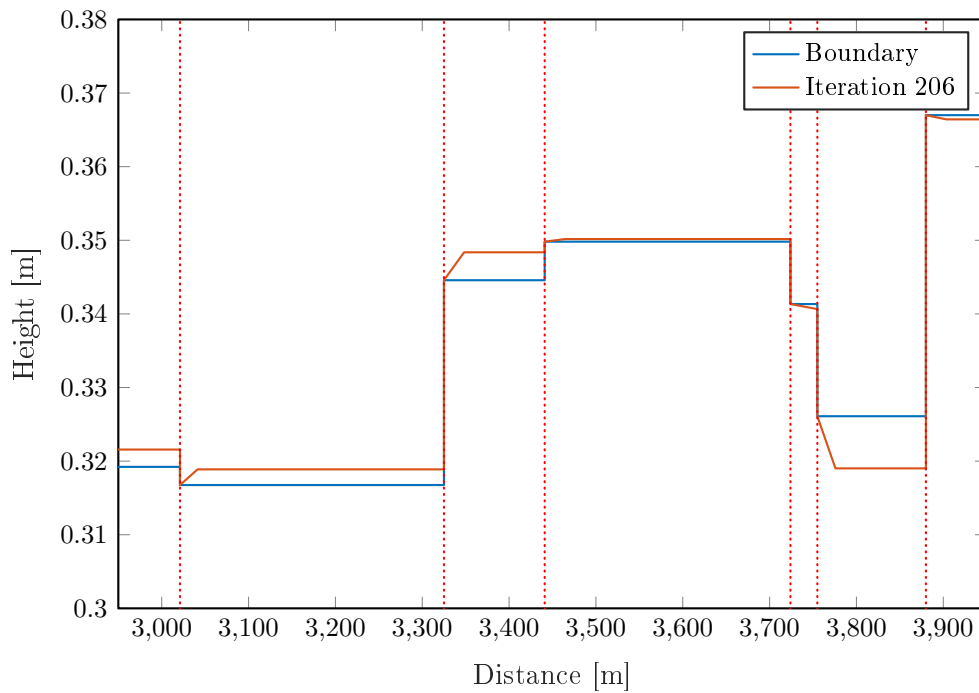


Figure 5.19: Segment of the height plot shown in figure 5.18. Pipe 10 and 16 is seen partially at the left and right side and 11 to 15 in between with a red stippled line separating pipes.

In the above figure, the obtained height from the fitted polynomial is at it worst off by almost a centimeter. But when simulating this offset will only occur in the first section of the pipe. This means that it will be a greater disturbance on short pipes with few sections than larger ones with more sections. An alternative method is attempted to conclude if the deviations of the curve fitted polynomial seen in figure 5.15 is the cause or if there is an unforeseen error in the Preissmann scheme. A lookup table, where the same data used to create the polynomial, is utilized. A simple implementation is made where the index in the vector of flow is found by subtracting the input flow from the vector. The desired index is then found by searching for the lowest absolute value. Finally the resulting height is given as the desired index of the height vector. The chosen scheme for creating the lookup table means that the height will in the worst case be rounded to the nearest step. But indexing the flow and height into the chosen 10.000 steps, it is assumed to be an insignificant error, and in the worst case the number of steps can be increased. In figure 5.20 an identical test of the pipe setup of Fredericia is performed at various iterations.

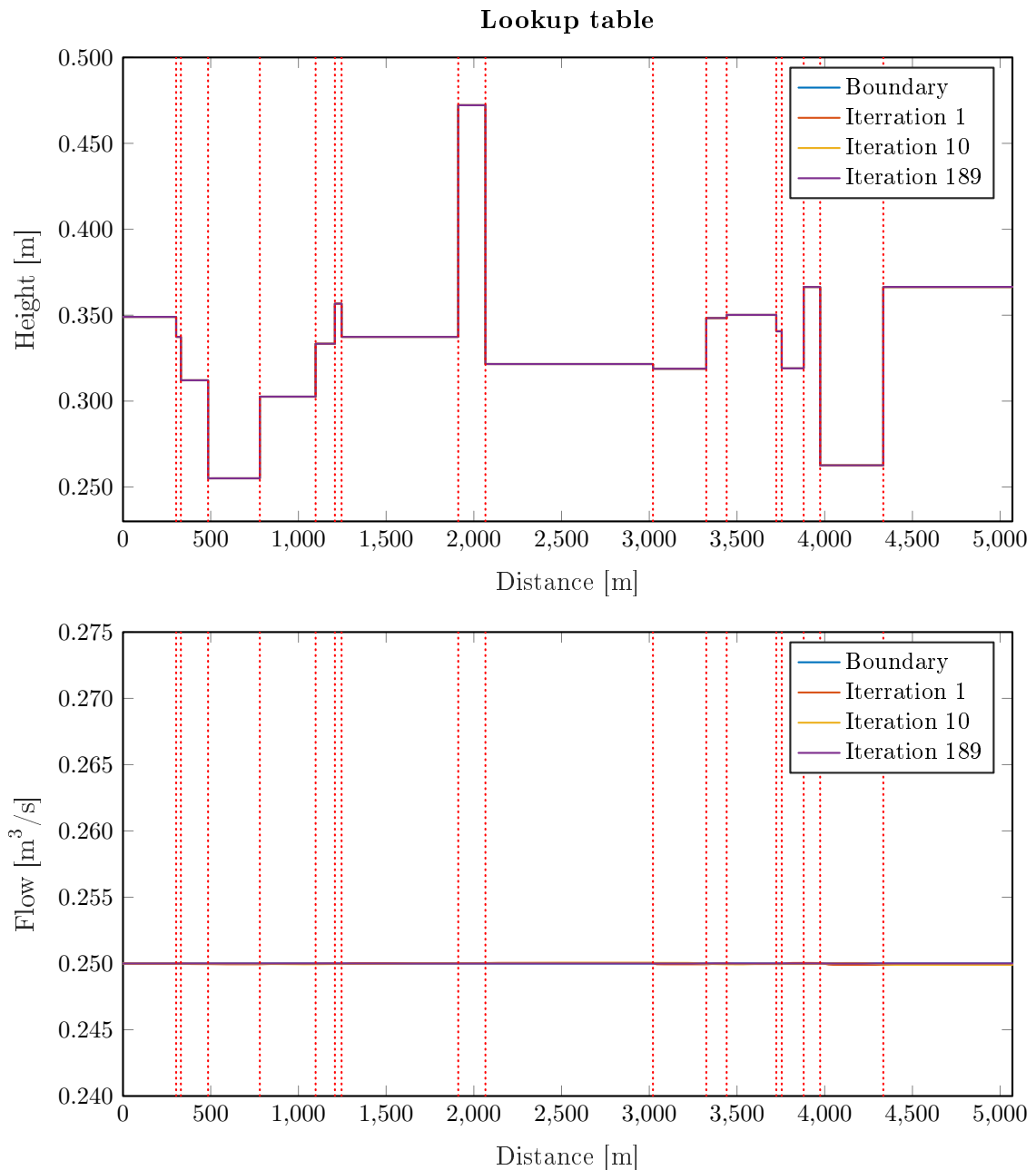


Figure 5.20: Height and flow of pipe setup from part of Fredericia, given by table 2.1 with corrections from table 2.2, where boundary conditions is found by lookup table. Various amount of iterations, with constant flow input of  $0,25 \text{ m}^3/\text{s}$ , is performed. The dotted line indicates pipe intersections.

It is clearly shown that the deviation between the boundary conditions found by the lookup table and the values found by the following iterations of the Preissmann scheme is significantly decreased. Something else to note is that even though the difference seem to be non-existent it still required 189 iterations before the flow error was minimized to the same  $1 \cdot 10^{-7}$  as before. For this reason, it is decided to implement the scheme which brings the adjoining pipe parts into steady state before the simulation starts. A decisive choice is not made at this point whether the curve fitted polynomial or the lookup table should be implemented. The reason for this is that some imprecision can be accepted if reduction in simulation time can be obtained. A test will therefore be performed, in the simulation

part of the implementation, to decided which scheme should be utilized. A flow chart of the initialization scheme, where initial values for the entire setup is found, can be seen in figure 5.21.

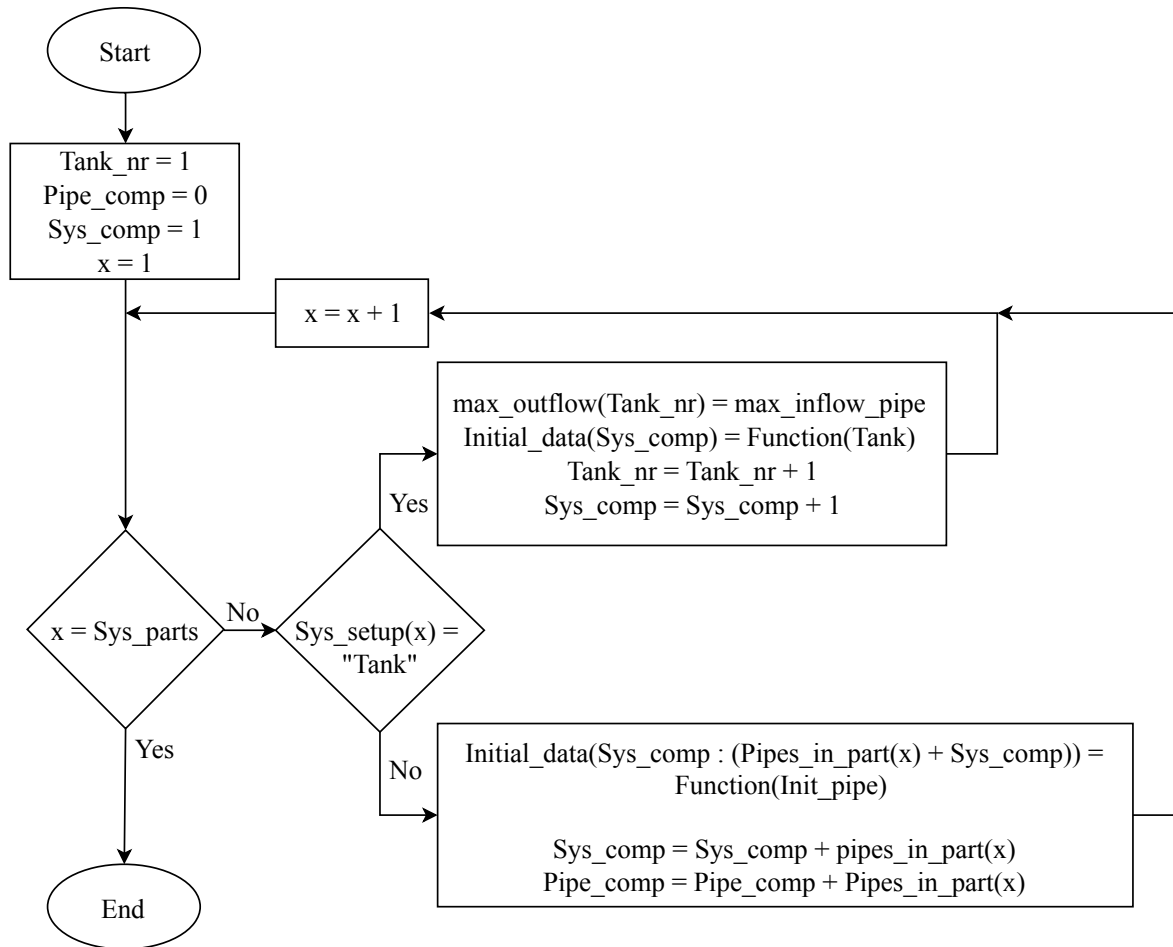


Figure 5.21: Initialization loop.

Two functions, namely “Tank” and “Init\_pipe”, is used to obtain the initial values for tanks and the boundary conditions, for the pipes, needed to start iterating with the Preissmann scheme. The tank function returns the initial flow, height and the input needed for the pump, such that inflow is equal to outflow in the tank. Due to MPC requiring constraints for the input to the pump in the tank and due to time constraint of the project, a limitation in the simulation is made. The limitation refers to tanks not being able to be the end point of the entire system setup. The reason for this is that a uniform control input of zero to one for all pumps, to ease constraint setup when utilizing MPC, is obtained. The following parameters are set in the tank function:

- $Q_{in} = Q_{initial} [m^3/s]$
- $Q_{out} = Q_{in} [m^3/s]$
- $u_{initial} = Q_{in}/Q_{max-outflow} [.]$
- $h = h_{initial} [m]$
- $C = C_{initial} [g/m^3]$

Where  $Q$  is flow,  $u$  is pump input,  $h$  is height and  $C$  is concentrate. The pipe function is given initial flow, a component number from the system setup list in figure 5.13, the corresponding pipe specifications to the number of pipes indicated by the system setup

list and an error value. The error value is the accepted error between desired flow and the flow obtained by iterating with the Preissmann scheme, which means that when the error is less than the error value the system is in the desired steady state. A flowchart of the pipe function can be seen in figure 5.22.

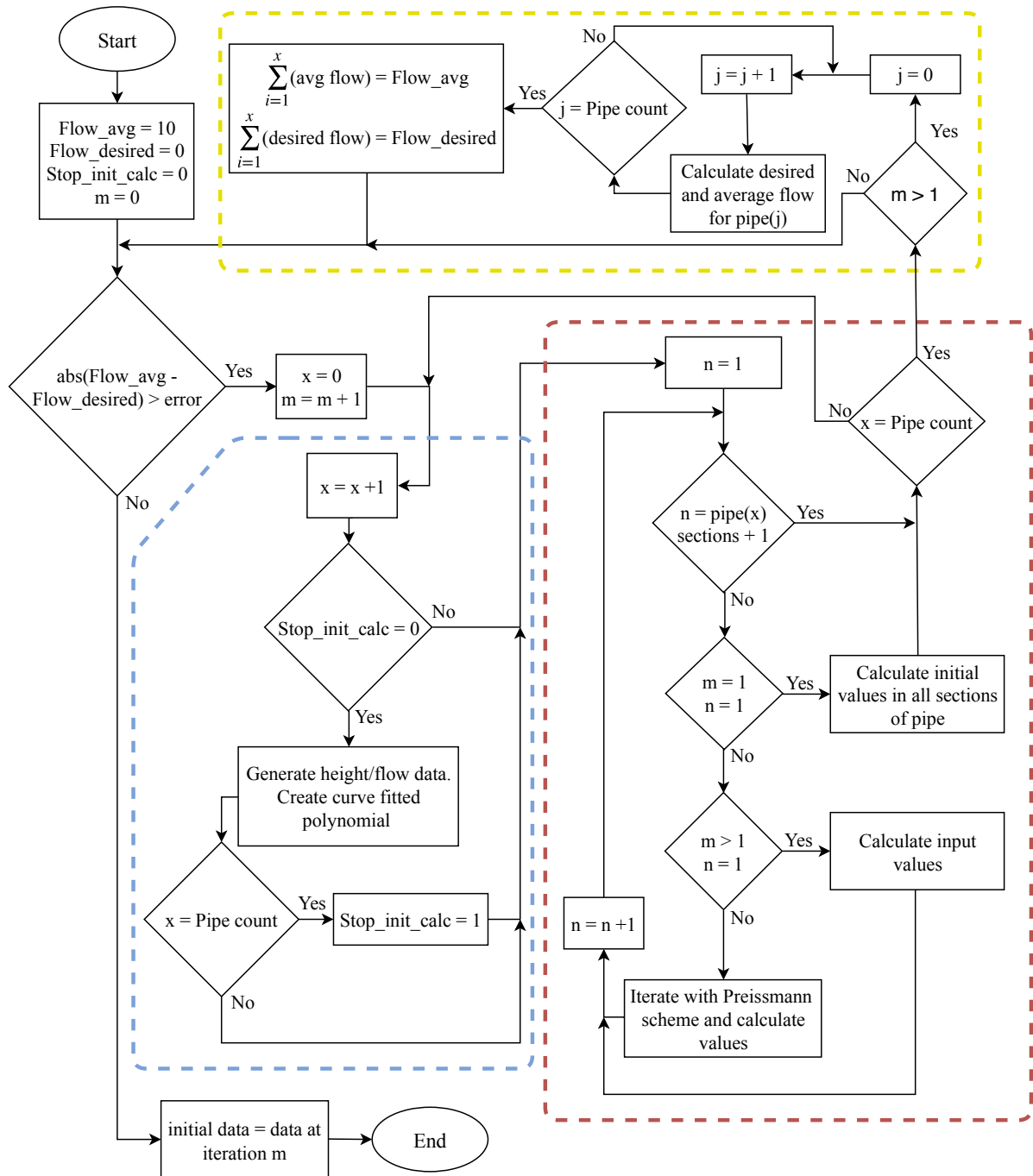


Figure 5.22: Flowchart of pipe initializing function where the blue box is the setup of the curve fitted polynomial for each pipe, the red box is the computation of data in pipes and the yellow box calculates desired and average flow for error stop condition. Furthermore “x” indicates a specific pipe, “m” is time step and “n” indicates the section in a pipe.

The pipe initialization function can be separated into three parts as indicated by the blue, red and yellow stippled boxes. In the blue stippled box the generated data, which can

also be used for a lookup table, is used to create the curve fitted polynomial. When data are generated for all the pipes given to the function, a flag is set such that unnecessary calculations are not performed further on.

In the red stippled box the calculations of the height and concentrate are performed. In the first time iteration “ $m = 1$ ” the initial boundary condition is set for all sections of pipe number “ $x$ ”. This corresponds to the  $i$ -th row of circles shown in figure 5.7. Furthermore, when iterating through the pipes the corresponding pipe specifications is checked to decide if the pipe has side inflow. If it is present then the inflow into the pipe is a simple summation of input flow and side inflow. The concentrate input in the case of side inflow is found by equation 4.40. For the next pipe, the input is then set to be the output of the previous pipe plus eventual side inflow. At the following time iterations, the input boundary condition is found at section “ $n = 1$ ”. The Preissmann scheme is then utilized to find the height, and the concentrate is calculated, for the remaining pipe sections. This is done for all the pipes given to the function.

Lastly, in the yellow stippled box the desired and average flow values in the pipe or pipes are calculated. At the first time iteration “ $m = 1$ ” the values of “Flow\_avg” and “Flow\_desired” are not updated. The reason is that the initial flow is inserted as the flow in all sections of all the pipes, which would give an error which is zero and stop the initialization loop. In the following iterations, disregarding the boundary condition which is still calculated, the flow is found from a height which can vary for some iterations as seen in figure 5.18. When the flow in all sections of all the pipes has an error which is sufficiently small from the desired flow the iterations is stopped. The flow, height and concentrate data from the latest iteration is returned and the simulation has a steady state point from where it can start. The amount of iterations and the accuracy of the steady state of course depends on the chosen error value. In figure 5.23, the result of various tested error values can be seen.

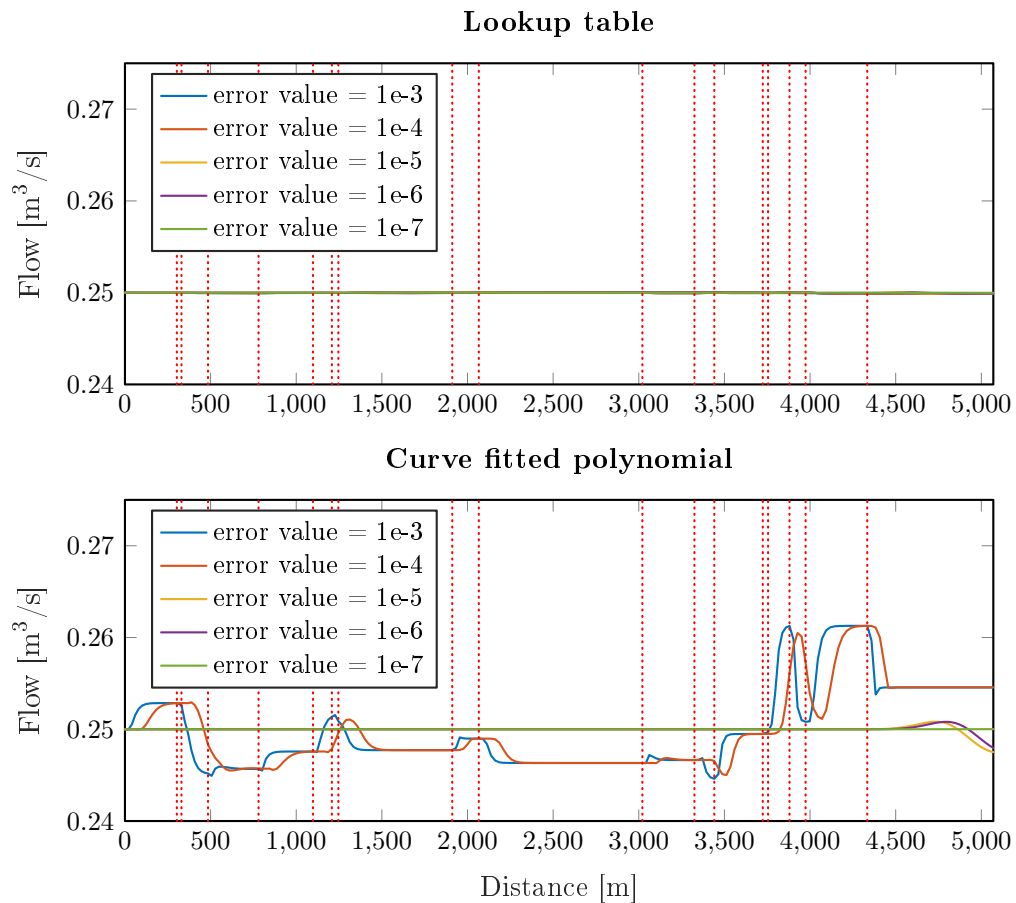


Figure 5.23: Various values of error value are tested with the lookup table and curve fitted polynomial tested on pipe setup shown in figure 5.17 of Fredericia.

If the curve fitted polynomial is utilized to obtain boundary conditions then an error value below  $1 \cdot 10^{-6}$  is preferable. But for setup's with more pipes, it can be necessary to lower this value even further. The lookup table, on the other hand, is due to its better precision not considerably affected in the first place, though some precision is obtained by lowering the error value. As the tested error value is performed on a simple test, and a final decision has not been made on which scheme to utilize an error value of  $1 \cdot 10^{-9}$  has been decided upon. The reason being the results shown in figure 5.23, and that various setup where more pipes with different initial flows might yield a worse result.

## Simulation

Having obtained initial data, for which iterating with the Preissmann scheme can begin, the next part to be implemented is the simulation of the initialized setup. To ease eventual future expansion of the simulation a simple design, where individual parts are simulated one at a time, is chosen. This is realized by nesting functions in two steps from the main simulation module which is seen in figure 5.24.

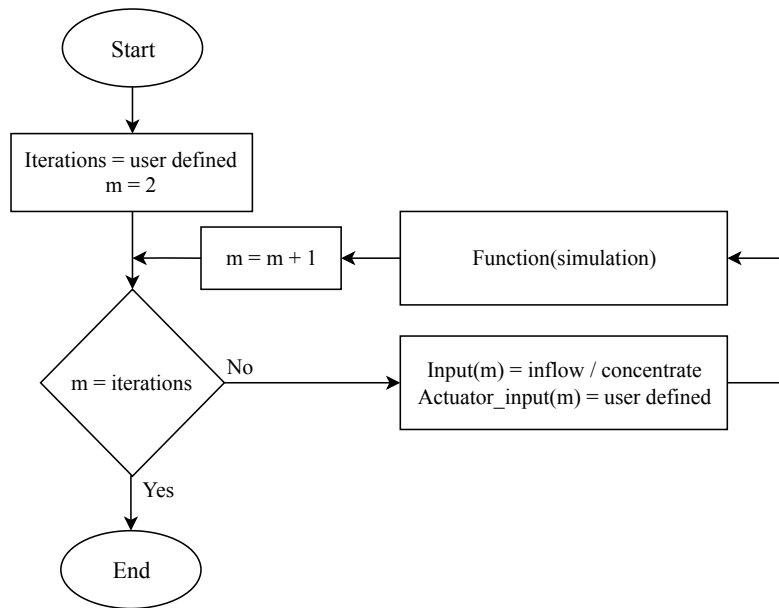


Figure 5.24: Main simulation loop.

The number of iterations desired to simulate the system for is chosen. As the system is already initialized and MATLAB does not have zero indexing the system is initialized at  $m$  equal to one. Therefore the first iteration is performed at  $m$  equal to two and proceeds until the chosen amount of iterations is reached. The function “simulation” is given flow and concentrate input, system specification ( $\text{Sys\_setup}$ ), pipe specification ( $\text{pipe\_spec}$ ). If a tank is present, actuator input and tank specification ( $\text{tank\_spec}$ ) are also needed. In figure 5.25 the simulation function is seen.

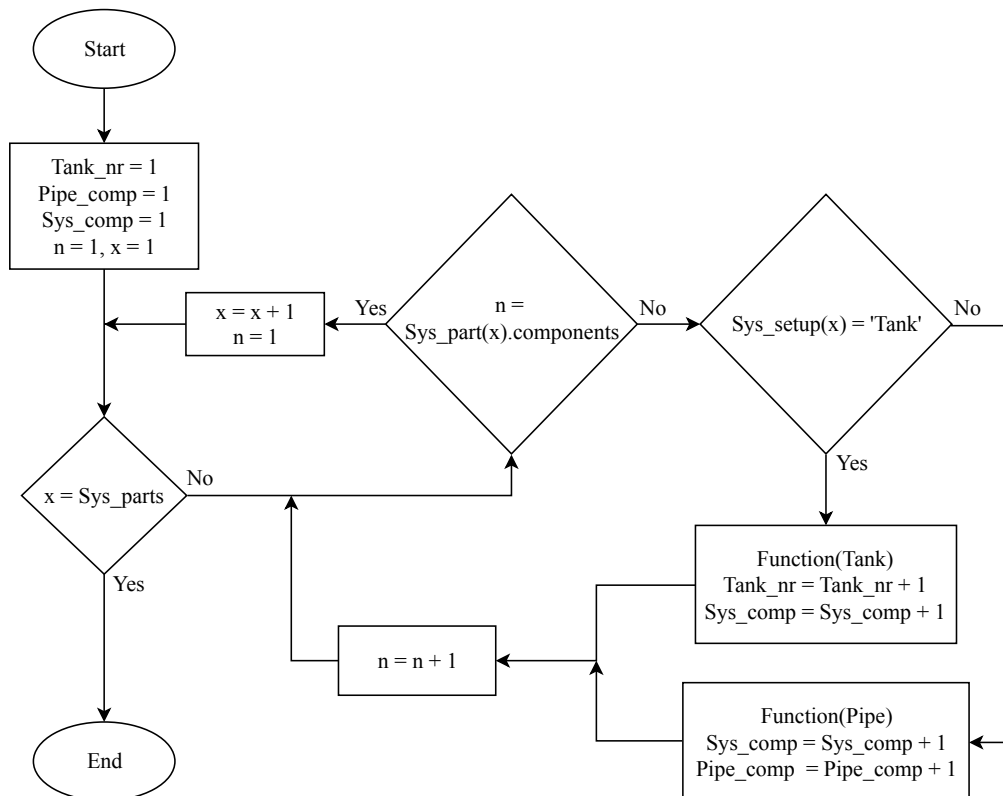


Figure 5.25: Simulation function.

The simulation function is given input of flow, concentrate and actuator for pipes and tanks respectively. Furthermore specifications of system, pipe and tank are given. The basic functionality is an outer and an inner loop. The outer loop iterates through the parts in “Sys\_setup” and the inner loop iterates through the components each part consists of. Iterating through the parts, checking whether the component is a tank or pipe, the respective function is called. The tank function is given tank specifications, current iteration value, flow and actuator input. Furthermore, the index number of the tank is given. The iteration value “m” is in the function used to index when logging data. Output flow is found by equation 4.45. The value of  $\bar{Q}$  in equation 4.45 is set to be the maximum inflow of the adjoining pipe as seen below.

$$Q_{out} = u_{pump} \cdot Q_{max\_outflow} \quad (5.28)$$

Where maximum outflow is equal to the maximum inflow of the downstream adjoining pipe. Doing so makes it possible to always have an actuator input which ranges from zero to one, which helps to minimize complexity when implementing control on large scale setups where several tanks of various sizes could be present. In figure 5.26 a flow chart of the tank function can be seen.

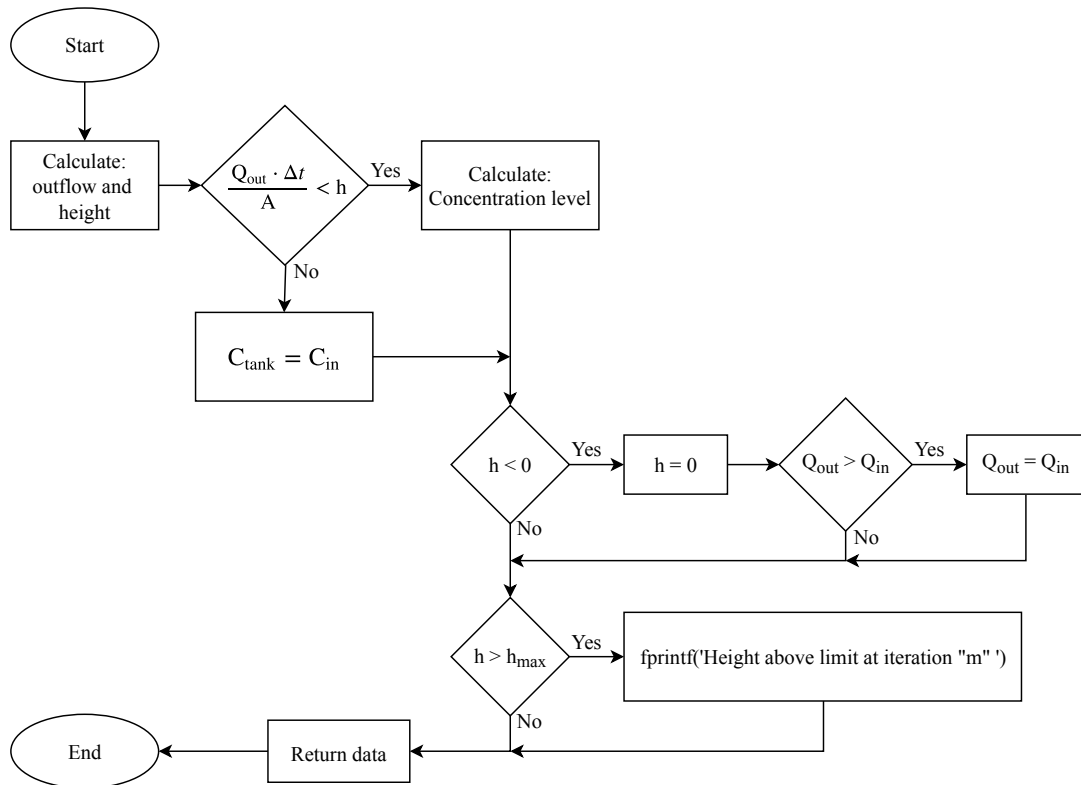


Figure 5.26: Tank function.

The tank function is given inflow, actuator input, “Tank\_nr”, tank specification, iteration value “m”, part index “x” and data stored at index “Sys\_comp”. Iteration and part index is used to fetch previous values of height and concentrate level, used in the calculation of new values. Furthermore the value of “Tank\_nr” is used as index in “Tank\_spec”. First, when the height and flow has been calculated, the condition mentioned in section 5.4 is checked to avoid oscillating concentrate level in the tank. Secondly, as seen in the flowchart, if the calculated height gives a result below zero the height is set to zero and maximum outflow is set equal to inflow. In the case of concentrate level, if height is less than  $Q_{out} \cdot \Delta t / A$  then the level in the tank is set equal to the inflow level. If the fluid level exceeds the

height of the tank a message is printed to the command windows which also contains at which iteration the overflow occurred. Instead of placing a hard limit on tank height, knowing when a tank overflow occurs, and how much the dimension of the tank needs to be adjusted, would be more valuable. In figure 5.27 the pipe function can be seen.

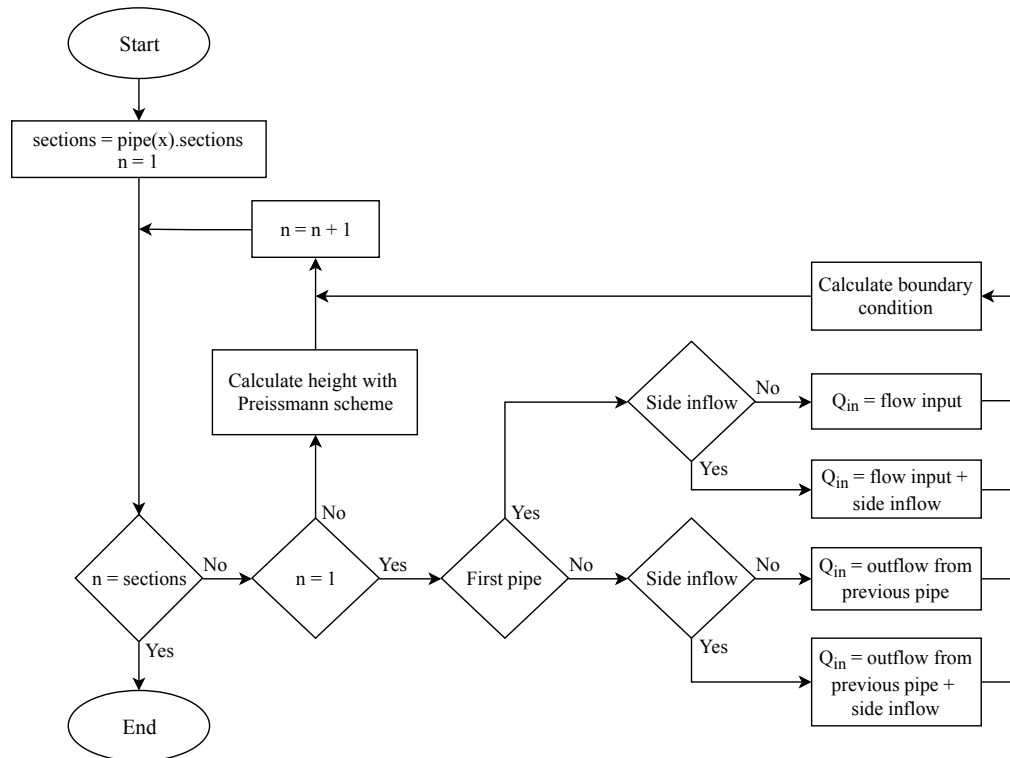


Figure 5.27: Pipe function.

The function is given inflow, pipe\_comp, pipe specifications, iteration value “m”, part index “x” and data stored at index “Sys\_comp”. Once again iteration and part index are used to fetch previous values of height and concentrate level, used in the calculation of new values. The value of pipe\_comp is used as an index in “pipe\_spec”. The functionality of the function is to iterate through the sections which the pipe consists of. At the first section,  $n = 1$ , it is determined if the pipe is the first in the specific part. Afterward, it is checked if side inflow is present. If the pipe is the first then inflow needs to be given, otherwise the flow out of the previous pipe is set as inflow. When inflow is obtained, height can be found from either curve fitted polynomial or lookup table as mentioned in the initialization part of the implementation. For the remaining sections in the pipe, the height is found by the Preissmann scheme. Finally, data is returned to the simulation function. To decided upon which of the curve fitted polynomial or lookup table, methods should be implemented a test with the pipe setup shown in figure 5.17 is performed for various iterations. Furthermore, two values of  $\Delta t$  are tested. A sinusoidal input is given for all tests to increase the computational power needed to solve the Preissmann scheme. The input can be seen in figure 5.28.

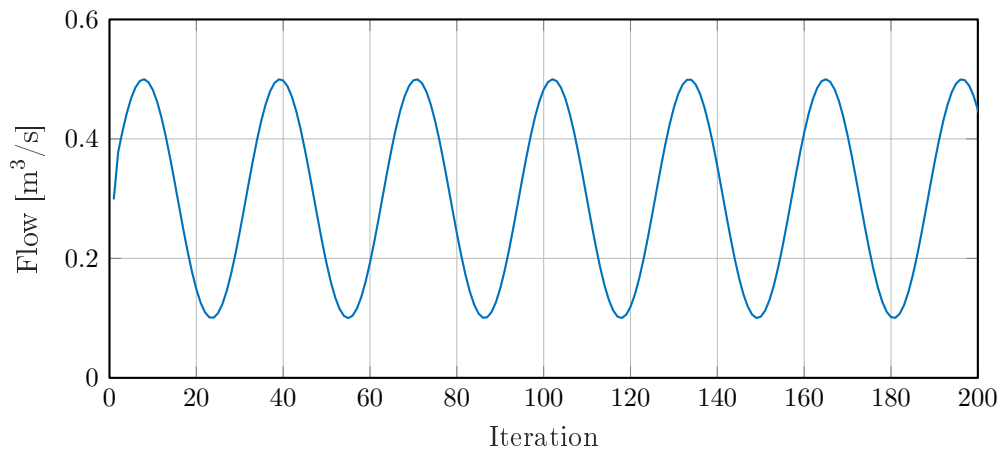


Figure 5.28: Input flow for the comparison test of lookup table and curve fitted polynomial.

The results of the computational tests can be seen in table 5.4, 5.5 and 5.6.

	Run 1	Run 2
$\Delta t$	15 s	20 s
lookup table	4,600 s	4,978 s
Curve fitted polynomial	5,554 s	5,893 s
Difference	20.722 %	18.393 %

Table 5.4: Computation time of 400 iterations.

	Run 1	Run 2
$\Delta t$	15 s	20 s
lookup table	10,073 s	10,574 s
Curve fitted polynomial	11,868 s	11,859 s
Difference	17.817 %	12.153 %

Table 5.5: Computation time of 800 iterations.

	Run 1	Run 2
$\Delta t$	15 s	20 s
lookup table	30,380 s	30,776 s
Curve fitted polynomial	33,247 s	34,194 s
Difference	9.437 %	11.105 %

Table 5.6: Computation time of 2000 iterations.

The results are obtained by using the MATLAB function “tic-toc” on the main simulation loop shown in figure 5.24. Furthermore, a laptop with an I7-4710MQ processor at 3,4 GHz is used for the test. Clearly, the lookup table is preferable both in accuracy and computational speed. For this reason, it is implemented as the solution to obtain fluid height boundary condition from an inflow of the pipe.

## Display result

The areas of interest chosen to be displayed are, as mentioned in section 5.1, flow, height, concentrate and concentrate flow. In figure 5.29 a flowchart of the constructed playback function to examine the simulation result is seen

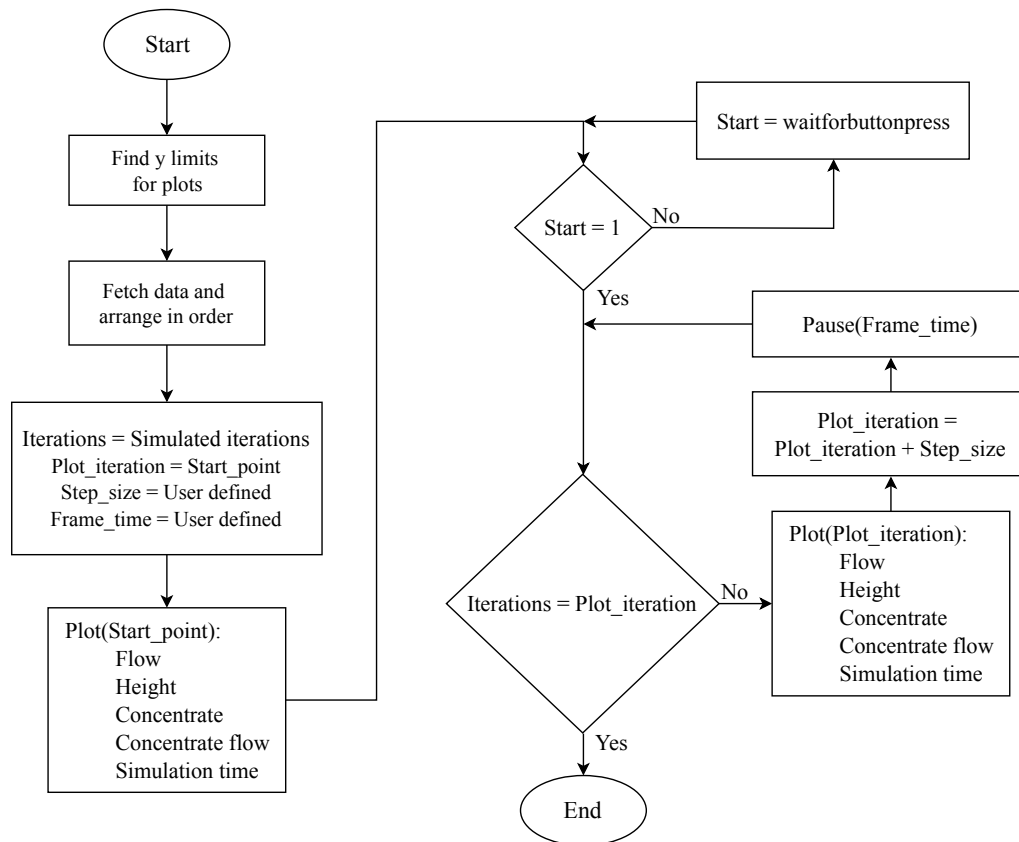


Figure 5.29: Flowchart of playback function.

The first thing that is done in the playback function is finding minimum and maximum values for the y-axis. This is done such that the graph can not move outside the plot. Furthermore, another setting where space, corresponding to a user defined percentage, at the top and bottom of the plot is unused. An initial value of ten percent at top and bottom is set, which leaves 80 percent of the window to be used by the graph during playback. Secondly, the data for all the components are fetched into a matrix such that the MATLAB plot function can be utilized. Furthermore, x-axis data is scaled correctly according to the number of components, various  $\Delta x$ , intersections and tanks. Afterward “Iteration” is set to the value of iterations which has been simulated, “Plot\_iteration” is set to the iteration from where the playback is to start from, “step\_size” is set to the number of iterations to skip during playback. Lastly “frame\_time” is set, which decides the speed of the playback. The maximum speed is in the end decided by the processor available to MATLAB and due to the plot function is known to be computationally demanding, a low amount of updates per second should be expected. The defined iteration or boundary conditions, if “Start\_point” is set to zero, is plotted before the playback is put on hold. Playback is now started by clicking on the window holding the plots and continues iterating in the predefined step size and frame time.

This concludes on the implementation part of the simulation. The next section will go into details about the setup of the model predictive control scheme chosen for this project.

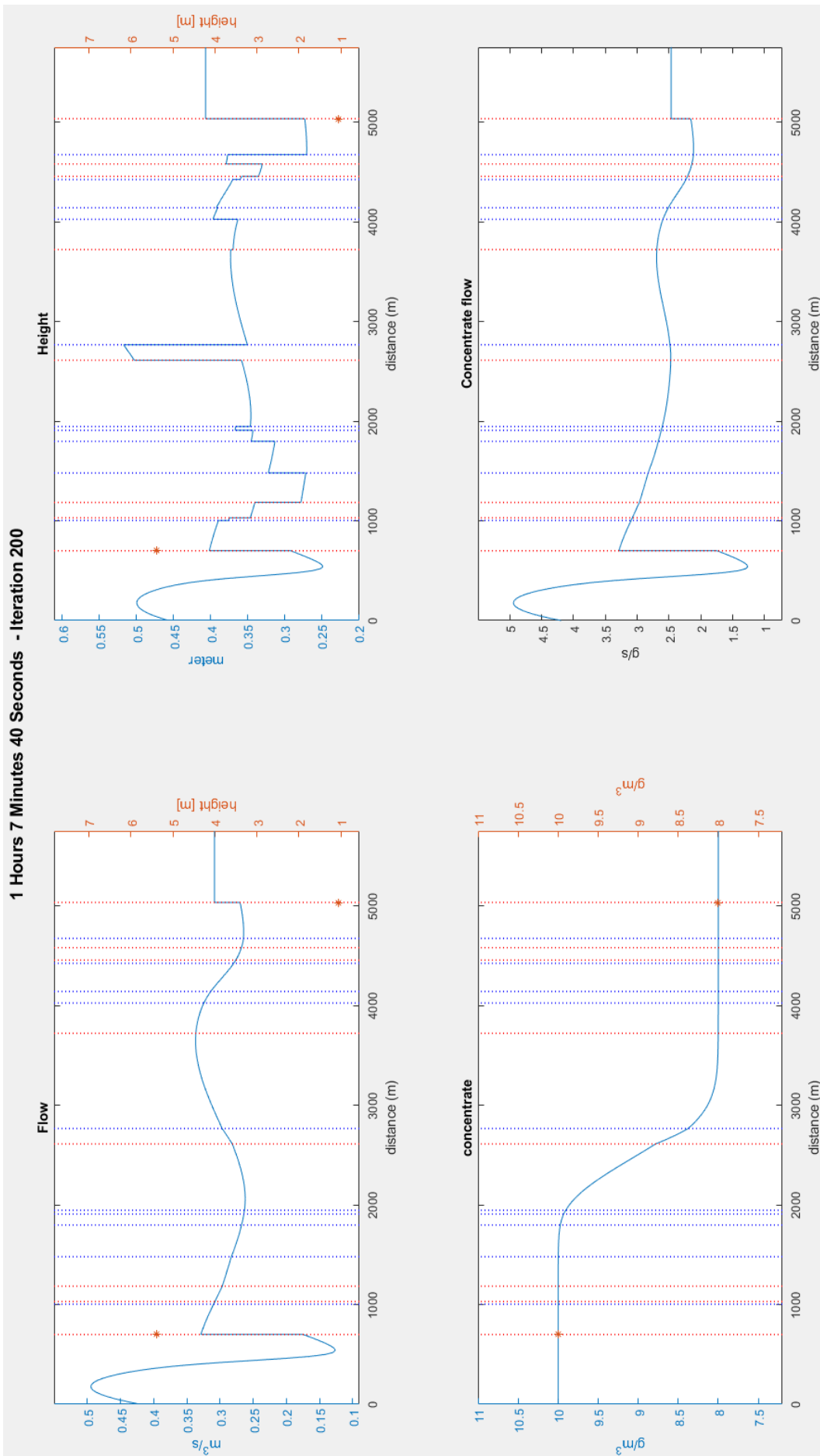


Figure 5.30: Screen shot of the plots made by the playback function where a sinusoidal flow input and step in concentrate is given, red dotted lines indicate pipe intersection and blue dotted lines are intersections with side inflow and stars are tanks inserted. In the simulation the pipe configuration seen in figure 5.17 is used and input to the side inflows is not given.



In this chapter the Model Predictive Control scheme is elaborated upon. Furthermore it is decided to construct a linearization function which can produce a linear model of the setup of pipes and tanks. This is to serve as the predictive model utilized in the MPC design. Due to time constraints a linear model containing flow of concentrate in sewer pipes and tanks has not been developed. In the following, the procedure to construct a linearized model of the sewer pipes and tanks from the nonlinear setup is elaborated on.

## 6.1 Linearization

The linearization of the setup can be split into two parts, the first being linearization of pipes and the second of tanks.

Linearization of pipes is elaborated in the following. If the simulation environment should be setup with a real sewer system it would be ideal to have a linear model which could mimic a real world situation. In real systems measurements from all states, which in this case is flow and height in the amount of sections each pipe consists of, is rarely available. In these cases states are often estimated by an observer or a Kalman filter. By the assumption that height measurements are a more obtainable solution, due to the hostile environment, which sewers typically consists of, it is decided to proceed with a linearized model where the states represent fluid height.

The continuity equation from section 4.1, and the equation that describes flow in a pipe knowing the height, is used.

$$\frac{\partial A(x, t)}{\partial t} + \frac{\partial Q(x, t)}{\partial x} = 0 \quad (6.1)$$

$$Q = f(h) = \left( 0.46 - 0.5 \cdot \cos\left(\pi \frac{h}{d}\right) + 0.04 \cdot \cos\left(2\pi \frac{h}{d}\right) \right) Q_f \quad (6.2)$$

First the continuity equations is expanded to the following:

$$\frac{\partial A(h)}{\partial h} \frac{\partial h(x, t)}{\partial t} + \frac{\partial Q(h)}{\partial h} \frac{\partial h(x, t)}{\partial x} = 0 \quad (6.3)$$

By applying equation 5.5 and 5.6, from the Preissmann scheme in section 5.2, on the

partial derivate of h in terms of time and position, the following is obtained:

$$\begin{aligned} \frac{\partial A(h)}{\partial h} \left( \frac{1}{2} \frac{h_{j+1}^{i+1} - h_{j+1}^i}{\Delta t} + \frac{1}{2} \frac{h_j^{i+1} - h_j^i}{\Delta t} \right) + \\ \frac{\partial Q(h)}{\partial h} \left( \theta \frac{h_{j+1}^{i+1} - h_{j+1}^i}{\Delta x} + (1 - \theta) \frac{h_{j+1}^i - h_j^i}{\Delta x} \right) = 0 \end{aligned} \quad (6.4)$$

Where the derivate of Q given h can be found by taking the derivate of equation 6.2 with respect to h, and the derivate of A can be found by taking the derivate of the following equation with respect to h:

$$A = \frac{d^2}{4} \cdot \operatorname{acos} \left( \frac{\frac{d}{2} - h}{\frac{d}{2}} \right) - \sqrt{h \cdot (d - h)} \cdot \left( \frac{d}{2} - h \right) \quad (6.5)$$

Setting equation 6.4 onto matrix form yields the following:

$$\begin{aligned} \left[ \underbrace{\frac{1}{2\Delta t} \frac{\partial A}{\partial h} - \frac{\theta}{\Delta x} \frac{\partial Q}{\partial h}}_a \quad \underbrace{\frac{1}{2\Delta t} \frac{\partial A}{\partial h} + \frac{\theta}{\Delta x} \frac{\partial Q}{\partial h}}_b \right] \begin{bmatrix} h_j^{i+1} \\ h_{j+1}^{i+1} \end{bmatrix} = \\ - \left[ \underbrace{\frac{-1}{2\Delta t} \frac{\partial A}{\partial h} - \frac{(1-\theta)}{\Delta x} \frac{\partial Q}{\partial h}}_c \quad \underbrace{\frac{-1}{2\Delta t} \frac{\partial A}{\partial h} + \frac{\theta}{\Delta x} \frac{\partial Q}{\partial h}}_d \right] \begin{bmatrix} h_j^i \\ h_{j+1}^i \end{bmatrix} \end{aligned} \quad (6.6)$$

This equation can be written on state space form, where the heights are the states of the state space system and a, b, c, and d are the parameters in the system matrix and the input vector.

$$x(k+1) = Ax(k) + Bu(k) + B_d d(k) \quad (6.7)$$

Where A is the system matrix, x is the states of the system, B is the input vector, u is the input,  $B_d$  is the input disturbance vector and d is the disturbance input. By utilizing equation 6.6 the following can be written:

$$\begin{aligned} \underbrace{\begin{bmatrix} 1 & 0 & 0 & \cdots & 0 \\ 0 & b_1 & 0 & \cdots & 0 \\ 0 & a_1 & b_2 & \cdots & \vdots \\ \vdots & \vdots & \ddots & \ddots & 0 \\ 0 & 0 & 0 & a_{m-1} & b_m \end{bmatrix}}_{\xi} \underbrace{\begin{bmatrix} h_0^{i+1} \\ h_1^{i+1} \\ h_2^{i+1} \\ \vdots \\ h_m^{i+1} \end{bmatrix}}_{x(k+1)} = \underbrace{\begin{bmatrix} 0 & 0 & 0 & \cdots & 0 \\ c_0 & d_1 & 0 & \cdots & 0 \\ 0 & c_1 & d_2 & \cdots & 0 \\ \vdots & \vdots & \ddots & \ddots & \vdots \\ 0 & 0 & 0 & c_{m-1} & d_m \end{bmatrix}}_A \underbrace{\begin{bmatrix} h_0^i \\ h_1^i \\ h_2^i \\ \vdots \\ h_m^i \end{bmatrix}}_{x(k)} + \\ \underbrace{\begin{bmatrix} 1 \\ -a_0 \\ 0 \\ \vdots \\ 0 \end{bmatrix}}_B h_0^{i+1} + \underbrace{\begin{bmatrix} \frac{dh}{dQ} \\ 0 \\ 0 \\ \vdots \\ 0 \end{bmatrix}}_{B_d} d_0^{i+1} \end{aligned} \quad (6.8)$$

Where  $m$  denotes the total amount of sections in the pipe. To obtain a state space form  $\xi$  needs to be inverted, thereby obtaining the following equation:

$$x(k+1) = \xi^{-1}(Ax(k) + Bu(k) + B_d d(k)) \quad (6.9)$$

By repeating this procedure the desired amount of pipes can be inserted into the linear model. Due to equation 6.6 containing discretizing elements in the form of  $\Delta t$  and  $\Delta x$  no discretizing of the state space system should be necessary. A verification in the form of a comparison of the nonlinear and linear system is performed further on.

The change of height within the tank is given by  $h = Q_{in} - Q_{out}$ .

As the input to the tank is a height in an adjoining pipe the inflow to the tank needs to be obtained from it. This means that the derivative of  $h(Q)$  is needed. As mentioned in section 5.5 equation 6.2 can not be solved for  $h$  analytically. Instead a curve fitted polynomial is created for the inflowing pipe and the derivative is obtained by the MATLAB function "differentiate". The increase in height within the tank by the inflow is given by:

$$h_{inflow} = h_{pipe} \cdot \frac{dh}{dQ} \cdot \frac{1}{A} \cdot \Delta t \quad (6.10)$$

Where  $h_{pipe}$  is the inflow height in the adjoining pipe and  $A$  is the vertical cross section area of the tank.

The outflow of the tank is due to being controlled by the pump split into two parts. The first being the change in height within the tank due to the pump, and secondly the height into the adjoining pipe due to the outflow controlled by the pump. As seen in equation 4.46 the outflow of the tank is already a linear term, therefore the reduction in height due to the pump is:

$$h_{pump} = u_{pump} \cdot Q_{max\_out} \cdot \Delta t \quad (6.11)$$

The change of height is then given by:

$$h_{tank} = h_{inflow} - h_{pump} \quad (6.12)$$

Finally the inflow to the adjoining pipe is given by:

$$h_{outflow} = \frac{dQ}{dh} \cdot u_{pump} \cdot Q_{max\_out} \quad (6.13)$$

Where the derivative is found by curve fitted polynomial and the MATLAB function "differentiate". Utilizing the same indexing scheme on equation 6.10, 6.11 and 6.13 as in equation 6.6 the following is given:

$$\underbrace{\frac{dh}{dQ} \cdot \frac{1}{A} \cdot \Delta t}_e, \underbrace{u_{pump} \cdot Q_{max\_out} \cdot \Delta t}_f, \underbrace{\frac{dQ}{dh} \cdot u_{pump} \cdot Q_{max\_out}}_g$$

An example of how the tank is implemented in a state space system in between two pipes,

can be seen in equation 6.14

$$\begin{aligned}
 & \underbrace{\begin{bmatrix} 1 & 0 & 0 & 0 & 0 & 0 & 0 \\ 0 & b_{1,1} & 0 & 0 & 0 & 0 & 0 \\ 0 & a_{1,1} & b_{1,2} & 0 & 0 & 0 & 0 \\ 0 & 0 & 0 & 1 & 0 & 0 & 0 \\ 0 & 0 & 0 & 0 & 1 & 0 & 0 \\ 0 & 0 & 0 & 0 & a_{2,1} & b_{2,2} & 0 \\ 0 & 0 & 0 & 0 & 0 & a_{2,2} & b_{2,3} \end{bmatrix}}_{\xi} \underbrace{\begin{bmatrix} h_{1,0}^{i+1} \\ h_{1,1}^{i+1} \\ h_{1,2}^{i+1} \\ h_{tank}^{i+1} \\ h_{2,0}^{i+1} \\ h_{2,1}^{i+1} \end{bmatrix}}_{x(k+1)} \\
 = & \underbrace{\begin{bmatrix} 0 & 0 & 0 & 0 & 0 & 0 & 0 \\ c_{1,0} & d_{1,1} & 0 & 0 & 0 & 0 & 0 \\ 0 & c_{1,1} & d_{1,2} & 0 & 0 & 0 & 0 \\ 0 & 0 & e & 1 & 0 & 0 & 0 \\ 0 & 0 & 0 & 0 & 0 & 0 & 0 \\ 0 & 0 & 0 & 0 & c_{2,0} & d_{2,1} & 0 \\ 0 & 0 & 0 & 0 & 0 & c_{2,1} & d_{2,2} \end{bmatrix}}_A \underbrace{\begin{bmatrix} h_{1,0}^i \\ h_{1,1}^i \\ h_{1,2}^i \\ h_{tank}^i \\ h_{2,0}^i \\ h_{2,1}^i \\ h_{2,2}^i \end{bmatrix}}_{x(k)} + \underbrace{\begin{bmatrix} 1 & 0 \\ -a_0 & 0 \\ 0 & 0 \\ 0 & -f \\ 0 & g \\ 0 & 0 \\ 0 & 0 \end{bmatrix}}_B \begin{bmatrix} h_0^{i+1} \\ u_{tank} \end{bmatrix} \tag{6.14}
 \end{aligned}$$

Where subscripts indicate pipe and section number, and for simplification the disturbance input is not shown.

A test of the linear system has been conducted to verify if the linear model has a similar response of the nonlinear model for small perturbations. In table 6.1 the system setup which is used to verify the linear model is seen.

Type	Components	Sections
Pipe	1	35
Tank	1	1
Pipe	18	227
Total	20	263

Table 6.1: System setup for verification of linear model.

What is important to remember before simulating is that the state space system is a small signal model. This is also the reason why the nonlinear systems needs to be brought into steady state before the linearized model is obtained. If the system is not in steady state the linearized model is most likely going to yield an undesirable result. The first part shown in table 6.1 has the specifications seen in table 6.2.

Part number	Length [m]	Sections	Dx [m]	Sb	d [m]	$\theta$	$Q_f [m^3/s]$
1	700	35	20	0,003	0,9	0,65	0,972

Table 6.2: Specification of the first pipe in the comparison of the nonlinear with the linear model.

Pipe specifications for the remaining 18 pipes can be seen in figure 5.17. In table 6.3 specifications of the tank can be seen.

Part number	2 (Tank)
Size [ $m^3$ ]	90
Height [m]	10
Area [ $m^2$ ]	9

Table 6.3: Tank specification of the tank used in comparison of the nonlinear model with the linear.

In figure 6.1 the input to the first pipe is seen.

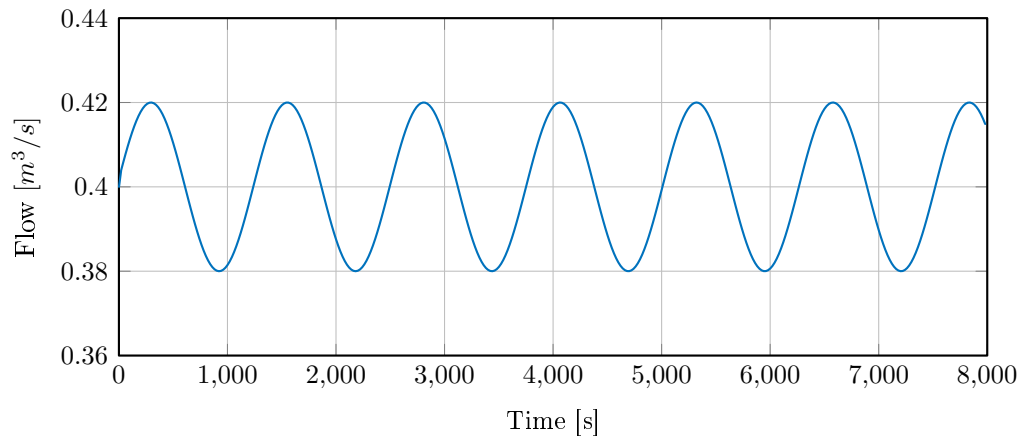


Figure 6.1: Input flow to the first pipe.

A sinusoidal input flow to the simulation setup is given, to compare the response of the nonlinear and linear model. In the following figures, comparisons are made between the nonlinear and linear model at different places in the simulation setup. In figure 6.2 the output of the first pipe is shown.

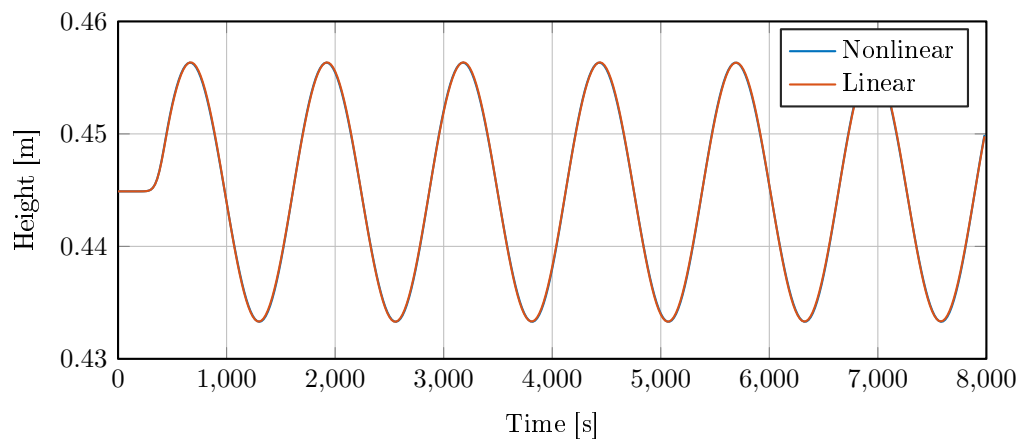


Figure 6.2: Comparison between the nonlinear and linear model at the output of the first pipe.

It can be seen that the linear and nonlinear model for the output of the first pipe are nearly identical, both in phase and amplitude as they follow each other throughout the simulation. In figure 6.3 the height of the tank for the linear and nonlinear model is shown.

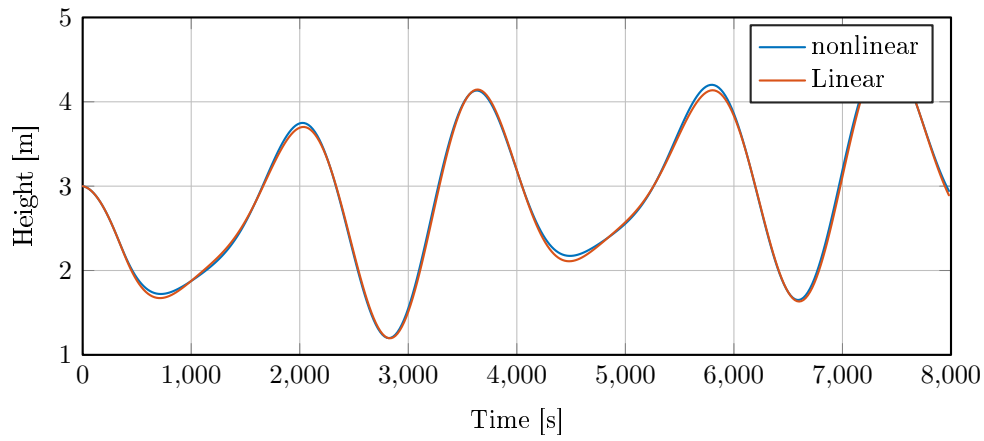


Figure 6.3: Comparison of the nonlinear and linear model for the tank.

It is clear that the nonlinear and linear model for the tank are very similar as they only deviate a small amount at the peaks. In figure 6.4 the output of the pipe after the tank is shown.

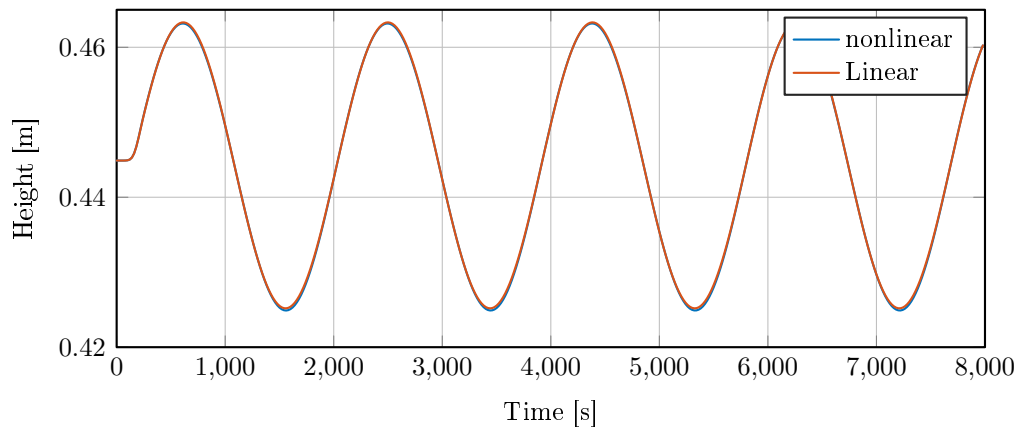


Figure 6.4: Comparison of the nonlinear and linear model of the pipe after the tank.

The output of the second pipe in the sewer network, also shows the linear and nonlinear model are very similar and it is difficult to separate the two plots from another. In figure 6.5 the output of the last pipe in the sewer network can be seen.

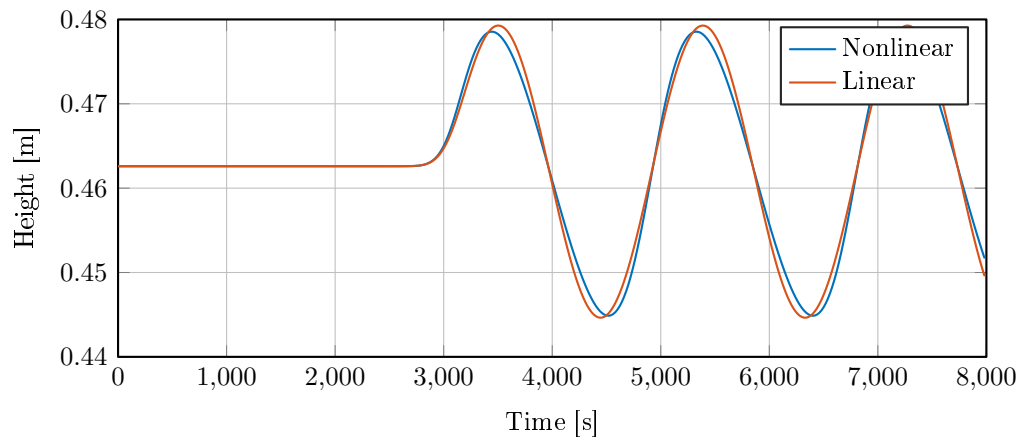


Figure 6.5: Comparison of the nonlinear and linear model at the last pipe in the setup.

A small difference can be seen at the peaks of the two graphs. The nonlinear model starts to rise faster and falls slower than the linear model. However, it can be seen that the two model crosses the operating point at each period and they are similar in phase and amplitude. The linear model, is therefore deemed to be an acceptable linearized model of the nonlinear system for small perturbations. It will therefore be used in the next section in the design of MPC.

## 6.2 Model predictive control

In this section, the design of the controller is elaborated. First the control problem is summarized thereafter Model predictive controller (MPC) is elaborated followed by the design of the MPC controller and ending with the implementation and results of the simulation.

The simulation covered in chapter 5 is to be controlled with respect to the problems elaborated in section 1.4 and stated below.

1. Flow variations due to large industries and natural phenomena
2. Concentration variations due to large industries and natural phenomena
  - a) Chloride variations
  - b) Phosphorus variations
  - c) Nitrogen variations
  - d) Organic matter variations

From the problem statement, it is given that flow and concentration variations must be kept to a minimum without causing overflow in the sewer. To achieve this, tanks are used. These are placed in the sewer network in locations where they are able to minimize flow and concentration variations into the WWTP. However, the output of these tanks must be controlled in a way such that overflow in the tank does not occur. Furthermore the size and location of these tanks can be hard to determine. Therefore implementing an optimal control, which can operate the system close to limits of the system, can help determine if the tank is located and dimensioned properly.

MPC algorithm consists of:

**Cost function** or control objective,  $\mathcal{J}$ , is a criterion when measuring e.g. the difference between future outputs and a reference while at the same time having in mind that any

control action is costly for the system. Therefore the price is measured in the cost function over the prediction horizon,  $H_p$ . This function is therefore minimized with respect to the future control input to minimize the cost [Ruscio, 2001].

**Constraints** is a unique advantage of MPC. They can be applied to the process variables e.g. on the states of the system to keep them within a defined limit. Furthermore, they are usually written as inequality constraints,  $Ax \leq b$ , where the optimization problem is subject to the constraint [Ruscio, 2001].

**Prediction model** is as the name indicates, able to predict future system behavior. The model describes the in- and output behavior of the system over the prediction horizon [Ruscio, 2001].

For MPC to optimize the system a cost function must be written to penalize variations of the flow output  $Q(k+i|k)$  and the concentration output  $C(k+i|k)$ . Where  $k$  defines the prediction time and  $i$  is a value going from 1 to  $H_p$ . The cost functions for flow and concentration are:

$$\begin{aligned}
\mathcal{J} = & \sum_{i=1}^{H_p-1} \|Q(k+i|k)C_1(k+i|k) - Q(k+i-1|k)C_1(k+i-1|k)\|_{\mathcal{Q}_1(i)}^2 \\
& + \sum_{i=1}^{H_p-1} \|Q(k+i|k)C_2(k+i|k) - Q(k+i-1|k)C_2(k+i-1|k)\|_{\mathcal{Q}_2(i)}^2 \\
& + \sum_{i=1}^{H_p-1} \|Q(k+i|k)C_3(k+i|k) - Q(k+i-1|k)C_3(k+i-1|k)\|_{\mathcal{Q}_3(i)}^2 \\
& + \sum_{i=1}^{H_p-1} \|Q(k+i|k)C_4(k+i|k) - Q(k+i-1|k)C_4(k+i-1|k)\|_{\mathcal{Q}_4(i)}^2 \\
& + \sum_{i=1}^{H_p-1} \|Q(k+i|k) - Q(k+i-1|k)\|_{\mathcal{Q}_5(i)}^2
\end{aligned} \tag{6.15}$$

Where  $\mathcal{J}$  is the cost function that needs to be minimized,  $Q$  is the flow,  $C$  is the concentration and  $\mathcal{Q}$  is a weighting parameter. The concentrations  $C_1, C_2, C_3$  and  $C_4$  are respectively chloride, phosphorus, nitrogen and organic matter levels in the wastewater. However, due to delimitations in section 2 the concentrate is limited to a single component. Due to time constraints, it has been decided to keep a focus on minimizing flow variations and limit the complexity of implementing MPC. The cost function is therefore limited to the following:

$$\begin{aligned}
\mathcal{J} = & \sum_{i=1}^{H_p-1} \|\hat{y}(k+i|k) - \hat{y}(k+i-1|k)\|_{\mathcal{Q}(i)}^2 \\
\text{s.t.} \quad & \hat{x}(k+i+1) = A\hat{x}(k+i|k) + B\hat{u}(k+i|k) + B_d\hat{d}(k+i|k) \\
& \hat{y}(k+i) = C\hat{x}(k+i|k) \\
& x_{min} \leq x \leq x_{max} \\
& u_{min} \leq u \leq u_{max}
\end{aligned} \tag{6.16}$$

Where  $Q$  has been replaced with the output  $y$  as it can be measured directly from the state space system. The hat denotes a small signal value of  $y$ . This notation is used throughout the chapter. Where  $y$  corresponds to the height of fluid in the pipe. Minimizing height difference corresponds to minimizing flow differences, as to both describe the variation in the output of the sewer. Furthermore, the cost function is subject to constraints on the states and the control input. Both the states and the control input have a lower and upper constraint corresponding respectively to the bottom of the pipe and the top of the pipe and respectively to the minimum and maximum control input to the pump. In order for the controller to minimize the variations in the output, it must be able to predict future events from the current state. Therefore, by iterating the linear model, obtained in section 6.1, for the duration of the prediction horizon the controller is able to predict future states [Maciejowski, 2002].

In equation 6.17 the recursively use of the state equation is seen.

$$\begin{aligned}
\hat{x}(k+1|k) &= A\hat{x}(k|k) + B\hat{u}(k|k) + B_d\hat{d}(k|k) \\
\hat{x}(k+2|k) &= A\hat{x}(k+1|k) + B\hat{u}(k+1|k) + B_d\hat{d}(k+1|k) \\
&= A^2\hat{x}(k|k) + AB\hat{u}(k|k) + AB_d\hat{d}(k|k) + B\hat{u}(k+1|k) \\
&\quad + B_d\hat{d}(k+1|k) \\
&\quad \vdots \\
\hat{x}(k+H_p|k) &= A\hat{x}(k+H_p-1|k) + B\hat{u}(k+H_p-1|k) + B_d\hat{d}(k+H_p-1|k) \\
&= A^{H_p}\hat{x}(k|k) + A^{H_p-1}B\hat{u}(k|k) + \dots + B\hat{u}(k+H_p-1|k) \\
&\quad + A^{H_p-1}B_d\hat{d}(k|k) + \dots + B_d\hat{d}(k+H_p-1|k)
\end{aligned} \tag{6.17}$$

Here the first equation  $\hat{x}(k+1|k)$  is inserted into the second and this is iterated up to the prediction horizon. This can be set up as prediction vectors and matrices denoted by  $\mathcal{X}$ ,  $\mathcal{A}$ ,  $\mathcal{B}$ ,  $\mathcal{U}$ ,  $\mathcal{B}_d$  and  $\mathcal{D}$  as shown in equation 6.18.

$$\begin{aligned}
\underbrace{\begin{bmatrix} \hat{x}(k+1|k) \\ \hat{x}(k+2|k) \\ \vdots \\ \hat{x}(k+H_p|k) \end{bmatrix}}_{\mathcal{X}} &= \underbrace{\begin{bmatrix} A \\ A^2 \\ \vdots \\ A^{H_p} \end{bmatrix}}_{\mathcal{A}} \hat{x}(k|k) \\
&+ \underbrace{\begin{bmatrix} B & 0 & \dots & 0 \\ AB & B & \dots & 0 \\ \vdots & \vdots & \ddots & \vdots \\ A^{H_p-1}B & A^{H_p-2}B & \dots & B \end{bmatrix}}_{\mathcal{B}} \underbrace{\begin{bmatrix} \hat{u}(k|k) \\ \hat{u}(k+1|k) \\ \vdots \\ \hat{u}(k+H_p-1|k) \end{bmatrix}}_{\mathcal{U}} \\
&+ \underbrace{\begin{bmatrix} B_d & 0 & \dots & 0 \\ AB_d & B_d & \dots & 0 \\ \vdots & \vdots & \ddots & \vdots \\ A^{H_p-1}B_d & A^{H_p-2}B_d & \dots & B_d \end{bmatrix}}_{\mathcal{B}_d} \underbrace{\begin{bmatrix} \hat{d}(k|k) \\ \hat{d}(k+1|k) \\ \vdots \\ \hat{d}(k+H_p-1|k) \end{bmatrix}}_{\mathcal{D}}
\end{aligned} \tag{6.18}$$

Where  $\mathcal{X}$  is the predicted state vector for the entire prediction horizon.  $\mathcal{A}$  is the state matrix up to the prediction horizon. The initial state is  $x(k|k)$  and is used to predict over

the prediction horizon,  $\mathcal{B}$  is the predicted input matrix over the prediction horizon,  $\mathcal{U}$  is the predicted input vector, which consists of all the predicted inputs from the current time step until  $(k + H_p - 1)$ .  $\mathcal{B}_d$  is the disturbance matrix for the prediction horizon and  $\mathcal{D}$  is the disturbance vector.

This iteration process is also performed for the output equation.

$$\hat{\mathcal{Y}}(k) = \underbrace{\begin{bmatrix} \hat{y}(k+1|k) \\ \hat{y}(k+2|k) \\ \vdots \\ \hat{y}(k+H_p-1|k) \end{bmatrix}}_{\mathcal{Y}} = \underbrace{\begin{bmatrix} C & 0 & \cdots & 0 \\ 0 & C & \cdots & 0 \\ \vdots & \vdots & \ddots & 0 \\ 0 & 0 & 0 & C \end{bmatrix}}_{\mathcal{C}} \underbrace{\begin{bmatrix} \hat{x}(k+1|k) \\ \hat{x}(k+2|k) \\ \vdots \\ \hat{x}(k+H_p|k) \end{bmatrix}}_{\mathcal{X}} \quad (6.19)$$

Where  $\mathcal{C}$  is a diagonal matrix with the output matrix  $C$  in the diagonal. By inserting the predicted state equation 6.18, into the predicted output equation 6.19 the following is achieved:

$$\hat{\mathcal{Y}}(k) = \mathcal{C}\mathcal{A}\hat{x}(k) + \mathcal{C}\mathcal{B}\hat{\mathcal{U}}(k) + \mathcal{C}\mathcal{B}_d\hat{\mathcal{D}}(k) \quad (6.20)$$

By using the following notation on equation 6.20:

$$\psi = \mathcal{C}\mathcal{A} \quad \gamma = \mathcal{C}\mathcal{B} \quad \Theta = \mathcal{C}\mathcal{B}_d \quad (6.21)$$

The predicted output equation can be rewritten as:

$$\hat{\mathcal{Y}}(k) = \psi\hat{x}(k) + \gamma\hat{\mathcal{U}}(k) + \Theta\hat{\mathcal{D}}(k) \quad (6.22)$$

To be able to utilize the cost function, in equation 6.16, it has to be rewritten in terms of the predicted output equation 6.22. Thereby replacing the output  $y$  with the predicted output  $\mathcal{Y}$ , the following is obtained:

$$\mathcal{J} = \|\hat{\mathcal{Y}}(k) - \hat{\mathcal{Y}}(k-1)\|_{\mathcal{Q}(i)}^2 \quad (6.23)$$

Where the difference between  $\hat{\mathcal{Y}}(k)$  and  $\hat{\mathcal{Y}}(k-1)$  can be expressed as:

$$\Delta\hat{\mathcal{Y}}(k) = \hat{\mathcal{Y}}(k) - \hat{\mathcal{Y}}(k-1) \quad (6.24)$$

Furthermore, it is desired to have the control input as  $\Delta\mathcal{U}$  as this will introduce integral action and thereby eliminate steady state error [Maciejowski, 2002]. Doing so, equation 6.22 is inserted into equation 6.24 and thereby obtaining:

$$\begin{aligned} \Delta\hat{\mathcal{Y}}(k) &= (\psi\hat{x}(k) + \gamma\hat{\mathcal{U}}(k) + \Theta\hat{\mathcal{D}}(k)) - (\psi\hat{x}(k-1) + \gamma\hat{\mathcal{U}}(k-1) + \Theta\hat{\mathcal{D}}(k-1)) \\ &= \psi\Delta\hat{x}(k) + \gamma\Delta\hat{\mathcal{U}}(k) + \Theta\Delta\hat{\mathcal{D}}(k) \end{aligned} \quad (6.25)$$

Thereby  $\Delta\mathcal{U}$  is introduced in the predicted output. The cost function in equation 6.23 can be reformulated to the following by using equation 6.24:

$$\begin{aligned}\mathcal{J} &= \|\Delta\hat{\mathcal{Y}}(k)\|_{Q(i)}^2 \\ &= \Delta\hat{\mathcal{Y}}(k)^T \cdot Q \cdot \Delta\hat{\mathcal{Y}}(k)\end{aligned}\tag{6.26}$$

To be able to write the cost function as quadratic and linear terms of the predicted input,  $\Delta\mathcal{U}$ , equation 6.25 is therefore inserted into the cost function, in equation 6.26, from which the following is obtained:

$$\mathcal{J} = (\psi\Delta\hat{x}(k) + \gamma\Delta\hat{\mathcal{U}}(k) + \Theta\Delta\hat{\mathcal{D}}(k))^T \cdot Q \cdot (\psi\Delta\hat{x}(k) + \gamma\Delta\hat{\mathcal{U}}(k) + \Theta\Delta\hat{\mathcal{D}}(k))\tag{6.27}$$

The term on the right hand side of equation 6.27 is equal to:

$$\begin{aligned} &(\psi\Delta\hat{x}(k) + \gamma\Delta\hat{\mathcal{U}}(k) + \Theta\Delta\hat{\mathcal{D}}(k))^T \cdot Q \cdot (\psi\Delta\hat{x}(k) + \gamma\Delta\hat{\mathcal{U}}(k) + \Theta\Delta\hat{\mathcal{D}}(k)) = \\ &\Delta\hat{x}(k)^T \psi^T Q \psi \Delta\hat{x}(k) + \underbrace{\Delta\hat{x}(k)^T \psi^T Q \gamma \Delta\hat{\mathcal{U}}(k)}_{\text{Linear}} + \Delta\hat{x}(k)^T \psi^T Q \Theta \Delta\hat{\mathcal{D}}(k) \\ &\underbrace{\Delta\hat{\mathcal{U}}(k)^T \gamma^T Q \psi \Delta\hat{x}(k)}_{\text{Linear}} + \underbrace{\Delta\hat{\mathcal{U}}(k)^T \gamma^T Q \gamma \Delta\hat{\mathcal{U}}(k)}_{\text{Quadratic}} + \underbrace{\Delta\hat{\mathcal{U}}(k)^T \gamma^T Q \Theta \Delta\hat{\mathcal{D}}(k)}_{\text{Linear}} \\ &\Delta\hat{\mathcal{D}}(k)^T \Theta^T Q \psi \Delta\hat{x}(k) + \underbrace{\Delta\hat{\mathcal{D}}(k)^T \Theta^T Q \gamma \Delta\hat{\mathcal{U}}(k)}_{\text{Linear}} + \Delta\hat{\mathcal{D}}(k)^T \Theta^T Q \Theta \Delta\hat{\mathcal{D}}(k)\end{aligned}\tag{6.28}$$

The quadratic and linear terms of  $\Delta\mathcal{U}$  are denoted respectively, the remaining terms which are not denoted in the equation are constants, that will be referred to in the following equations as the constant  $c$ . The quadratic variables are collected in:

$$\mathcal{H} = \gamma^T Q \gamma\tag{6.29}$$

And the linear variables are collected in:

$$\mathcal{G} = 2\Delta\hat{x}(k)^T \psi^T Q \gamma + 2\Delta\hat{\mathcal{D}}(k)^T \Theta^T Q \gamma\tag{6.30}$$

Thereby inserting these expressions in equation 6.28 the following cost function is obtained:

$$\min_{\Delta\mathcal{U}(k)} \mathcal{J}(\Delta\mathcal{U}(k)) = \min_{\Delta\mathcal{U}(k)} \Delta\mathcal{U}(k)^T \mathcal{H} \Delta\mathcal{U}(k) + \mathcal{G} \Delta\mathcal{U}(k) + c\tag{6.31}$$

In the following the constraints, which the cost function is subject to, will be elaborated.

### 6.2.1 Constraints

In order to apply the constraints, shown in equation 6.16 on the states, to the optimization problem in equation 6.31 the constraints must be reformulated so they are a constraint of the control input  $\Delta\mathcal{U}$ . Therefore it is required to reformulate the inequality constraints.

The constraints applied to the states are upper and lower bound to the pipe and the tank. This will if possible limit over- and underflow in pipes and tanks due to the nature of the linearized model. In the following equation the constraints for the predicted states are shown:

$$x_{min} \leq \mathcal{X}(k) \leq x_{max} \quad (6.32)$$

Where  $x_{min}$  and  $x_{max}$  are respectively lower and upper bound. Considerations are needed as the linear model is a small signal model and the constraints are made for the nonlinear simulation. The linearization point therefore needs to be subtracted from the lower and upper bounds which thereby transforms the constraints into small signal constraints.

$$x_{min} - \bar{x} \leq \hat{\mathcal{X}}(k) \leq x_{max} - \bar{x} \quad (6.33)$$

To reformulated the constraints the predicted state equation in equation 6.18 is inserted in place of the state vector.

$$x_{min} - \bar{x} \leq \mathcal{A}\hat{x}(k) + \mathcal{B}\hat{\mathcal{U}}(k) + \mathcal{B}\hat{\mathcal{D}}(k) \leq x_{max} - \bar{x} \quad (6.34)$$

However, to make the constraints depending on  $\Delta\mathcal{U}$ , the predicted input can be formulated as  $\mathcal{U}(k) = \mathcal{V}u(k-1) + W\Delta\mathcal{U}(k)$ , where  $\mathcal{V}$  is a vector and  $W$  is a matrix on the form:

$$\mathcal{V} = \begin{bmatrix} \mathcal{V}_1 \\ \mathcal{V}_2 \\ \vdots \\ \mathcal{V}_{H_p} \end{bmatrix} = \begin{bmatrix} 1 \\ 1 \\ \vdots \\ 1 \end{bmatrix} \quad (6.35)$$

$$W = \begin{bmatrix} w_{1,1} & w_{1,2} & w_{1,3} & w_{1,H_p} \\ w_{2,1} & w_{2,2} & w_{2,3} & w_{2,H_p} \\ w_{3,1} & \vdots & \ddots & w_{3,H_p} \\ w_{H_p,1} & w_{H_p,2} & \cdots & w_{H_p,H_p} \end{bmatrix} = \begin{bmatrix} 1 & 0 & 0 & 0 \\ 1 & 1 & 0 & 0 \\ 1 & \vdots & \ddots & 0 \\ 1 & 1 & \cdots & 1 \end{bmatrix} \quad (6.36)$$

Inserting this into equation 6.34 the following is obtained:

$$x_{min} - \bar{x} \leq \mathcal{A}\hat{x}(k) + \mathcal{B}\mathcal{V}\hat{u}(k-1) + \mathcal{B}W\Delta\hat{\mathcal{U}}(k) + \mathcal{B}\hat{\mathcal{D}}(k) \leq x_{max} - \bar{x} \quad (6.37)$$

Having set the constraints up as a constraint on the input signal they furthermore has to be set up as equality constraints. Therefore are they divided into two constraints one for the upper bound and one for the lower bound.

$$x_{max} - \bar{x} \geq \mathcal{A}\hat{x}(k) + \mathcal{B}\mathcal{V}\hat{u}(k-1) + \mathcal{B}W\Delta\hat{\mathcal{U}}(k) + \mathcal{B}\hat{\mathcal{D}}(k)$$

$$\underbrace{\mathcal{B}W}_{\Lambda} \Delta\hat{\mathcal{U}}(k) \leq \underbrace{x_{max} - \bar{x} - \mathcal{A}\hat{x}(k) - \mathcal{B}\mathcal{V}\hat{u}(k-1) - \mathcal{B}\hat{\mathcal{D}}(k)}_{\Gamma_1} \quad (6.38)$$

$$x_{min} - \bar{x} \leq \mathcal{A}\hat{x}(k) + \mathcal{B}\mathcal{V}\hat{u}(k-1) + \mathcal{B}W\Delta\hat{\mathcal{U}}(k) + \mathcal{B}\hat{\mathcal{D}}(k)$$

$$\underbrace{\mathcal{B}W}_{\Lambda} \Delta\hat{\mathcal{U}}(k) \leq \underbrace{-x_{min} + \bar{x} + \mathcal{A}\hat{x}(k) + \mathcal{B}\mathcal{V}\hat{u}(k-1) + \mathcal{B}\hat{\mathcal{D}}(k)}_{\Gamma_2} \quad (6.39)$$

Constraints are also applied to the control output. The reason for these constraints is to not allow the controller to produce an output that will cause overflow in the pipe after the tank. The constraint on the control output is constructed in the same way as for the states. Below the constraint for the control output is shown:

$$u_{min} \leq \mathcal{U}(k) \leq u_{max} \quad (6.40)$$

The constraint needs to be written for small signal values, and need to depend on  $\Delta\mathcal{U}$ :

$$u_{min} - \bar{u} \leq \mathcal{V}\hat{u}(k-1) + W\Delta\hat{\mathcal{U}}(k) \leq u_{max} - \bar{u} \quad (6.41)$$

The constraint is split up into lower and upper bound for the signal, the upper bound is:

$$\mathcal{V}\hat{u}(k-1) + W\Delta\hat{\mathcal{U}}(k) \leq u_{max} - \bar{u}$$

$$W\Delta\hat{\mathcal{U}}(k) \leq \underbrace{u_{max} - \bar{u} - \mathcal{V}\hat{u}(k-1)}_{\Gamma_3} \quad (6.42)$$

And the lower bound:

$$u_{min} - \bar{u} \leq \mathcal{V}\hat{u}(k-1) + W\Delta\hat{\mathcal{U}}(k)$$

$$-W\Delta\hat{\mathcal{U}}(k) \leq \underbrace{\mathcal{V}\hat{u}(k-1) - u_{min} + \bar{u}}_{\Gamma_4} \quad (6.43)$$

The constraints can be put on standard inequality constraint form and thereby be included in the algorithm for the MPC implementation.

$$\begin{bmatrix} \Lambda \\ -\Lambda \\ W \\ -W \end{bmatrix} \Delta\mathcal{U} \leq \begin{bmatrix} \Gamma_{1.max} \\ \Gamma_{2.min} \\ \Gamma_{3.max} \\ \Gamma_{4.min} \end{bmatrix} \quad (6.44)$$

In the following section, the implementation of the cost function and constraints, shown in this section, in MATLAB will be elaborated

### 6.2.2 Implementation of MPC

In this section the implementation of MPC in MATLAB will be elaborated.

The cost function in equation 6.31 is a quadratic problem. In order to solve this minimization problem and find a global minimum, quadratic programming (QP) is utilized. In MATLAB there exist several solvers for QP problems, in this project Quadprog is the chosen solver. Quadprog solves the minimization problem subject to constraints to the specified convex cost function. The model used as the predictive model is the linear model obtained in section 6.1. Furthermore, the constraints the cost is subject to, as explained in the previous section, is also included.

In figure 6.6 an illustration of a MPC controller is shown.

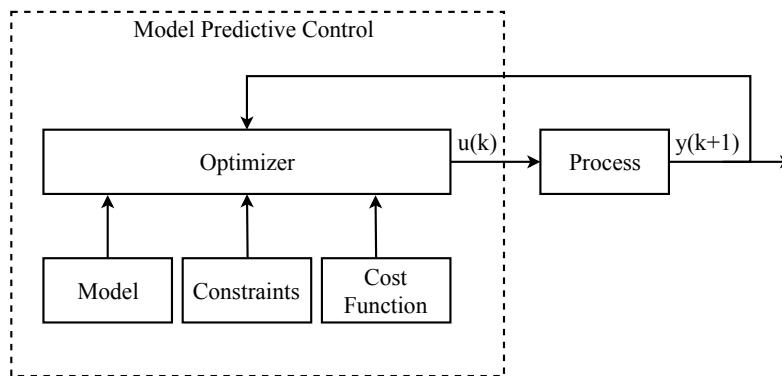


Figure 6.6: Diagram of MPC controller.

Here it is illustrated that the model, constraint and cost function will be used in the optimizer to generate a control output. This will be used in the process, which in this case is the nonlinear model. The output  $y(k+1)$  is the output height at the end of the last pipe in the sewer network, which corresponds to the input of the WWTP. At each time step, the current value of the output is returned to the MPC controller. Here the MPC will at each iteration calculate up to  $H_p$  control inputs, however, only the first element within the  $u$  vector will be used to control the process. Thereafter a new measurement will be taken and a new control output will be calculated. This procedure will iterate for the entire simulation.

In determining the length of the prediction horizon several considerations were taken into account. In figure 1.5 a daily flow from the households is shown. The flow is illustrated for working days and weekend. By knowing the wastewater flow pattern from households the MPC would be able to include this knowledge in the prediction model. Thus an ideal prediction horizon would be 24 hours, as it would be able to see the disturbance across a whole day.

However, as the households are not the only disturbance in this setup this is not entirely true. Because the output from the larger industry e.g. the bottling plant and the brewery are stochastic can be let into the sewer without warning and the periodicity between the

outlets are unknown. Furthermore, the amount of wastewater coming from the industry also varies between outlets. Therefore, it would be preferable not to place the tank next to the industry as it would not be able to predict the disturbance. Thus the tank should be placed at a distance from the industry, where the distance can be used in the prediction model by measurements obtained at the outlet of the industry.

During implementation of the MPC controller, it was discovered that the prediction horizon was restricted. It was not possible to set it higher than 20 iterations or 400 seconds, as the quadratic matrix  $\mathcal{H}$  then became non-convex. The reason is most likely to be found in the linearized model, as some of the elements in the matrices are small, which can result in numerical problems. Therefore, when the system is predicted, it would cause the  $\mathcal{H}$  matrix to have negative eigenvalues. Several tests were conducted to find a prediction horizon that did not result in a negative eigenvalue. A prediction horizon of 400 seconds equal to 20 iterations, would give a quadratic matrix which was convex. However, this restricts the distance from the tank, as the MPC were not able to predict far enough into the future to see the point where the flow variations are to be minimized. Therefore, in the simulation of the MPC controller, this must be kept in mind.

## Results

In this subsection, the results obtained from testing the MPC controller will be covered. Two simulations will be conducted, one where the constraints are neglected and therefore the problem is minimized without any restriction and another simulation where the constraints are included.

The pipe and tank setup for the simulation includes two pipes and one tank, where the tank is placed in between of the pipes. The specification for both pipes and the tank can be seen in tabular 6.4 and 6.5 respectively.

Pipe number	Length [m]	Sections	Dx [m]	$S_b$	d [m]	$\theta$	Qf [ $m^3/s$ ]
1	100	5	20	0,003	0,9	0,65	0,97
2	100	5	20	0,003	0,9	0,65	0,97

Table 6.4: The pipe specification for the simulation.

Size [ $m^3$ ]	90
Height [m]	10
Area [ $m^2$ ]	9
Q_out_max [ $m^3/s$ ]	0,97

Table 6.5: Tank specification for the simulation.

In the first simulation the MPC controller is minimizing the output variations of the tank without any constraints. The input signal into the first pipe is shown in figure 6.7.

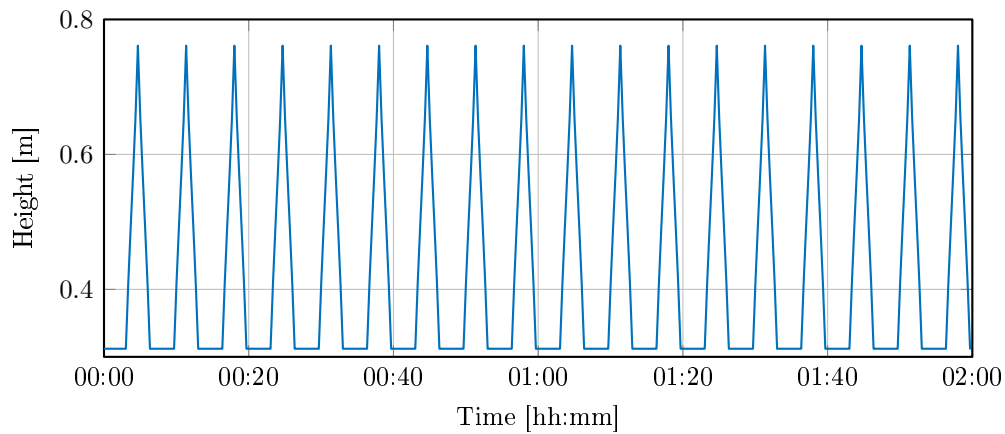


Figure 6.7: Input to the first pipe.

A constant input of  $0,2 \text{ m}^3/\text{s}$ , which results in a height of  $0,31$  meters in the pipe is given. On top of the input, a disturbance signal is added. This is done to verify the functionality of the MPC, being able to keep the flow variations out of the tank at a minimum. The disturbance signal is a triangular signal which spans from zero up to  $0,7 \text{ m}^3/\text{s}$ , which is equal to a height of  $0,75$  meters in the pipe when taking the constant input into consideration. The time between each disturbance peak is  $200$  seconds and the period of the disturbance is  $100$  seconds. The simulation conducted for two hours where  $\Delta t$  is set to  $20$  seconds. In figure 6.8 the output of the last pipe is shown.

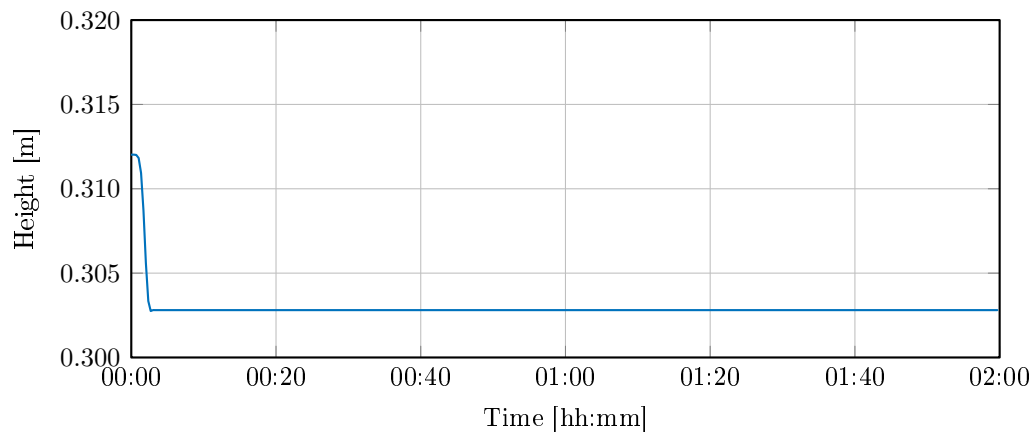


Figure 6.8: Output of the last pipe.

Here it can be seen that the MPC controller is able to minimize the disturbance coming from the first pipe as the output is constant. At the beginning the height of the output is a bit higher, this is due to that the tank holds wastewater at the beginning of the simulation. After it is emptied the height falls to a constant level. In figure 6.9 the fluid height within the tank can be seen.

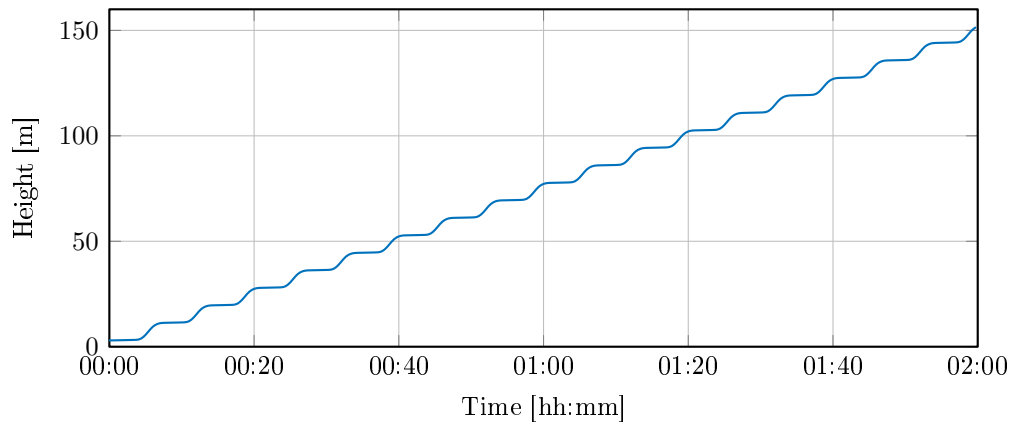


Figure 6.9: Height in the tank.

As expected the tank would be overfilled, as the disturbance coming from the first pipe is much higher than the output of the second. However, the cost function does what is expected, as it keeps a steady output of the tank and has no knowledge about the limitations of the tank and therefore causes overflow. In the second simulation the same input is applied to the first pipe, where the constraints shown in equation 6.2.1 is utilized. In this simulation, only constraints regarding the tank and the control input to the pump is applied. The reason for not having constraints on the height in the second pipe is, that it should be sufficient to have constraints on the control input to the pump. As only inputs between zero and one is allowed. Furthermore, the height constraints for the tank goes from 0 to the maximum height which is set to 10 meters, in this simulation, as seen in table 6.5. The reason for not having constraints on the first pipe is, that it is impossible for the MPC controller to regulate the height in that part. In figure 6.10 the height of the tank is shown from the second simulation.

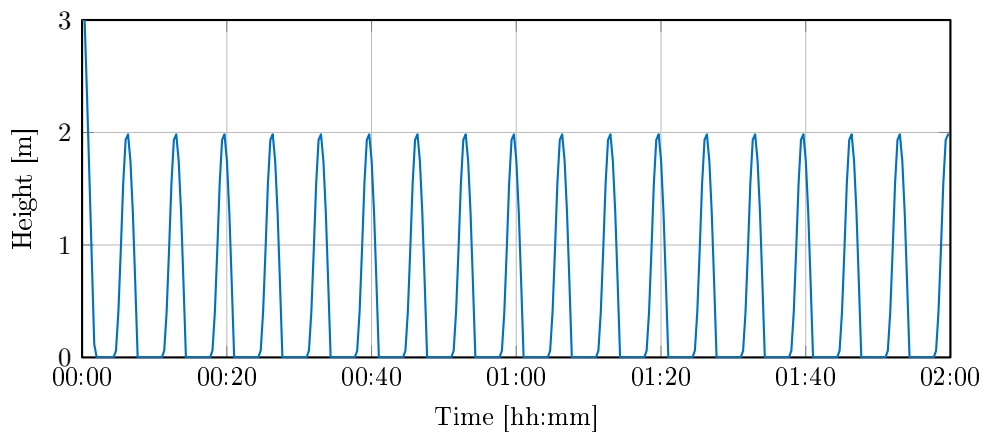


Figure 6.10: Height in the tank at the second simulation run.

It can be seen that the tank does not overflow, thereby it is within the constraints of the tank. At the start of the simulation, the tank is emptied once again. Hereafter the tank is continuously filled with fluid to a level of two meters and then emptied again. In figure 6.11 the output of the second pipe is shown.

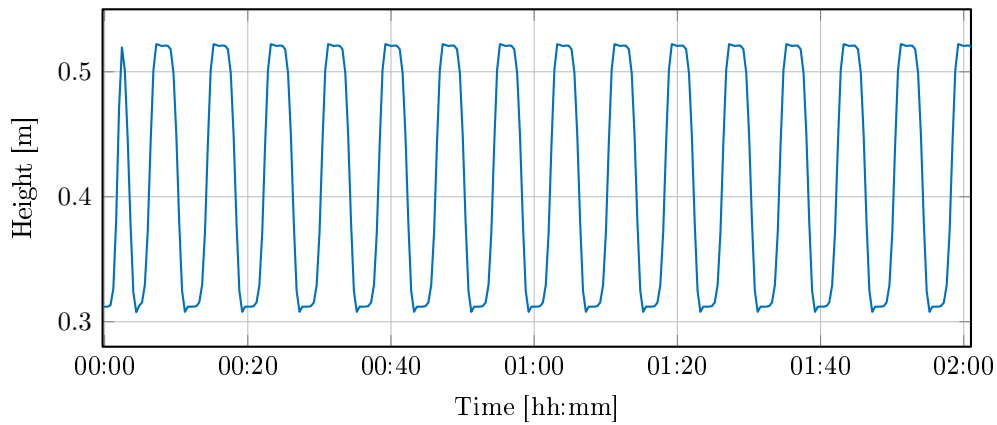


Figure 6.11: Output of the last pipe in the second simulation run.

It is clear from the figure that the variations in the output are not minimized. It fluctuates between two values, the constant input of approximately 0,31 meters and 0,51 meters. In the top and bottom of the curve, it can be seen that the curve flattens. The bottom is due to the tank is empty and therefore, the input, that goes into the tank from the first pipe, goes right into the second pipe without any storage occurring in the tank. When the top flattens the tank start to be filled up, and as it goes down the tank is emptied. It was discovered that the reason for the top is due to constraints on the upper bound for the input, this however, is not a wanted feature. It was desired to get a constant output or a minimum of variations in the output, which is not achieved. Through several tries of changing the parameters of the constraints, e.g. lessen the controller constraints and trying to changing the height of the tank. However, a solution was not found.

The MPC controller does not function as intended and will be concluded upon in the discussion, however in the following chapter the results of the simulation model over the northern part of Fredericia is shown.

# Results 7

In this chapter, a simulation of the northern part of Fredericia will be conducted.

The goal of this simulation is to simulate a daily flow in the northern part of Fredericia. For this purpose the simulation environment explained in chapter 5 is utilized. The pumping station, illustrated with the blue dot in figure 2.1, is not included in this simulation, the reason is that it will have a dampening effect on the disturbances from the larger industry and the surrounding urban areas. To generate the disturbances from the residential and industrial areas, shown in figure 2.1, the flow profiles in appendix A.3 is used. These disturbance models are not simulated in pipes from the various areas into the main sewer line but are directly added into the main sewer line. Therefore the results are expected to have higher peaks, as these models are not attenuated, as they would have been if they were simulated in pipes from the various areas. It has been chosen to only use the disturbance from the brewery and bottling plant, as the data from the refinery weren't available. The disturbances from the brewery and bottling plant are shown in figure 2.4. The pipe specifications for this simulation can be seen in table 7.1.

Component number	Length [m]	Sections	Dx [m]	$S_b$	d [m]	$\theta$	$Q_f$ [ $m^3/s$ ]	side inflow
1	700	35	20	0,003	0,9	0,65	0,973	0
3	303	15	20,2	0,003	0,9	0,65	0,973	0
4	27	2	13,5	0,003	1	0,65	1,284	1
5	155	8	19,4	0,0041	1	0,65	1,50	0
6	295	14	21	0,0122	0,8	0,65	1,438	0
7	318	15	21,2	0,0053	0,9	0,65	1,293	1
8	110	5	22	0,0036	0,9	0,65	1,066	1
9	38	2	19	0,0024	1	0,65	1,149	1
10	665	30	22,2	0,003	1	0,65	1,284	1
11	155	7	22,1	0,0008	1	0,65	0,663	0
12	955	47	20,3	0,0029	1,2	0,65	2,041	1
13	304	15	20,3	0,003	1,2	0,65	2,076	0
14	116	5	23,2	0,0021	1,2	0,65	1,737	1
15	283	12	23,6	0,0017	1,4	0,65	2,346	1
16	31	2	15,5	0,0019	1,4	0,65	2,480	1
17	125	6	20,8	0,0021	1,6	0,65	3,707	0
18	94	4	23,5	0,0013	1,5	0,65	2,461	0
19	360	18	20	0,0046	1,6	0,65	5,487	1
21	736	38	19,4	0,0012	1,6	0,65	2,802	0

Table 7.1: Specification of pipes used in the final simulation.

Tank specifications can be seen in table 7.2.

Part	2 (Tank)	20 (Tank)
Size [ $m^3$ ]	90	90
Height [m]	10	10
Area [ $m^2$ ]	9	9
$Q_{out_{max}}$ [ $m^3/s$ ]	0.973	2.80

Table 7.2: Tank specification for the final simulation.

Furthermore, table 7.3 show the system setup.

Type	Component	Sections
Pipe	1	35
Tank	1	1
Pipe	17	207
Tank	1	1
Pipe	1	38
Total	21	282

Table 7.3: The system setup.

The first pipe and the two tanks have been added to the original sewer network shown in figure 2.2. The first pipe is connected from the larger industrial area to the main sewer line indicated by a black circle in figure 2.1, where the first tank is placed as well. The reason for placing the tank there is, that it should be able to reduce variations in the flow of wastewater coming from the larger industry. Furthermore, the pipe is placed, such that the MPC should be able to use the delay for prediction. However, as this is not possible, due to the problems experienced with the MPC controller, as explained in section 6.2.

The second tank is placed just before the WWTP with the purpose of reducing all variations in flow into the WWTP. Due to the lack of a controller the tanks is given a static input during the simulation.

In figure 7.1 the output of a simulated period of two days can be seen.

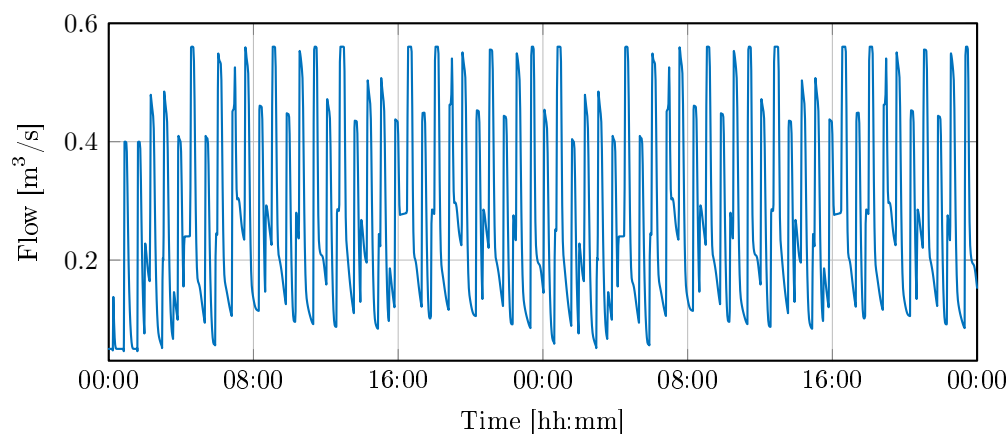


Figure 7.1: Output of the last pipe into the WWTP.

The flow varies considerable as can be seen in figure 2.5 from the real measurements from the WWTP at Fredericia. However, these two can not be directly compared, as the data

from Fredericia also includes the wastewater from the southern part of the city. However, the simulated data results in a greater variation in flow than the data obtained from Fredericia. This could be due to the pumping station, as mentioned previously, that reduces variation in flow from the northern part of the city. Therefore the variations seen on figure 2.5 from Fredericia is likely to be due to disturbance coming from the southern part of the city. By taking the mean of the data in figure 2.5 an inflow of  $0,28 \text{ m}^3/s$  is obtained and doing the same for the data in figure 7.1 a mean of  $0,273 \text{ m}^3/s$  is obtained. This means that the designed flow profiles are over dimensioned.

As no data were available which could give an indication of the amount of COD the brewery or bottling plant produces the output of concentrate is set to  $0,1 \text{ g/m}^3$ . As mentioned in the summary of the meeting with Fredericia which can be seen in appendix A.1 a person produces approximately 120 COD or  $0,2 \text{ g/m}^3$  per day. Therefore it has been chosen to spread this amount per citizen over an entire day such that it fits the flow pattern shown in figure 2.3. In figure 7.2 the concentration at the output of the last pipe is shown.

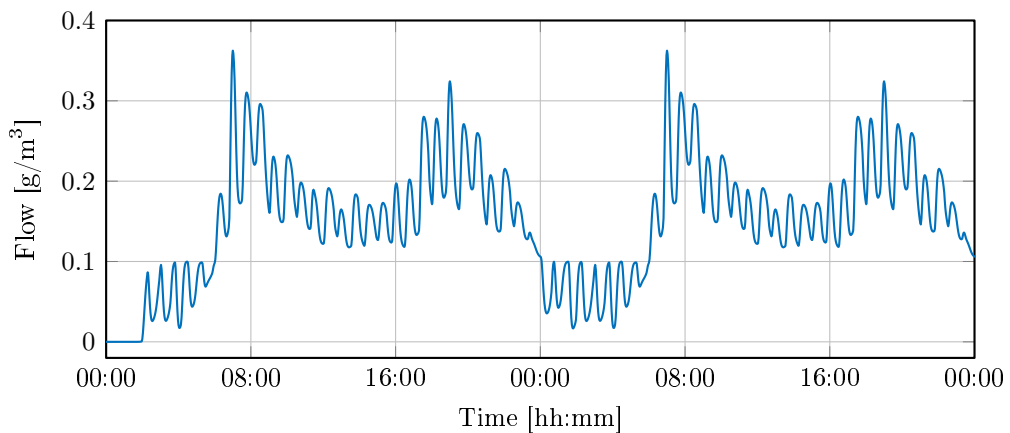


Figure 7.2: Simulation of COD output of the last pipe into the WWTP.

It is clear that the flow pattern is visible in the concentration output, as it can be seen the COD amount is high in the morning when people prepare for work and low during the night as people are at sleep.

A final test was conducted to investigate what a tank could do to the flow if the tank was large enough to contain the wastewater coming from the city. In this test, the tank before the WWTP was increased to  $300 \text{ m}^3$  with a height of 5 m and an area of  $60 \text{ m}^2$ .

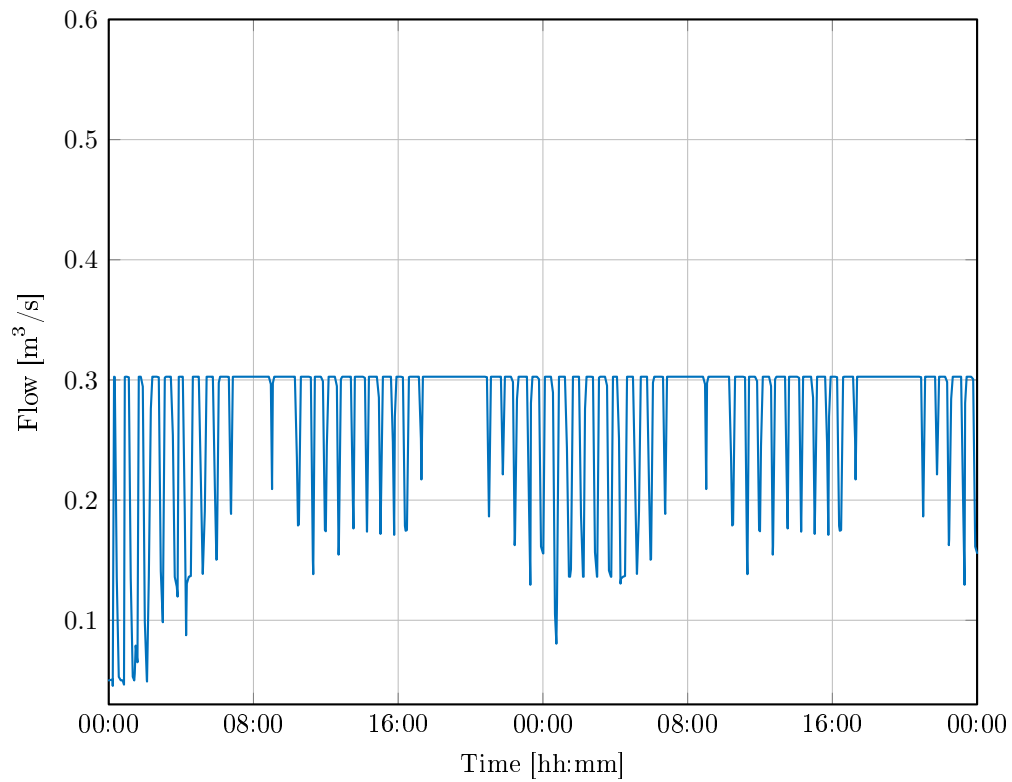


Figure 7.3: Output of the last pipe in to the WWTP, where a tank has been placed in front to reduce variation in flow into WWTP.

The pump has a constant output of  $0,3 \text{ m}^3/\text{s}$ , however, if the tank is empty it will follow the flow from the input of the tank. It can be seen by comparing figure 7.1 and figure 7.3 that the top has been reduced and thereby a less fluctuated input to the WWTP is obtained.

# Discussion 8

---

A basic study of how a WWTP works is performed, and from this, a problem statement is formulated. A simulation environment is constructed which can simulate setups which can easily be expanded by adding pipes and tanks in a setup function. Limitations are put on the chemical reactions occurring in sewer lines partly because of the delimitations made but also because of the complexity of it. Further research could be made into the Wastewater of Aerobic/Anaerobic Transformation in Sewers (WATS) model, which specifically is made to simulate chemical reactions in sewer lines. Assumptions are made utilizing the Saint-Venant equations, which simplifies the flow in the sewer line greatly. Even though simplifications are made, numerical errors in the chosen solution can be utilized to obtain a wave which mimics the real world. By utilizing Courant's number the degree of numerical error can to some extent be known during simulation. It is seen that an accurate computation can be obtained if  $\Delta t$  and  $\Delta x$  is chosen precisely. But an accurate result does not represent a real world scenario as well. Instead some discrepancy is desired such that effects such as a hydraulic jump in front of a wave going through the sewer line occurs. Therefore a Courant's number close to one is preferable to obtain some realism when simulating.

Another problem is that if  $\Delta x$  is chosen small the computational task can increase considerably if a large setup of pipes is simulated. Furthermore, the increase in size causes severe problems when linearizing a model to be utilized with MPC. The reason for this, is in part the chosen linearization method which causes the state space system to be ill conditioned, which gets worse when more sections are added. When predicting the state equations the problem is worsened and causes a numerical error, which minimizes the prediction horizon considerable. Solutions could be to create a simple model such that MPC could be used as a top level controller, or sample iterations of the state space system and do zero order hold at the MPC. But common for both is that prediction into the future is necessary, but not always available, depending on the location of the tank compared to where the disturbance is located.



# Conclusion 9

---

The focus of this project was to create a simulation model that was able to mimic the behavior of a real sewer system. Furthermore, MPC were to be implemented to obtain a low varying input into the WWTP based on the problem statement from section 1.4.

*How can a simulation environment be constructed, which mimic the behavior of a real sewer system, where MPC is utilized as the control scheme to obtain stable sewage output such that optimal performance can be obtained from a WWTP.*

A simulation model has been designed where it is possible to create a sewer system consisting of several pipes, tanks and side inflows. It is able to simulate wastewater flow and concentrate throughout a city. Furthermore, it is constructed in a way, where it can be reconfigured to fit other setups by changing the order of pipes and tanks to obtain a desired simulation setup. The results show that even though a simplified numerical scheme was chosen to simulate flow in pipes, some realism could be attained by utilizing numerical errors.

An MPC controller was constructed to control the output of a tank such that output variations were to be minimized. However, due to the rapid increase in size caused by a large number of sections numerical problems related to the linearized model appeared. Specifically, the prediction horizon was found to be limited in size if the quadratic problem could be solved. A controller was designed and tested but the results were less than satisfying.

Even though the project is not in its current form finalized, advantages can be seen in the simulation model as a tool to implement counter measures against flow variations.



# Bibliography

---

- [AquaEnviro, 2010] AquaEnviro (2010). Fungal problems in wastewater treatment works. Website. Posted 16th June 2010 - <https://www.aquaenviro.co.uk/fungal-problems-in-wastewater-treatment-works/>.
- [College, 2018] College, M. E. C. (2018). Biological components of wastewater. Website. <http://water.me.vccs.edu/courses/ENV149/biological.htm>.
- [Cunge et al., 1980] Cunge, J. A., Holly, F. M., and Verwey, A. (1980). Practical aspects of computational river hydraulics.
- [Dansk-betonforening, 2013] Dansk-betonforening (2013). Betonhåndbogen. Online.
- [Emerson, 2009] Emerson (2009). Dissolved oxygen measurement in wastewater treatment. [http://www2.emersonprocess.com/siteadmincenter/PM%20Rosemount%20Analytical%20Documents/Liq\\_ADS\\_4950-01.pdf](http://www2.emersonprocess.com/siteadmincenter/PM%20Rosemount%20Analytical%20Documents/Liq_ADS_4950-01.pdf).
- [Eniro, ] Eniro. krak. website.
- [EPA, 1994] EPA (1994). How wastewater treatment works... the basics. website. <https://www3.epa.gov/npdes/pubs/bastre.pdf>.
- [Eschooltoday, 2017] Eschooltoday (2017). Liquid waste (sewage/wastewater) treatment. Website.
- [Fredericia-Spildevand, 2018a] Fredericia-Spildevand (2018a). Geographical information systems. A map to describe the length, slope and size of the different sewers in Fredericia. <http://frsp.webgrafkort.dk/Mainpage.aspx>.
- [Fredericia-Spildevand, 2018b] Fredericia-Spildevand (2018b). Summary of company visits. Summary from a meeting with Fredericia Spildevand og Energi A/S can be found in appendix A.1.
- [Hvitved-Jacobsen et al., 2013] Hvitved-Jacobsen, T., Vollertsen, J., and Nielsen, A. H. (2013). *Sewer processes: microbial and chemical process engineering of sewer networks*. CRC press.
- [Institute of hydromechanics, ] Institute of hydromechanics. Concepts, definitions and the diffusion equation. Technical report, Karlsruhe Institute of Technology.
- [Maciejowski, 2002] Maciejowski, J. M. (2002). *Predictive control: with constraints*. Pearson education.
- [Mays, 2001] Mays, L. W. (2001). *Stormwater collection systems design handbook*. McGraw-Hill Professional.
- [Michelsen, 1976] Michelsen, H. (1976). Ikke-stationær strømning i delvis fyldte kloakledninger. Master's thesis, Den kongelige veterinær og landbohøjskole.
- [Nykredit, 2018] Nykredit (2018). Familietyperne. website.
- [Rinkesh, 2009] Rinkesh (2009). What is wastewater treatment. website.

- [Rossi et al., 2014] Rossi, F., Motta, O., Matrella, S., Proto, A., and Vigliotta, G. (2014). Nitrate removal from wastewater through biological denitrification with oga 24 in a batch reactor. *Water*, 7(1):51–62.
- [Ruscio, 2001] Ruscio, D. D. (2001). Model predictive control and optimization. Lecture notes. Lecture notes on Model Predictive Control.
- [Schlütter, 1999] Schlütter, F. (1999). *Numerical modelling of sediment transport in combined sewer systems*. PhD thesis, The Hydraulics and Coastal Engineering Group, Dept. of Civil Engineering, Aalborg University.
- [Schütze et al., 2011] Schütze, M., Butler, D., and Beck, B. M. (2011). *Modelling, simulation and control of urban wastewater systems*. Springer Science & Business Media.
- [Sjøholm, 2016] Sjøholm, P. (2016). Rensningsanlæg (wastewater plant). Video. [https://www.youtube.com/watch?v=cEQ\\_IN0601E](https://www.youtube.com/watch?v=cEQ_IN0601E).
- [Statistics-Denmark, 2018] Statistics-Denmark (2018). Population according to cities in 2017. <https://www.dst.dk/en>.
- [Szymkiewicz, 2010] Szymkiewicz, R. (2010). *Numerical modeling in open channel hydraulics*, volume 83. Springer Science & Business Media.
- [Szymkiewicz, 1998] Szymkiewicz, R. (1998). *Numerical Modeling in Open Channel Hydraulics*. Springer.
- [Vestergaard, 1989] Vestergaard, K. (1989). *Numerical Modelling of Streams: Hydrodynamic models and models for transport and spreading of pollutants*. PhD thesis, Hydraulic & Coastal Engineering Laboratory, Department of Civil Engineering, Aalborg University.
- [Vojtesek et al., ] Vojtesek, J., Dostal, P., and Maslan, M. Modelling and simulation of water tank.

## A.1 Summary of company visits

This appendix contains a summary from a meeting with the Fredericia wastewater department. The summary is in danish.

Virksomheds besøg 19/03/2018

Spildevand der kommer til rensning ved Fredericia rensningsanlæg stammer hovedsageligt fra industrien, 60-65 %. Ved Carlsberg og Arla er der flow målinger. Der er ikke målinger fra beboelse, hverken flow eller koncentrat, dog er der flow målinger ved nogle af pumpe stationer, samt flow og koncentrations målinger ind på rensningsanlægget. Stofmængden er ukendt fra det meste af industrien. Der er biotector ved Carlsberg (TOC) og COD måler ved Arla. Fredericia kunne evt. skaffe flowmålinger til os efter kontakt med industrien. På nuværende tidspunkt regulerer Carlsberg deres spildevand så det har en pH værdi mellem 6 og 9. Carlsberg har også et spare bassin. Arla har to spare bassiner, hvor de også kontrollerer deres pH udledning. Shell har deres eget rensningsanlæg. Industrien er typisk gode til at holde en konsistent udledning af flow og koncentrat, der kan dog forekomme uheld. Fordelene ved Fredericia er, at temperaturen på spildevandet i kloakkerne ligger omkring 16-17 grader året rundt. Dette hjælper bakterierne med denitrificering af spildevandet. Bakterierne er mindre aktive med nitrificeringen og denitrificering når temperaturen kommer under 10 grader celsius. Hvilket betyder, at fjernelsen af nitrogen går langsommere.

- Der er problemer i ledningsnettet når der falder kraftig regn, der kan forekommer overløb, derudover gør man rensningsprocessen hurtigere ved kun at føre vandet igennem den mekaniske rensning og derefter udlede det til Lillebælt.
- Der er kul filter på næsten alt for at fjerne lugtgener, såsom dæksler, overtryksventiler og lukkede bassiner.
- Man vil gerne minimere opholdstid i spare bassiner for at undgå produktion af hydrogen sulfid.
- Ved vedligeholdelse af rensningsanlægget lukkes hovedledningen ind til rensningsanlægget, hvor det er muligt at stuve spildevand op i hoved ledning i 3-4 timer i tørvejr.
- Grundvandsindtrængning er forhøjet under regnvejr, samt forhøjet når vandstanden i Lillebælt er over normen.
  - Forhøjet vandstand kan øge klorid indholdet i spildevandet både ved at trænge ind gennem grundvandet, men også ved tilbageløb i overløbsanlæg beliggende ud til Lillebælt. Dette er et problem, da bakterierne fungerer bedst med en konstant mængde af klorid i spildevandet. Variationer i klorid gør, at bakteriernes nedbrydningsproces af de forskellige stoffer i spildevandet er nedsat for en periode. Når indholdet af klorid er konstant igen tilpasser bakterierne sig og deres nedbrydningsproces går tilbage til normal kapacitet.
- Der er ingen forfældning i rensningsanlægget pga. lugtgener.

- Har tidligere udtaget primær slam ved bundfældning, det blev stoppet pga. høj gas udvikling, da dette gav lugtgener.
- Der planlægges igen at udtage primær slam ved en filtreringsproces for at undgå lugtgener.
- Fosfor kommer hovedsageligt fra industri ca. 300-500 kg/døgn under normal drift. Fosfor er nødvendigt da dette indgår i processen til at nedbryde kvælstof.
- Varierende indhold af klorid i spildevandet er et problem for bakterierne, dette er især et problem under 10 mg/l.
- Rensningsanlægget har en kapacitet på 420.000 People Equivalent (PE), PE svarer til 120 COD/døgn eller 0,2 mg/l/døgn for en person.
- Når der er tørvejr er der et typisk flow på 800-1200  $m^3/time$  ind til rensningsanlægget.

Det ideelle scenarie er,

- Konstant flow og koncentrat
- Fast indhold af koncentrat (Klorid bl.a.)
  - Nødvendigvis ikke et lavt indhold

Prioriteringer i forhold til forstyrrelse i styring af ledningsnetværk.

- Små klorid variationer
- Slam/bakterier nok til at kunne omsætte kvælstof
  - Dette reguleres der for i rensningsanlægget.
- Der skal være en hvis mængde kulstof
  - Hvis spildevand flowet er konstant, er dette ikke et problem for rensningsanlægget.
- Små flow variationer
- Lav opholdstid i bassiner

## A.2 Pump information

Information regarding some of the pumps in Fredericia.

In tabluar A.1 information regarding the pumps located in Fredericia can be found. These values have been given by Fredericia.

Location	Pump capacity [ $m^3/s$ ]	Number of pumps	Surface area of the well [ $m^2$ ]	Start stop level [m]	Wear reduction [%]	Total pumping capacity [ $m^3/s$ ]
Damvej P215	0,0478	2	12.56	0,7/0,37	5-10	0.0956
Thulesvej P217	0,0719	2	12.56	0,59/0,07	25-30	0.1438
Treldevej P218	0,0206	1	7.06	0,67/0,17	25-30	0,0206
Treldevej east P219	0,0214	2	12.56	0,79/0,34	25-30	0,0428
Lillebælts allé P221	0,0138	2	6	1,06/0,7	5-10	0,0276
Benzinvej P254	0,0476	2	12.56	1/0.36	5-10	0,0952
Norgesgade P255	0,350	3	N/A	N/A	N/A	1,05
Vesthavnsvej P256	0,240	5	N/A	N/A	N/A	1,2

Table A.1: Information for the different pumps located in Fredericia

### A.3 Flow profiles

In this appendix the flow profiles that describes the flow from the residential, industrial, brewery and bottling plant used in the simulation is shown. Furthermore, profiles that describes the concentration intake to the WWTP is also included.

In table 2.3 the population of each residential areas are shown. This, together with figure 1.5 is used to estimate the flow profiles for each residential area in Fredericia. By constructing a flow profile identical to Frejlev, shown in figure 1.5, and by knowing the population of Frejlev, the population in the residential areas shown in 2.3 is scaled accordingly to the constructed flow profile for Frejlev.

For the industrial areas, shown in figure 2.1, it has been decided to use the flow profile for the respectively residential area, where a factor of 1/5 has been multiplied on the industrial flow profiles. The reason for this is, that no information about the flow from these industrial areas are accessible. Therefore, it is assumed that 1/5 of the people living in the respectively residential area works in the industrial area. Thereby, the flow profiles for the industrial areas are obtained.

From some of the residential and industrial areas located far away from the main sewer line a transport delay has been added to the flow profile. These areas are seen in table A.2.

Area	Distance [m]	Time [s]
1,1	500	250
1,2	1000	500
1,3	2000	1000
3	800	400
4,1	1500	750
4,2	1400	700
4,3	1100	550
7	1000	500
10	900	450
11	300	150

Table A.2: Specification on the distance from the areas furthest away from the main sewer line. Furthermore, the time it takes for the wastewater to be transported from there respectively area to the main sewer line.

The distance is an estimate of the pipe length for each area. A velocity of 2 m/s has been chosen as the transport speed of the wastewater. This however variates with the flow, wetted area and the slope of the pipe, however it is deemed as a appropriated size, due to the flow profiles also variates in flow.

The legend and the figure text, throughout this appendix, references to the figure 2.1 shown in chapter 2.

In figure A.1 the difference flow profile for the residential and industrial areas for area one is shown.

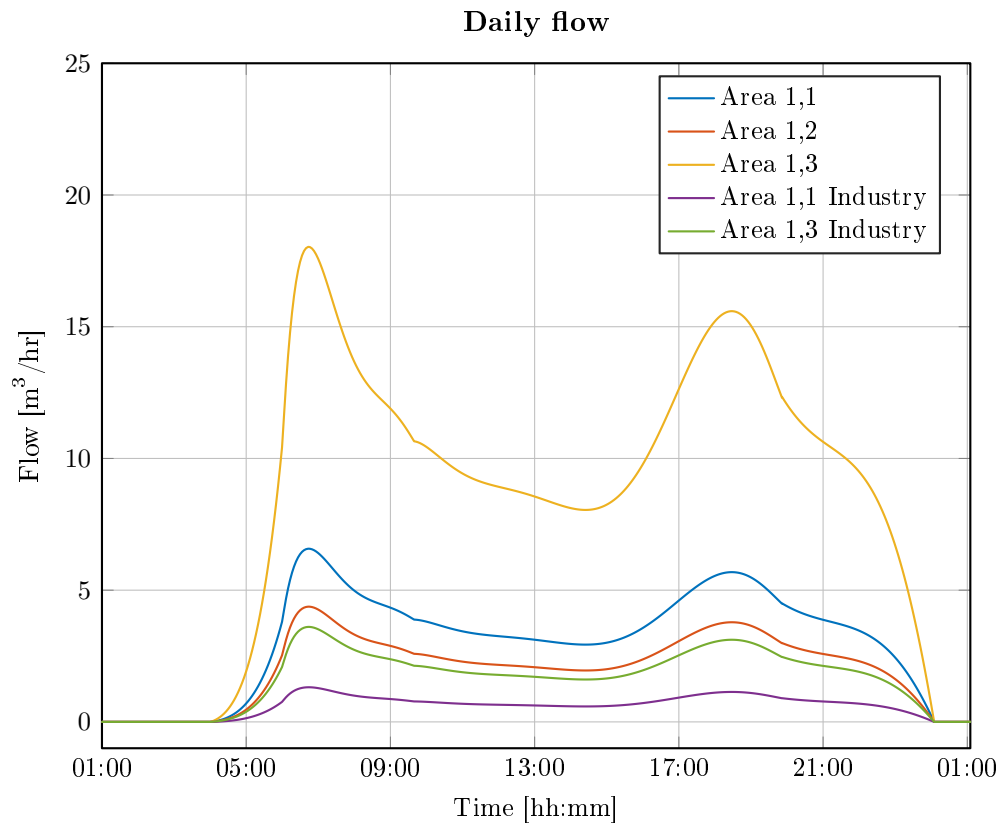


Figure A.1: A daily flow profile of area 1.

In figure A.2 the combined disturbance from area one is shown with transport delay.

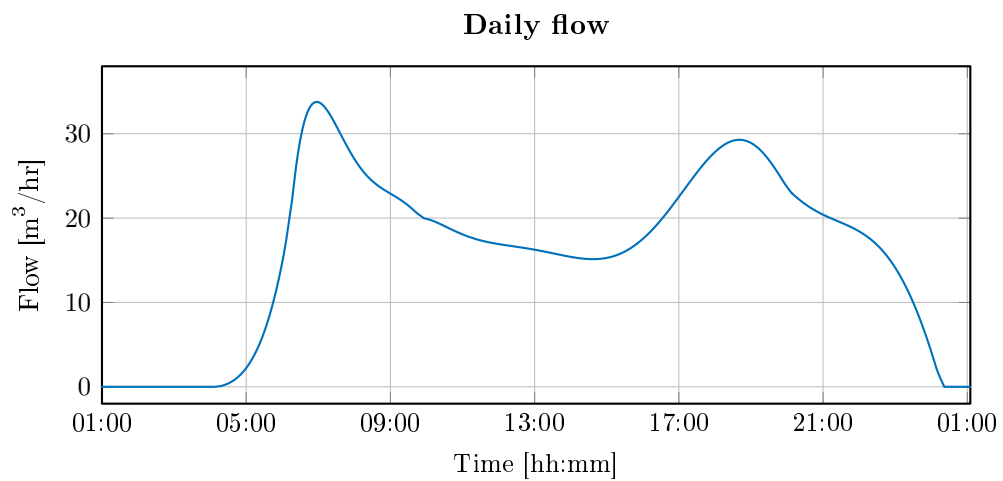


Figure A.2: A daily combined flow profile of area 1, where a transport delay is added to the pipes.

In figure A.3 the flow profile for area two is shown, and as it is so close to the main sewer line no transport delay is added.

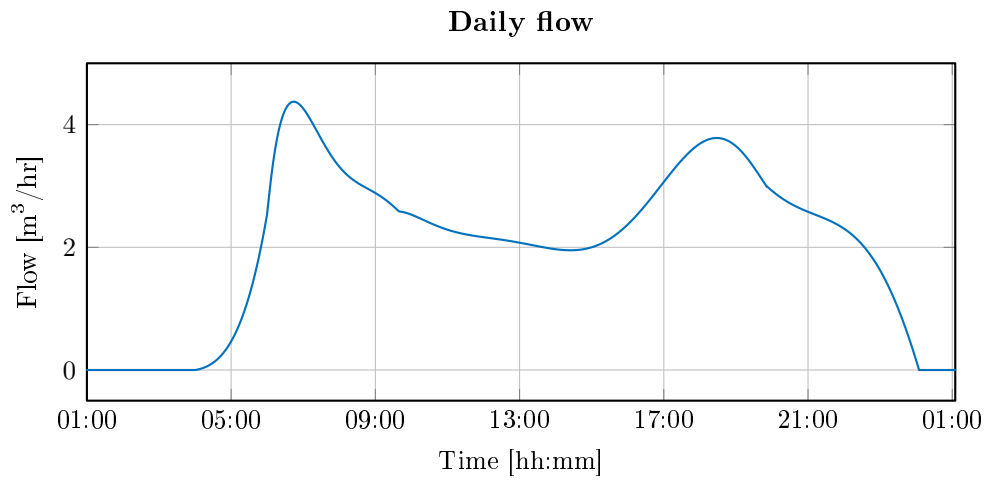


Figure A.3: A daily flow profile of area 2.

In figure A.4 the flow profile for area three is shown.

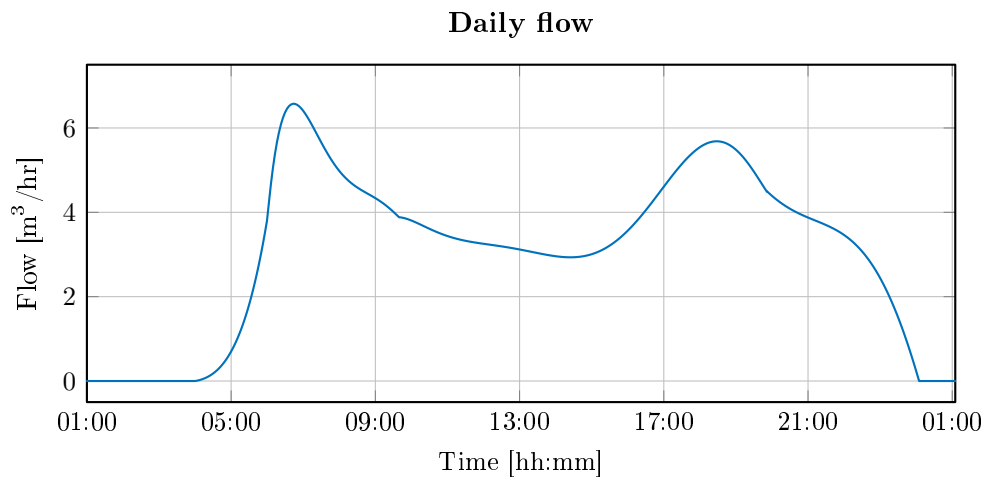


Figure A.4: A daily flow profile of area 3.

In figure A.5 the disturbance from area three is shown with transport delay.

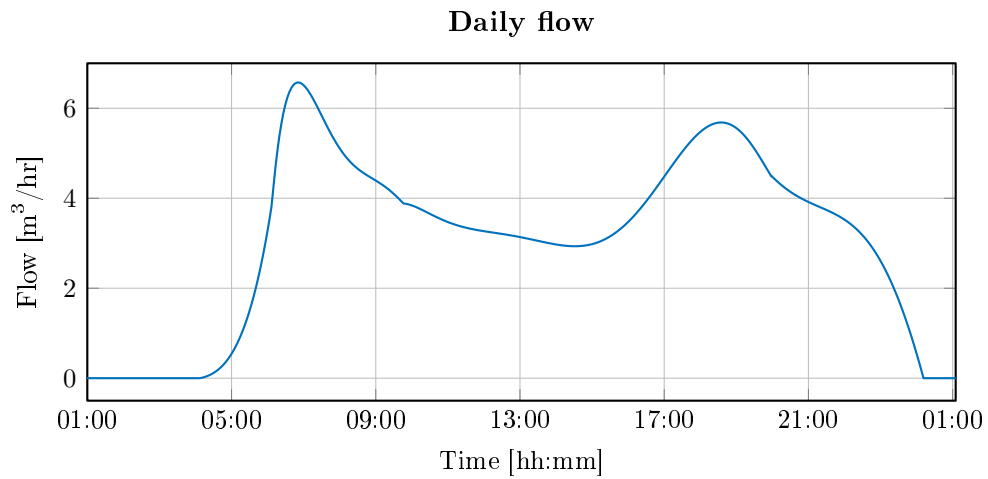


Figure A.5: A daily combined flow profile of area 3, where a transport delay is added to the pipes.

In figure A.6 the difference flow profile for the residential and industrial areas for area four is shown.

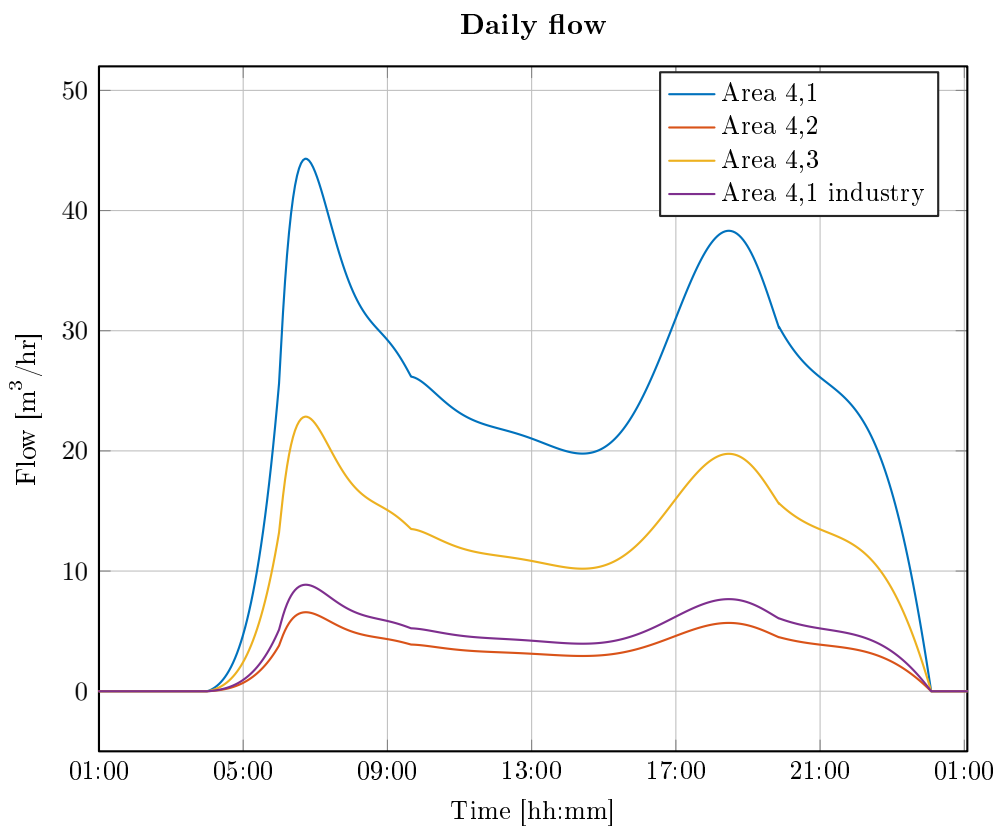


Figure A.6: A daily flow profile of area 4.

In figure A.7 the combined disturbance from area four is shown with transport delay.

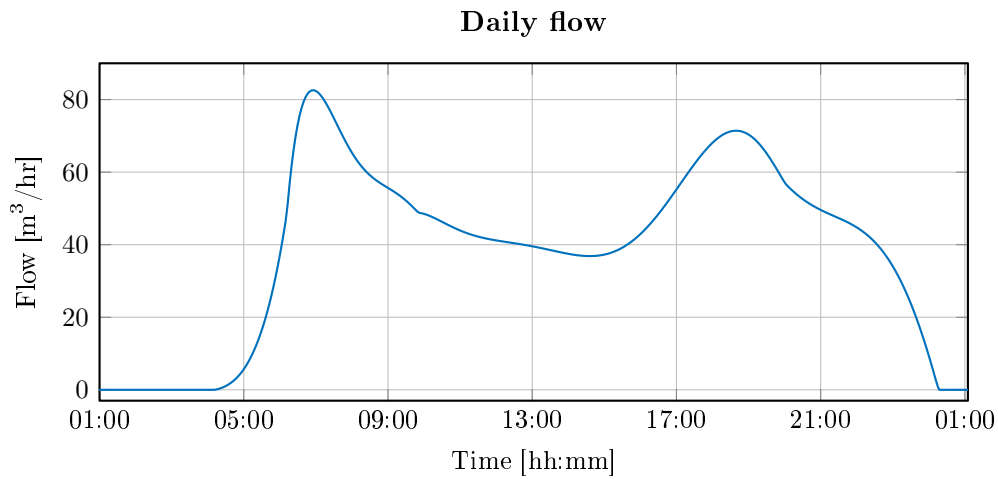


Figure A.7: A daily combined flow profile of area 4, where a transport delay is added to the pipes.

In figure A.8 the flow profile for area five is shown, and as it is so close to the main sewer line no transport delay is added.

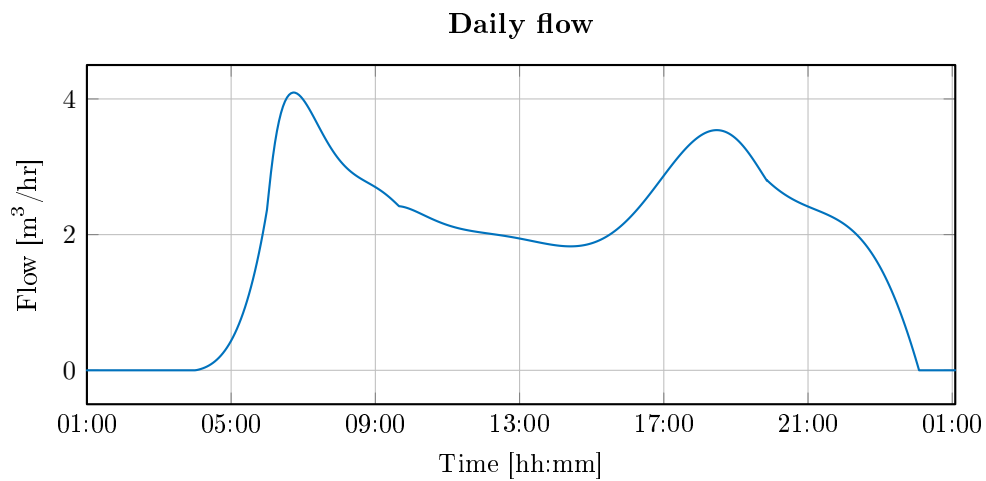


Figure A.8: A daily flow profile of area 5.

In figure A.9 the flow profile for area six is shown, and as it is so close to the main sewer line no transport delay is added.

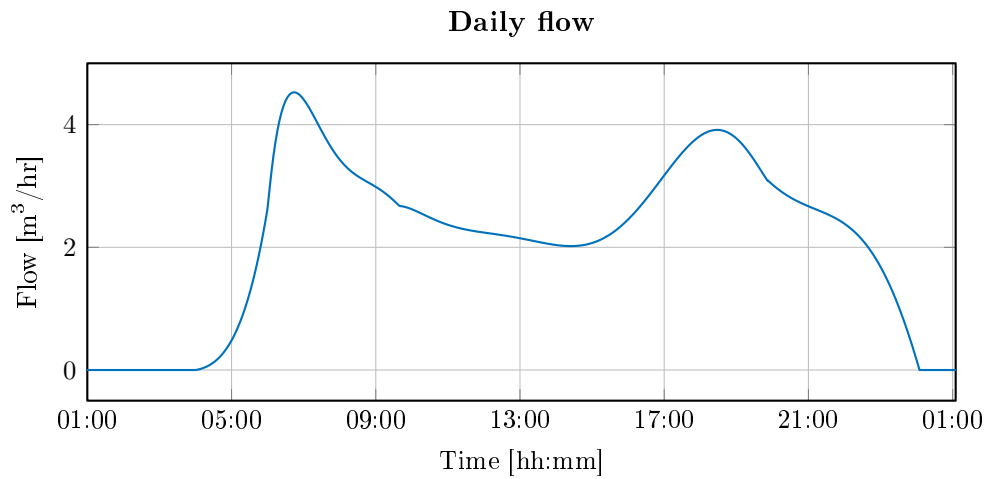


Figure A.9: A daily flow profile of area 6.

In figure A.10 the flow profile for area seven is shown.

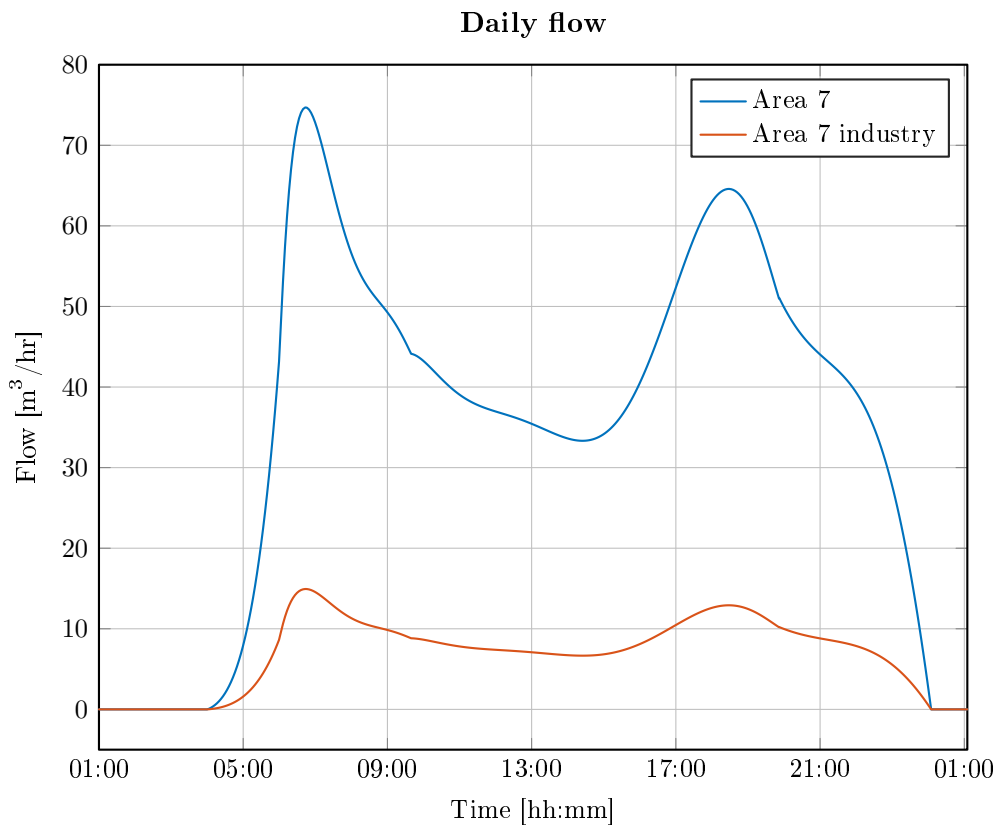


Figure A.10: A daily flow profile of area 7.

In figure A.11 the combined disturbance from area seven is shown with transport delay.

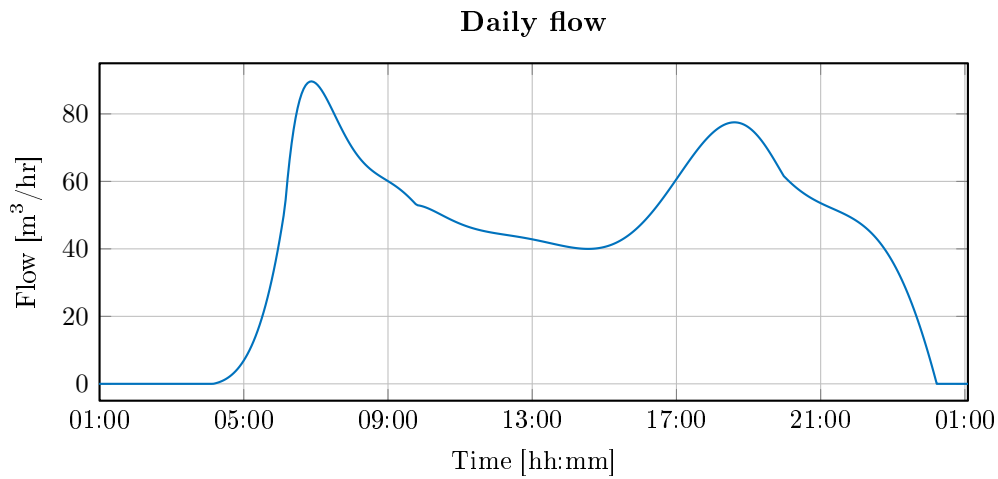


Figure A.11: A daily combined flow profile of area 7, where a transport delay is added to the pipes.

In figure A.12 the flow profiles for area eight and nine is shown.

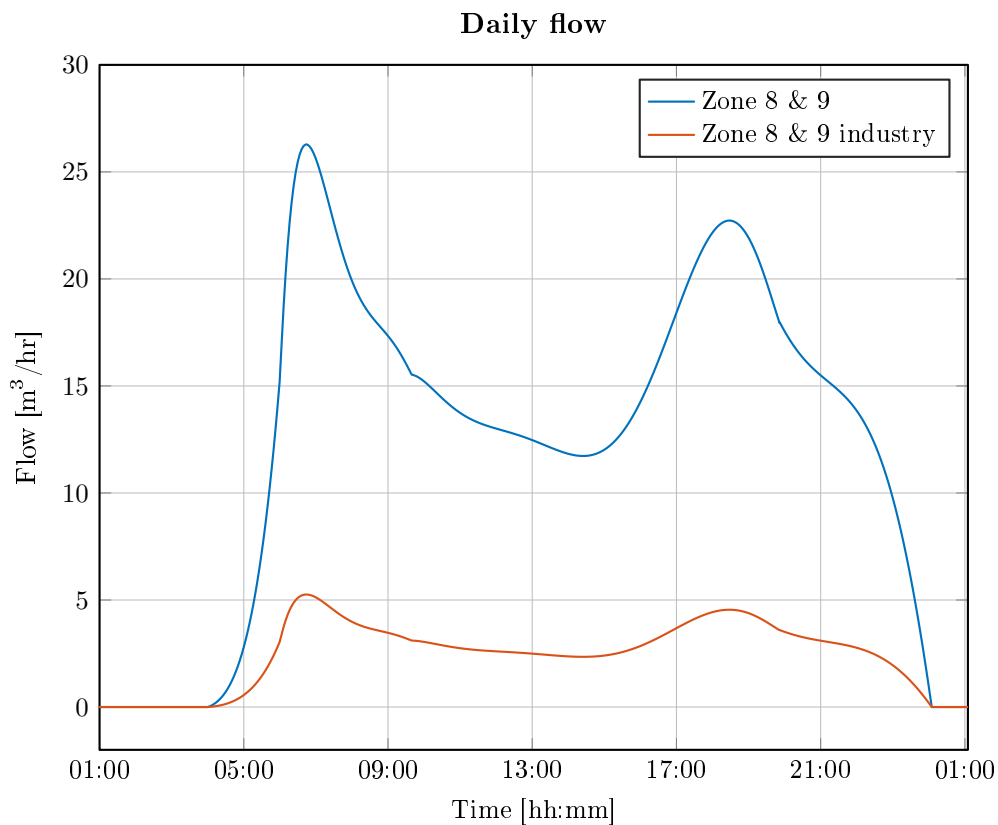


Figure A.12: A daily flow profile of area 8 and 9.

In figure A.13 the combine flow profile for area eight and nine is shown.

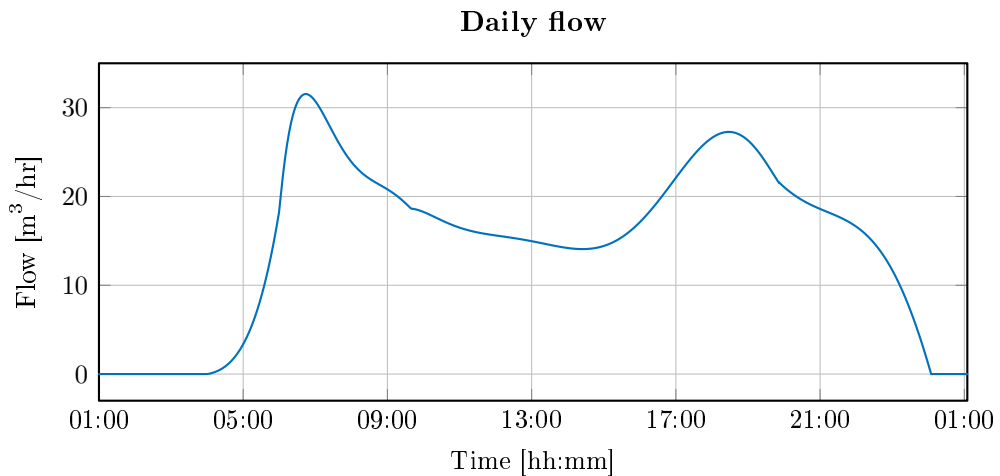


Figure A.13: A daily combined flow profile of area 8 and 9, where a transport delay is added to the pipes.

In figure A.14 the flow profile for area ten is shown.

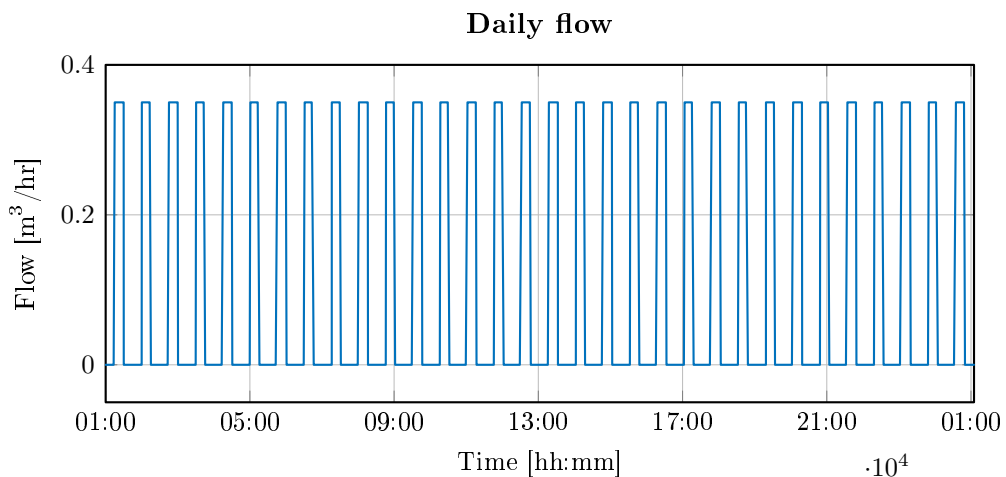


Figure A.14: A daily flow profile of area 10.

From area ten a pump is pumping the wastewater to the main sewer line every 30 minutes for a period of 15 minutes. The pump has a pumping capacity of  $0,350 \text{ m}^3/\text{s}$  which has been stated by Fredericia and seen in table A.1. Therefore the flow profile of this area will be a constant input of  $0,350 \text{ m}^3/\text{s}$  for 15 minutes every 30 minutes. The pipe from area ten is a pressurized pvc pipe and therefore the resistance within the pipe is less than the resistance in a concrete pipe. However, the velocity of this pipe is deemed to be the same as for concrete pipe, as these flow profiles are just an estimate. In figure A.15 area ten is shown with the transport delay.

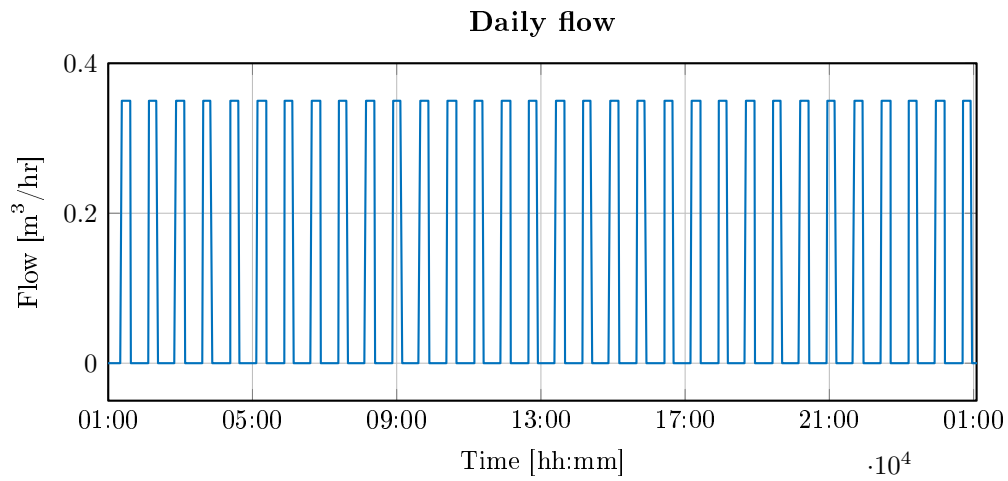


Figure A.15: A daily combined flow profile of area 10, where a transport delay is added to the pipes.

In figure A.16 the flow profile for area eleven is shown.

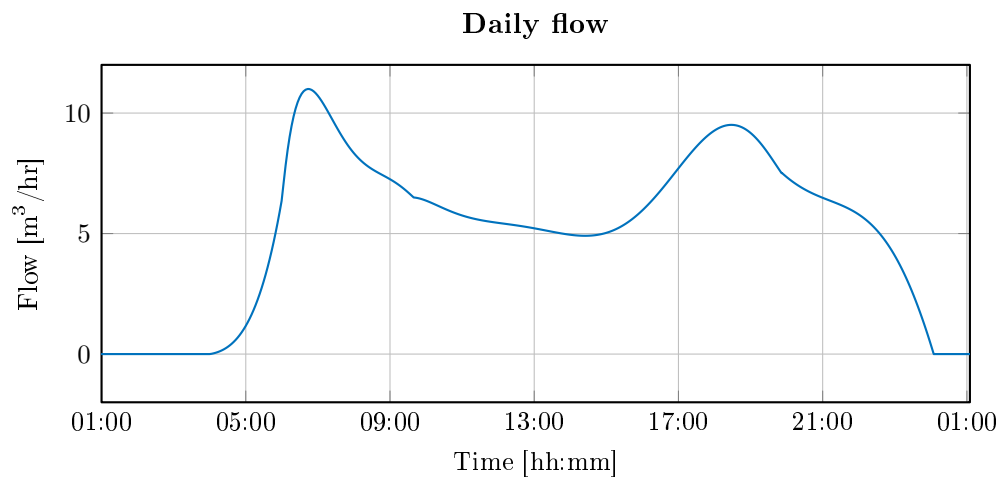


Figure A.16: A daily flow profile of area 11.

In figure A.17 the flow profile for area eleven is shown with time delay.

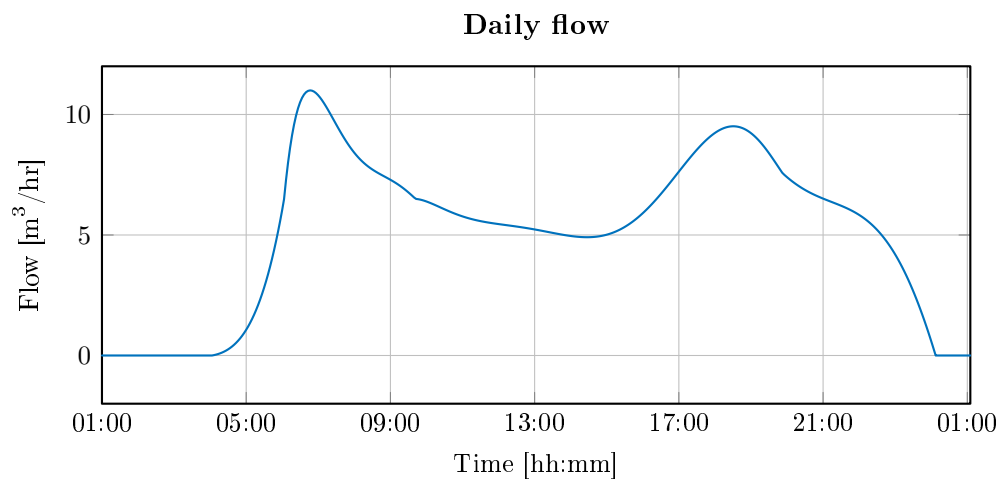


Figure A.17: A daily combined flow profile of area 11, where a transport delay is added to the pipes.

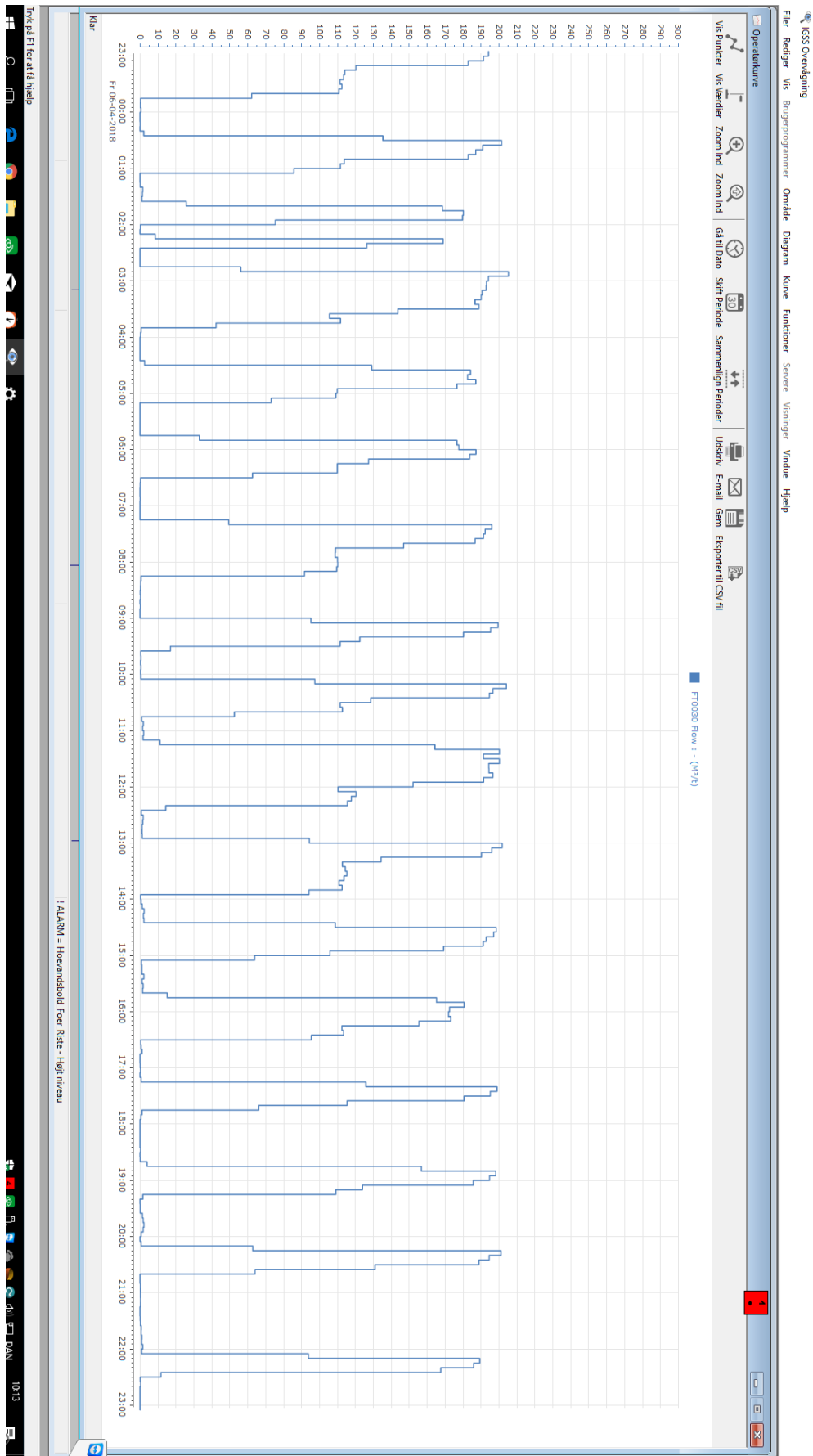


Figure A.18: Daily flow from a brewery and bottling plant in Fredericia.

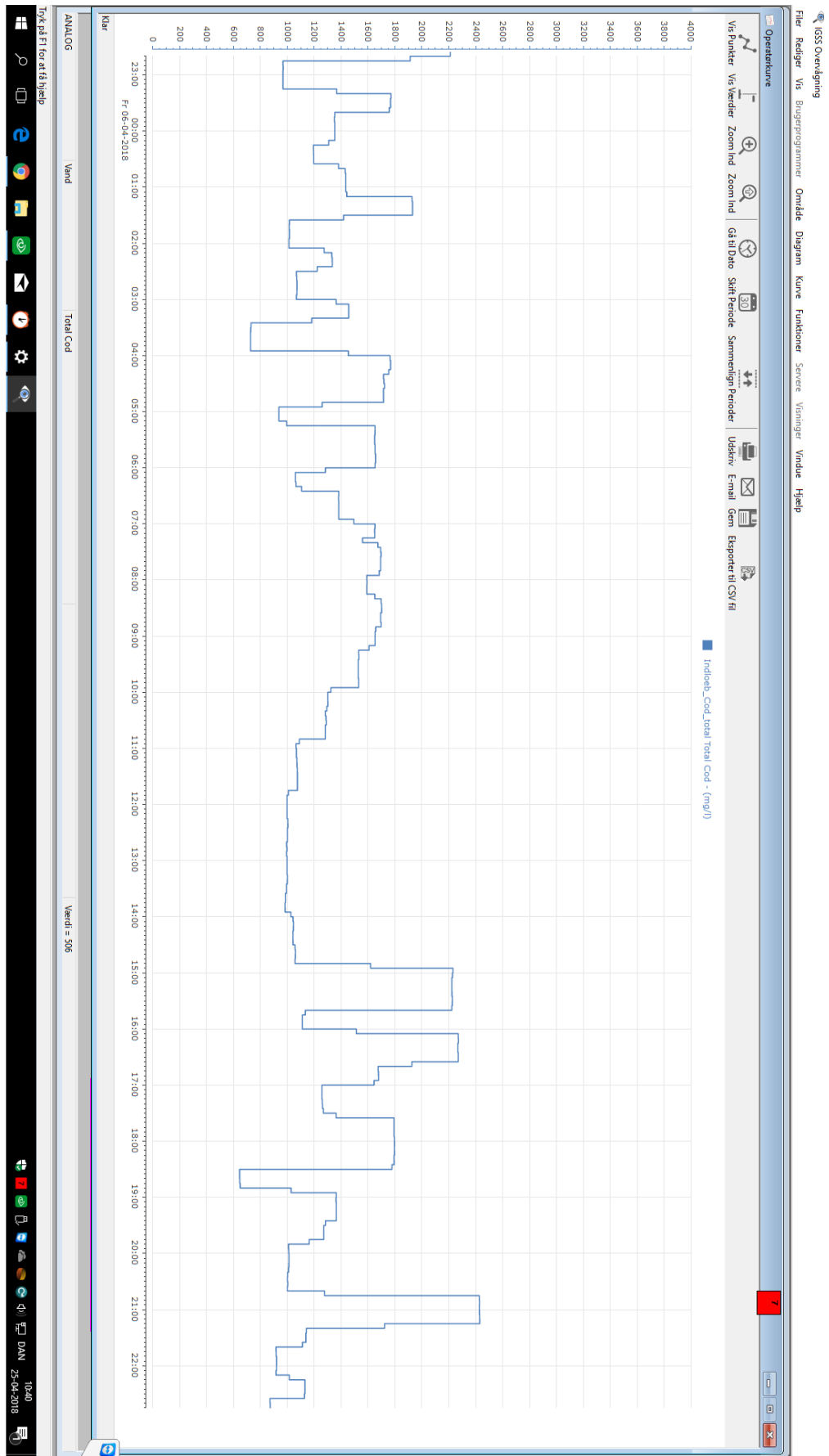


Figure A.19: COD inflow to the WWTP.

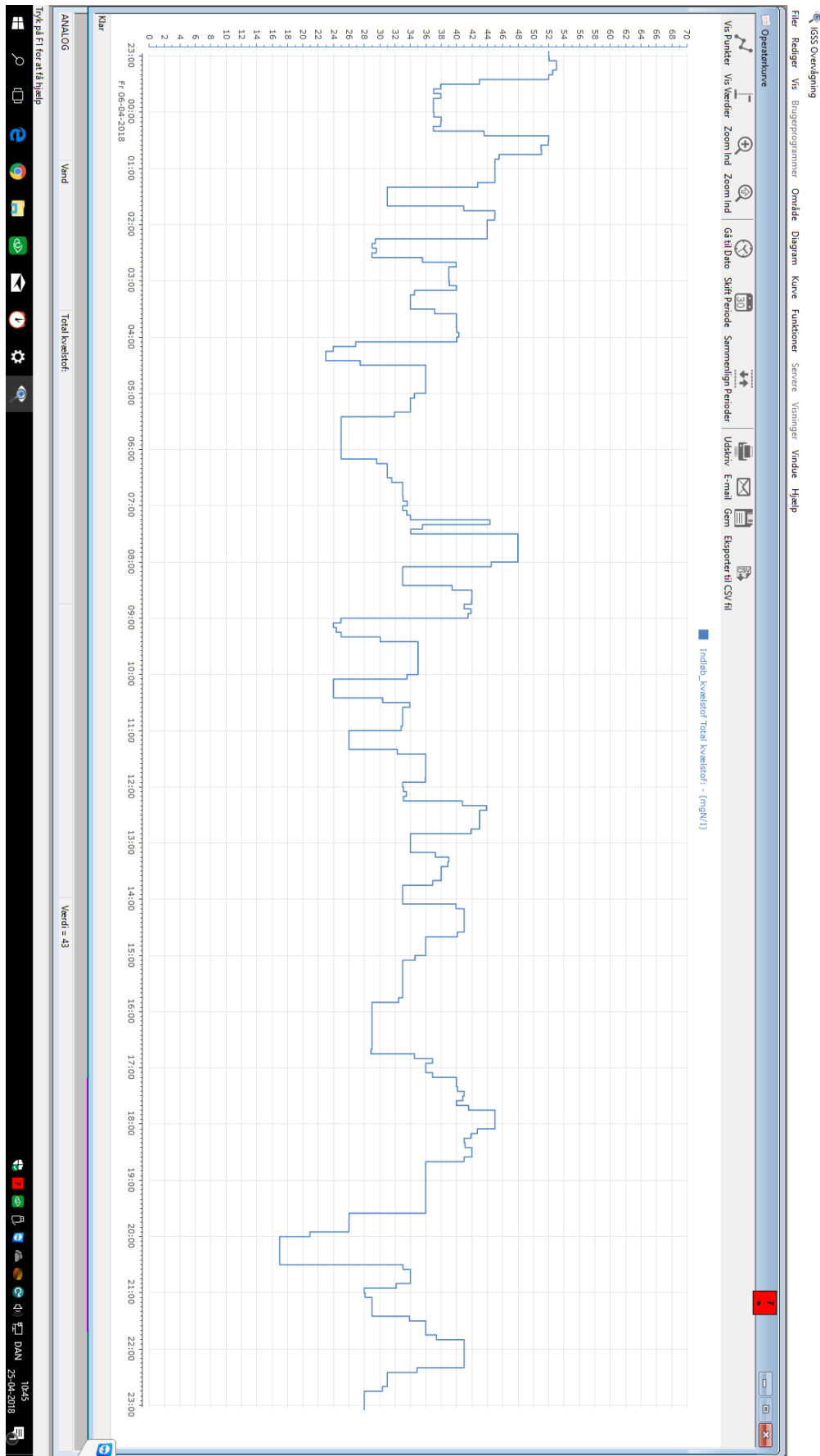


Figure A.20: Phosphorus inflow to the WWTP.

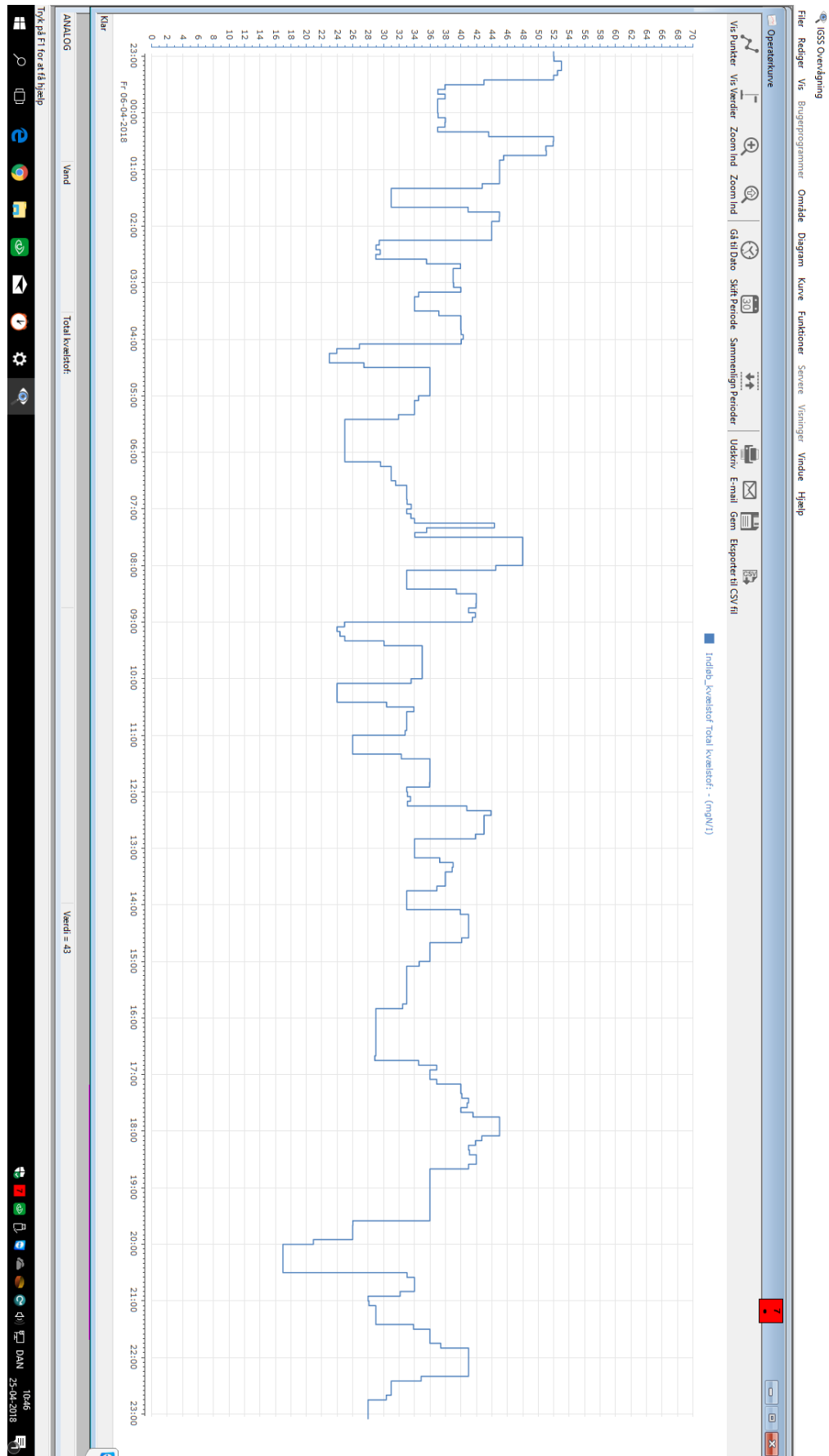


Figure A.21: Nitrogen inflow to the WWTP.

## A.4 Formulas

In this section the equations for calculation the area, water width and flow in a pipe will be shown.

In figure A.22 a illustration a cross view of a circular pipe is shown

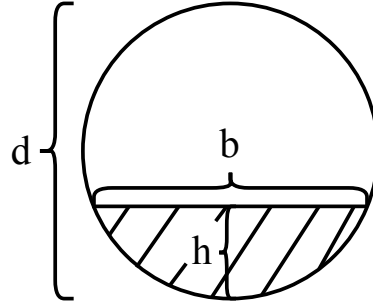


Figure A.22: Cross section view of a circular pipe. Where  $d$  is the diameter,  $b$  is the width of the water in a given height,  $h$  is the height and the crossed section in the bottom illustrates the area of the water in the pipe.

The area of the water in a circular pipe is calculated with the following [Michelsen, 1976]:

$$A = \frac{d^2}{4} \cdot \arccos\left(\frac{\frac{d}{2} - h}{\frac{d}{2}}\right) - \sqrt{h \cdot (d - h)} \cdot \left(\frac{d}{2} - h\right) \quad (\text{A.1})$$

The water width in a pipe to a given height is calculated with the following equation [Michelsen, 1976]:

$$b = 2 \cdot \sqrt{-h + h \cdot d} \quad (\text{A.2})$$

The flow in a filled pipe can be calculated with the equation describing the friction in a pipe [Michelsen, 1976]:

$$S_f = \frac{n^2 Q^2}{A^2 R^{4/3}} = \frac{n^2 v^2}{R^{4/3}} \quad (\text{A.3})$$

Where  $n$  is Mannings roughness factor [ $sm^{-1/3}$ ], which is 0,0139 for concrete pipe,  $S_f$  is a friction coefficient,  $R$  is the hydraulic radius [m],  $A$  is the area [ $m^2$ ] and  $Q$  is the flow [ $m^3/s$ ]. This equation is solved for the flow:

$$Q = \frac{1}{n} \cdot A \cdot R^{2/3} S_f^{1/2} \quad (\text{A.4})$$

Taking the square root on both sides and assuming that the equation is for a filled pipe, the following can be written:

$$Q_f = \frac{1}{n} A_f R_f^{0.635} S_f^{0.5} \quad (\text{A.5})$$

Where  $Q_f$ ,  $A_f$  and  $R_f$  are flow, wetted area and hydraulic radius for a filled pipe. For a filled pipe the formula for the area of a circle is used,  $\pi \cdot r^2$ . The hydraulic radius is the wetted area divided by the wetted perimeter. As the wetted area, is the area of a circle, and the wetted perimeter is equal to the perimeter of a circle,  $2\pi r$ , the following can be written:

$$Q_f = \frac{1}{n} \pi r^2 \left( \frac{\pi r^2}{2\pi r} \right)^{0,635} S_f^{0,5} \quad (\text{A.6})$$

This can be simplified to the equation for a filled pipe:

$$Q_f = \frac{1}{n} \pi \left( \frac{d}{2} \right)^2 \left( \frac{d}{4} \right)^{0,635} S_f^{0,5} \quad (\text{A.7})$$

The flow in a pipe given a height can be calculated with the following equation [Michelsen, 1976]:

$$Q = \left( 0,46 - 0,5 \cdot \cos \left( \pi \frac{h}{d} \right) + 0,04 \cdot \cos \left( 2\pi \frac{h}{d} \right) \right) \cdot Q_f \quad (\text{A.8})$$